



Deliverable 14.1: Initial State of the art report
Review of different designs/safety concepts and
processes governing the performance of engineered
barriers in near-surface disposal facilities

Work Package 14

DOI: 10.5281/zenodo.18174019



Co-funded by the European Union under Grant Agreement n°101166718

Document information

Project Acronym	EURAD-2
Project Title	European Partnership on Radioactive Waste Management-2
EC grant agreement No.	101166718
Work Package Title	SUDOKU: Near-Surface Disposal Optimization based on Knowledge and Understanding
Deliverable No.	Deliverable 14.1 State of the art report (initial)
Deliverable Title	Review of different designs/safety concepts and processes governing the performance of engineered barriers in near-surface disposal facilities
Lead Beneficiary	SCK CEN
Contractual Delivery Date	September 2025
Actual Delivery Date	November 2025
Dissemination level	PU
Authors	D. Jacques (SCK CEN), C. Bucur (Raten ICN), M. Gran (Amphos 21), F. Lemy (ONDRAF), P. Henocq (Andra), T. Missana (CIEMAT), M. Arribas (Enresa), D. Karastanov (GI-BAS), B. Tchakalova (GI-BAS), P. Balcius (LEI), D. Grigaliuniene (LEI), P. Poskas (LEI), G. Chen (SCK CEN), Y. Li (SCK CEN), O. Fabritius (UHel), G. Law (UHel), T. Vierinen (UHel), B. Zajec (ZAG)
Reviewers	Crina Bucur (RATEN ICN), Peter Ormai (PURAM)

To be cited as:

D. Jacques et al. D., (2025): Review of different designs/safety concepts and processes governing the performance of engineered barriers in near-surface disposal facilities. Final version as of 04.11.1025 of deliverable D14.1 of the European Partnership EURAD-2. EC Grant agreement n°:101166718.

Disclaimer

All information in this document is provided "as is" and no guarantee or warranty is given that the information is fit for any particular purpose. The user, therefore, uses the information at its sole risk and liability. Views and opinions expressed are however those of the author(s) only and do not necessarily reflect those of the European Union or European Atomic Energy Community. Neither the European Union nor the granting authority or the individual Colleges of EURAD-2 can be held responsible for them.

Acknowledgement

This document is a deliverable of the European Partnership on Radioactive Waste Management 2 (EURAD-2). EURAD-2 is co-funded by the European Union under Grant Agreement N° 101166718.

Status of deliverable		
	By	Date
Delivered (Lead Beneficiary)	D. Jacques (SCK CEN)	11/09/2025
Verified (WP Leader)	C. Bucur (RATEN ICN)	18/09/2025
Reviewed (Reviewers)	C. Bucur (RATEN ICN) P. Ormai (PURAM)	29/09/2025
Approved (PMO)	P. Ormai (PURAM)	28/10/2025
Submitted to EC (Coordinator)	ANDRA	06/11/2025

Executive Summary

SUDOKU, a work package in the EURAD-2 Partnership, is the acronym for Near-Surface Disposal Optimization based on Knowledge and Understanding. Its general objective is understanding the behaviour and performances of covers and cementitious barriers of near-surface disposal facilities for short lived waste (ground level facilities) and ILW (shallow deep facilities) in view of these barriers optimization to ensure the long-term safety of disposal facilities. A special focus is on the long-lived mobile radionuclides which mobility through the disposal zone depends closely on the properties of these engineered barriers.

Chapter 2 describes near-surface disposal concepts from the different countries represented by partners in SUDOKU. Safety functions in support of the general safety functions isolation and containment related to the multi-layer cover and the cementitious barriers are discussed as well.

Chapter 3 focusses on the multi-layer cover and describes water infiltration and degradation. An overview of the experimental studies both at laboratory scale and in-situ mock-ups (existing and planned) is given.

Chapter 4 describes the chemical and mechanical degradation of cementitious barriers as well as the effect of corrosion.

Finally, Chapter 5 discusses the migration of the main safety relevant radionuclides (^{36}Cl , ^{14}C , ^{99}Tc , ^{129}I ...) in degraded cementitious barriers, including the effect of degradation on sorption and diffusion of these radionuclides that are very mobile in the geosphere.

Key challenges addressed in SUDOKU are summarized in Chapter 6.

Keywords

(near-)surface repository, multi-layer cover, cementitious barriers, mobile radionuclides

Table of content

Executive Summary.....	4
Keywords	4
Table of content.....	5
List of figures	7
List of Tables	10
Abbreviations	11
1 Introduction	12
2 Near-surface Disposal concepts and safety functions associated to different EBS.....	14
2.1 Near-Surface disposal concepts	14
2.2 Status of selected near-surface disposal concepts.....	15
2.2.1 Belgium	15
2.2.2 Bulgaria.....	16
2.2.3 Finland	20
2.2.4 Czech Republic.....	21
2.2.5 France.....	22
2.2.6 Lithuania	26
2.2.7 Romania.....	28
2.2.8 Slovenia	29
2.2.9 Spain.....	31
2.3 R&D aspects	33
2.3.1 Belgium.....	33
2.3.2 Bulgaria.....	34
2.3.3 Finland	34
2.3.4 France.....	35
2.3.5 Lithuania	35
2.3.6 Romania.....	36
2.3.7 Slovenia	36
2.3.8 Spain.....	39
2.4 Safety functions.....	40
2.4.1 Belgium	40
2.4.2 Bulgaria.....	45
2.4.3 Finland	45
2.4.4 France.....	46
2.4.5 Lithuania	48
2.4.6 Romania.....	49
2.4.7 Slovenia	52
2.4.8 Spain.....	54
3 Multi-layer covers.....	58
3.1 Processes.....	58

3.1.1	Water infiltration and energy balances	58
3.1.2	Processes affecting long term performance	60
3.2	Experimental studies	61
3.2.1	Laboratory studies	61
3.2.2	In-situ Mock-ups.....	63
3.3	Modelling	70
3.3.1	Flow and Energy	70
3.3.2	Degradation processes	71
4	Durability of cementitious materials under surface disposal condition	73
4.1	Cementitious materials in disposal systems	73
4.2	Degradation processes	74
4.2.1	Chemical processes.....	74
4.2.2	Mechanical processes	77
4.2.3	Corrosion	78
4.2.4	Consequences	79
4.3	Modelling the degradation processes	79
4.3.1	Chemical processes.....	79
5	Mobility of RN in degraded concrete	81
5.1	Properties in solution.....	81
5.2	Sorption properties	81
5.2.1	^{14}C	82
5.2.2	^{36}Cl	83
5.2.3	^{129}I	84
5.2.4	^{93}Mo	86
5.2.5	^{99}Tc	87
5.3	Diffusion properties	89
5.3.1	Introduction	89
5.3.2	Diffusion in cracked samples	89
5.3.3	Transport/diffusion in unsaturated conditions	92
5.3.4	Diffusion of the studied radiotracers	93
5.4	Modelling transport of radionuclides in degraded cement	95
6	Concluding remarks	97
	References	98

List of figures

Figure 2-1 Overview of the disposal site during operations and of nearby facilities on the Belgoprocess site (A = Disposal site during operation of the first 20 disposal modules, B = Existing storage building, C = Plant for the production of monoliths, D = Plant for the production of concrete containers).....	15
Figure 2-2 Different types of monoliths (before backfilling with mortar).	16
Figure 2-3 Overview of the disposal facility right before closure.....	16
Figure 2-4 Location and boundaries of the Radiana site (on the Google Earth image).....	17
Figure 2-5 Radiana site geological cross-section with NDF foundation.....	18
Figure 2-6 Plan of the construction stages of the NDF	18
Figure 2-7 Overview of the NDF Stage 1	18
Figure 2-8 Outline of the NDF engineered barrier system	19
Figure 2-9 Main phases, processes and evolution of the barriers of the NDF (WP: waste package) ..	20
Figure 2-10 Schematic of the TVO's (Teollisuuden Voima Oy) VLLW surface disposal concept.....	20
Figure 2-11 TVO VLLW waste packages for eventual disposal in a shallow landfill facility	21
Figure 2-12 Disposal chamber of Dukovany near-surface disposal facility	22
Figure 2-13 CSA disposal facility in Aube (France).....	24
Figure 2-14 Disposal vaults at CSA	24
Figure 2-15 Metallic waste packages in vault.....	25
Figure 2-16 Containers for waste disposal in Lithuanian NSR (INPP, 2025).....	26
Figure 2-17 Main components of the disposal system at Stabatiškė site (INPP, 2025)	27
Figure 2-18 Conceptual model of NSR at Stabatiškė site: top – during operation, Bottom – closure ..	27
Figure 2-19 Saligny site position at local scale	28
Figure 2-20 Schematic cross-section representation of silo during operation	31
Figure 2-21 Schematic cross-section representation of silo after closure	31
Figure 2-22 El Cabril disposal site.....	32
Figure 2-23 Principle design for construction of multi-layer cover of the Bulgarian NDF-Radiana site	34
Figure 2-24 Timeframes considered in the Belgian surface disposal programme and period to which the long-term safety concept applies.....	40
Figure 2-25 Evolution of the radiotoxicity considering that all the radionuclides present in the waste inventory start to decay at the end of the operational phase. The radiotoxicity is calculated by multiplying the activities by the (isotope-specific) dose conversion factor for ingestion.	41
Figure 2-26 Evolution of radiotoxicity and related containment strategy. The radiotoxicity is calculated by multiplying the activities by the (isotope-specific) dose conversion factor for ingestion.	42
Figure 2-27 Barriers and safety functions contributing to containment between closure and ~1000 years.....	42
Figure 2-28 Barriers contributing to the limitation of water infiltration towards the waste after ~1000 years.	43
Figure 2-29 Processes contributing to containment inside monoliths after ~1000 years.....	44

Figure 2-30 Containment outside monoliths after ~1000 years.	44
Figure 2-31 SSCs contribution to the long term safety at CSA	47
Figure 2-32 Disposal module before backfilling with mortar (left) and disposal cell	50
Figure 2-33 Multibarrier system.....	55
Figure 2-34 Packages into a disposal unit	55
Figure 2-35 Disposal units into a vault	56
Figure 2-36 Waste disposal diagram.....	57
Figure 2-37 VLLW Storage.....	57
Figure 2-38 VLLW Cells	57
Figure 3-1 Picture of the Experimental Cover Structure in 1995	63
Figure 3-2 Schematic view of the Experimental Cover Structure.....	63
Figure 3-3 View of the Experimental Cover Structure in 2010	64
Figure 3-4 Measurement of the water content in clay layer of the SEC (10/05/2021)	65
Figure 3-5 General layout of two multilayer systems (Test I and Test II) of the El-Cabril mock-up cover.	67
Figure 3-6 Detailed layering of the two multilayer systems of the El-Cabril mock-up cover.	67
Figure 3-7 Example of sensor types and location in Test I.	68
Figure 3-8 Details of the drainage water collection system of the El-Cabril mock-up cover.	68
Figure 3-9 Layout of the test cover in the Belgian cAt program.	69
Figure 3-10 The two profiles considered in the test cover of the Belgian cAt program.	69
Figure 4-1 Schematic of degradation mechanism effects on cementitious materials and possible impacts	74
Figure 4-2 Schematic diagram illustrating the evolution of pH in hydrated cement pore fluid as a result of cement degradation.	80
Figure 5-1 Evolution of ^{14}C distribution ratios (Rd) vs time on non-carbonated CEM V HCP (a) and carbonated CEM V HCP (b). Initial ^{14}C concentration is $6 \cdot 10^{-8} \text{ mol.L}^{-1}$	83
<i>Figure 5-2 Cl-36 distribution ratio, Rd evolution onto HCP and concrete as a function of sorption contact time and chloride concentration in solution.....</i>	83
<i>Figure 5-3 Distribution coefficients (Rd) determined in this work (solid symbols) or reported in the literature (empty symbols) for the uptake of Cl by HCP in the degradation stage I (or otherwise at pH > 12.8).....</i>	84
<i>Figure 5-4 Rd values for the sorption of I⁻ on hemicarbonate, monosulfate and HS-AFm for a S/L ratio of $5 \cdot 10^{-3} \text{ kg/l}$ and pH 13</i>	84
<i>Figure 5-5 Iodide (left) and Iodate (right) sorption onto C-S-H as a function of C/S ratio and ageing at 25°C.</i>	85
<i>Figure 5-6 Iodide sorption onto HCPs</i>	86
<i>Figure 5-7 Dependency of MoO₄²⁻ retention on C-S-H phases as function of the Ca/Si ratio and time (Mo initial concentration 10. 6 M)</i>	86
<i>Figure 5-8 Kinetics of the molybdate uptake by various model hydration phases in different solutions: ES for “equilibrium solution”, and ACW for “artificial young cement water (pH 13.3)”</i>	87

<i>Figure 5-9 Uptake kinetics for 99 Tc(VII) by HCP made from CEM I and Cebama reference blend</i>	88
<i>Figure 5-10 Effective diffusion coefficient of tritiated water in CEM I and CEM V HCPs for different W/C ratio.....</i>	89
<i>Figure 5-11 Effect of crack width on diffusion coefficient through the crack.</i>	90
<i>Figure 5-12 Comparison of Diffusion coefficient vs. crack width for mortar deformed under bending load</i>	90
<i>Figure 5-13 ³⁶Cl autoradiographies (colorscale) and tomography images (greyscale) for cracked mortar CEM I (left) and mortar CEM V (right)</i>	91
<i>Figure 5-14 ¹³⁷Cs autoradiographies (colorscale) and tomography images (greyscale) for cracked mortar CEM I (left) and mortar CEM V (right)</i>	92
<i>Figure 5-15 – Influence of saturation degree on the relative diffusivity (compared to diffusivity under saturated conditions) in cement-based materials.....</i>	92
<i>Figure 5-16 Comparison of breakthrough curves for carrier-free ³⁶Cl and ¹²⁵I in NRVB equilibrated water</i>	94
<i>Figure 5-17 Simultaneous diffusion of I⁻ and Cs⁺ through hydrated sulphate resisting Portland cement at 30°C from a maximum concentration (side 1) of 10⁻⁴ mol/L for each species. The straight lines indicate steady-state diffusion</i>	94
<i>Figure 5-18 ³⁶Cl autoradiographies for mortars CEM I and CEM V compared to microscopic images</i>	95

List of Tables

Table 2-1. Conceptual multilayer cover layers and their functions (Bulgaria).....	45
Table 2-2 Surface landfill facility barrier materials and their safety functions (Finland)	46
Table 2-3 Multilayer cover materials and safety functions (Lithuania)	48
Table 2-4 Disposal vault components and safety functions (Lithuania).....	49
Table 2-5 Geological system and its safety functions	49
Table 2-6 Safety functions allocated to engineered barriers (Romania)	51
Table 2-7 Safety functions allocated to engineered barriers (Slovenia).....	53
<i>Table 5-1 Iodide Uptake onto Cement Hydrate Phases (% of Total I Added)</i>	85
<i>Table 5-2 Distribution coefficients (Rd) for the uptake of 99 Tc by cement hydration phases in various solutions (ES: equilibrium solution; ACW: artificial young cement water (pH 13.3); CH: saturated portlandite solution (pH 12.3)).</i>	88
<i>Table 5-3 Results of the field investigation (mean value)</i>	90

Abbreviations

ABS	Anti-bathtub system
ACD	Waste Conditioning Workshop
ASL	Above sea level
CIC	Corrosion-induced cracking
DFDSMA	Disposal facility for short-lived low and intermediate level waste in Romania
EBS	Engineered Barrier Systems
FE	Finite element
FoS	Factor of safety
GCL	Geosynthetic Clay Liner
HCP	Hardened Cement Paste
HDPE	High-Density Polyethylene
ISA	Isosaccharinic acid
LAI	Leaf area index
LEM	Limit equilibrium methods
LILW	low and intermediate level
LILW-SL	Low- and intermediate-level short-lived waste
LL&IL	Low level and intermediate level
LLDPE	Linear Low-Density Polyethylene
INPP	Ignalina Nuclear Power Plant
NEK	Krško Nuclear Power Plant
NPP	Nuclear power plant
NDF	National Disposal Facility (in Bulgaria)
NSR	Near-surface Repository
PMF	Probable maximum flood
OIT	Oxidative Induction Time
RCC	Reinforced concrete containers
R&D	Research and Development
RD&D	Research, Development and Demonstration
RN	Radionuclide
RSGE	Gravitational Separation System
SA	Safety Assessment
SL	Short-lived
SLF	Shallow landfill facility
SSCs	System, structures and components
VLLW	Very low-level waste
WAC	Waste Acceptance Criteria
WCB	Water Collection Building

1 Introduction

The objective of (near)-surface radioactive repositories is to safely dispose of low level and intermediate level (LL&IL) short-lived (SL) radioactive waste¹. Such repositories are designed to contain and isolate the radioactive waste sufficiently long such that the radiological impact remains below the dose constraint/dose limit² and/or other regulatory limits for current and future human generations and for non-human biota following national regulations and international recommendations. Contrary to repositories for high-level and/or long-lived waste, many such repositories are in construction, in operation or even closed.

The containment and isolation safety functions are, amongst others, guaranteed by a multi-layer barrier system consisting of an engineered barrier typically containing cementitious components and a multi-layer cover consisting mainly of natural materials. In many concepts, the geological environment such as the underlying aquifer system is also part of the safety concept. The SUDOKU (Near-Surface Disposal Optimization based on Knowledge and Understanding), work package of the EURAD-2 project, focusses on the multi-layer cover and the cementitious barriers.

This state-of-the-art report has two main objectives:

- To set the basis of the scientific understanding of the engineered barriers in a near-surface repository, with focus on the multi-layer cover and the cementitious barriers.
- To compile information on transport of geosphere-mobile radionuclides in degraded cementitious materials.

The report forms also the input towards task 5 in SUDOKU on (integrated) modelling of near-surface disposal systems. Therefore, to find a common basis for the modelling, a description of near-surface disposal concepts for the countries of partners in SUDOKU is given.

The concepts of (near-)surface disposal facilities have been evolved significantly during the last decades (Ormai, 2018) and depend also on requirements, specification and limitations in each country. A more detailed description on recent concepts is given in section 2.2. These examples are limited to those relevant for the SUDOKU consisting of existing or planned near-surface repository of the countries from different partners in SUDOKU. We limit ourselves to those repositories in line with the objective of the SOTA within SUDOKU, i.e. to provide (i) information on the concepts and status of near-surface repositories to the partners within SUDOKU, and (ii) the basis for the definition of models to be developed and applied within SUDOKU. For these near-surface repositories, an overview of the most urgent R&D topics is given as well (section 2.3).

Safety functions attributed to the multilayer cover and the cementitious engineered barriers are discussed in section 2.3 for the different disposal concepts described in section 2.2. A critical factor are the long-lived mobile radionuclides which mobility through the disposal zone depends closely on the properties of these engineered barriers. The water flux passing through the disposal facility is strongly linked to the durability of the engineered barriers and influences the migration of mobile radionuclides (³⁶Cl, ¹⁴C, ⁹⁹Tc, ¹²⁹I,...). The impacts of cracks and steel corrosion products on radionuclide transfer in cementitious barriers are not yet very well characterised and need to be appropriately addressed in safety assessments.

The multi-layer cover limits water infiltration into the underlying cementitious barriers and protects these from (early or fast) degradation. It is thus crucial to understand the important processes (water flow, heat, erosion, stability, amongst others) within different combinations of layers in the multilayer cover

¹ The exact definition of radioactive waste fit for (near)-surface disposal may be (slightly) different between different countries.

² Terminology may be different between countries, assessment period, stage of the repository etc.

structure and the long-term performances of the cover. This understanding is crucial in view of, beside long-term performance, the optimisation of these covers. The main objective within SUDOKU for the multi-layer cover is to improve the current knowledge of processes that control infiltration in multilayer covers for surface disposal facilities and to evaluate cover effectiveness and its long-term performance. This will be achieved by performing in-situ monitoring on under construction and existing multilayer cover mock-ups, complemented by laboratory scale experiments to study separately and under controlled conditions the behaviour of different barriers or combinations of layers that form the cover. Processes governing water infiltration and barrier degradation are described in section 3.1. Overview of existing laboratory experiments and in-situ mock-ups are listed in section 3.2. Modelling approaches for water flow and some degradation processes are described in section 3.3.

Cementitious barriers in a (near-)surface disposal have an important containment safety function. However, it is expected in all national programs that these barriers will degrade with time and thus lose gradually their capacity to contain radionuclides, specifically the geosphere-mobile ones(i.e. with no sorption in geosphere and for which the cement barrier can have a significant impact in terms of migration, that were identified as highly relevant in the case of shallow and surface repositories). The main objective within SUDOKU is to improve the understanding of the cementitious barrier degradation and its effect on the transfer properties of geosphere-mobile radionuclides. An important aspect is the coupling of mechanical constraints and chemical alterations on unreinforced cement-based materials (mortars and concretes) on the behaviour of the cementitious matrix including aggregates. The above-mentioned coupled effect is complemented in the reinforced materials by the effect of corrosion which may result in cracking and diffusion of corrosion products. The migration of geosphere-mobile radionuclides will be studied in degraded samples. Chapter 4 describes chemical and mechanical degradation processes and corrosion. Chapter 5 discusses the transport of radionuclides in intact and degraded cementitious materials and collects information on sorption and diffusion of the mobile radionuclides.

Engineered barriers performances and optimization are identified in the EURAD Roadmap (Beattie et al., 2021) under the following Themes and corresponding Domains:

- **Theme 5 - Disposal facility design and optimization**, Sub-theme 5.1 *Design and develop a disposal system for the national radioactive waste inventory (Design):*
 - o Domain 5.1.3: Based on the *design requirements and safety assessments*, define detailed *specifications for the design of the geotechnical barrier system* (Design specifications, component-scale)
 - o Domain 5.1.4 Develop and establish qualification procedures, especially with regard to manufacturing and testing requirements, as well as *safety demonstration concepts to confirm that structures, systems and components* will perform their allocated safety function(s) in all normal operational, fault and accident conditions identified in the safety case and for the duration of their operational lives (Design qualification);
- **Theme 3 Engineered Barrier Systems (EBS)**, Sub-Theme 3.4 *Confirm integrated EBS system understanding* and identify compatible EBS designs and materials for facilities containing multiple wasteforms (EBS system integration), Domain: 3.4.1 *Confirm complete and integrated EBS system understanding*, including the design of an optimized interface EBS/repository and the understanding of the interaction with the repository nearfield environment (EBS)

2 Near-surface Disposal concepts and safety functions associated to different EBS

2.1 Near-Surface disposal concepts

In general, different types of near-surface disposal concepts can be defined roughly discriminated as vault-types, trench/mould-types and underground near-surface (tens of meters below the soil surface accessible typically via a ramp or shafts)-types (Bergström et al., 2011; Finster and Kamboj, 2011). A summary of the main types is given below:

- Trench. Structures below soil surface without highly engineered cementitious barriers, suitable for e.g. very low radioactive waste. Typically, waste conditioning is limited and engineered barriers consists of compacted clay layers, High-Density Polyethylene (HDPE) and/or geomembranes. During waste emplacement, shelter systems can be placed. Examples are the VLLW repositories in El Cabril (Spain), and CIRES (France). Such types of repositories are already being used for several decades starting in the late 1950s in e.g. India, United States and United Kingdom (Drigg) (Ormai, 2018). Typically, such older repositories do not have engineered systems as drainage systems, liners or covers/caps. Sometimes, they do not meet sufficient safety standards and require remediation.
- Mound (above surface). Waste is emplaced directly on the surface or on a (cementitious) liner; after emplacement a cap covers the waste. Examples are the closed repository at Manch (CSM, France) and the Olkiluoto surface repository (section 2.2.3).
- Surface concrete vaults. Concrete vaults (thick-walled structure) are filled with conditioned waste. During operation, the concrete vaults are either open to the air or protected by a (movable) roof structure. After filling, a concrete cap is placed on the values and at the end of the operational phase and during closure, a (multi-layer) cover is placed to protect the underlying concrete System, structures and components (SSCs) from (rapid) degradation and to limit water infiltration. After closure, it forms a mound or hill in the landscape. The combination of the different engineered barriers prevents, limits or delays water entering the disposed waste, at least for a limited amount of time typically in the order of a few hundreds of years. There are a few of such disposal concepts in operation e.g., Centre de Stockage de l'Aube (France, see section 2.2.5) and El Cabril (Spain, see section 2.2.9). Many are planned or under construction e.g., cAt Dessel (Belgium, see section 2.2.1), Dukovany repository (Czech Republic, see section 2.2.4), Radiana (Bulgaria, see section 2.2.2), and Saligny (Romania, see section 2.2.9).
- Shallow and deeper near-surface concrete vaults. The concrete vaults are constructed below soil surface – the term shallow or deeper is relative as it might differ in different contexts of countries; deeper near-surface concrete repositories are build/planned within maximum a few tens of meters from the soil surface. The “Radon” facilities in eastern Europe and former Soviet Union are of this type (although with a quite simple vault construction). Examples are the (shallow) National repository for LLIL-SL waste in Slovakia (Mochovce) and the (deeper) Rokkoasho-mura repository in Japan. The Vrbina Low and Intermediate-Level Waste (LILW) Repository (Slovenia, see section 2.2.8) is special as the concrete wall form a silo.
- Shallow rock cavern. Waste disposal rooms are excavated in a suitable bedrock and are accessible via a shaft or ramp. Examples of purpose-built (alternatively, existing caverns can be used e.g. from old mines) shallow rock cavern repositories are those in Sweden (adjacent to the Forsmark Nuclear Power Plant) at approximately 50 m below seabed and in Finland (at nuclear power plant sites) although at depths of more than 50 m.

2.2 Status of selected near-surface disposal concepts

The detailed description of different concepts of near-surface disposal is limited to the countries involved in SUDOKU (see introduction). All of them are of the vault-type above the ground level, except the concept of Slovenia which is an underground vault (silo) concept. Many more are in operation, closed or under implementation (Ormai, 2024). The reader is referred to other reports in which descriptions for other countries are available (Bergström et al., 2011; Finster and Kamboj, 2011; Garamszeghy, 2021).

2.2.1 Belgium

In 2006, the federal government opted for surface disposal in the Dessel municipality for the long-term management of short-lived low- and intermediate-level (i.e. category A in the Belgian programme) radioactive waste. The safety case was compiled by the Belgian waste management organization ONDRAF/NIRAS (e.g. NIRAS (2019a; 2019b; 2019c; 2019d)). The license for the construction and operation of the disposal facility was granted to ONDRAF/NIRAS in 2023. Construction is scheduled to start in late 2025 and operation is expected to start in 2029.

The disposal site is located next to the site of Belgoprocess, i.e. close to the buildings where the existing category A waste is currently stored and monoliths will be produced (Figure 2-1). The waste is first emplaced in concrete containers. The voids left in these containers are filled with mortar to form monoliths. Depending on the type of waste (packages or bulk waste), different types of monoliths can be used (Figure 2-2). The actual disposal operations begin with the transport of the monoliths to the disposal modules. Two series of modules are planned. Only the first series consisting of 20 modules (two rows of 10 modules) will be built on the short term.



Figure 2-1 Overview of the disposal site during operations and of nearby facilities on the Belgoprocess site (A = Disposal site during operation of the first 20 disposal modules, B = Existing storage building, C = Plant for the production of monoliths, D = Plant for the production of concrete containers).



Figure 2-2 Different types of monoliths (before backfilling with mortar).

The monoliths are placed in concrete modules (Figure 2-3). Between the double row of modules is a central inspection gallery that provides access to inspection rooms below each module. The modules are built on a sand-cement embankment. After the disposal operations, the modules are covered with a multilayer cover, consisting of an impervious concrete top slab reinforced with fibers and an earth cover. A drainage system in the inspection rooms and gallery ensures that any water that might come into contact with the waste before closure in case of unexpected events (e.g. after an earthquake of exceptional magnitude) can be collected in the 'Water Collection Building' (WCB).



Figure 2-3 Overview of the disposal facility right before closure.

When there is sufficient confidence in the correct functioning of the facility, closure can be initiated. The repository is then brought into its final passive configuration by dismantling the drainage system and WCB and backfilling the inspection rooms and galleries.

2.2.2 Bulgaria

The so-called National Disposal facility (NDF) of Bulgaria will ensure multi-barrier isolation of low and intermediate level (short-lived) radioactive waste (LILW-SL) from the environment for a period of more than 300 years. It will be used to dispose of the radioactive waste generated from existing and future

NPPs. The repository is a vault-type near-surface facility, with the reference design similar to the Spanish El Cabril repository for low and intermediate level radioactive waste (see section 2.2.9).

The NDF is being constructed at the Radiana site, located next to the Kozloduy NPP, at about 200 km to the north of the Capital Sofia. The NDF site is positioned 3.3 km south-east from the town of Kozloduy and about 4.2 km south-west from the right bank of the Danube River. It covers approximately a rectangular area of 46 hectares (Figure 2-4), with maximum dimensions 470 x 1250 m. The Radiana site was selected based on the multi-criteria analysis after comparison with three other potential sites (EIA, 2015; Stefanova, 2024).

Geomorphologically the site is situated between the second (T_2) and sixth (T_6) unflooded loess terraces of the Danube River. The site elevation varies from +40 m to +95 m above sea level. The slope of the original terrain varies between 3% and 12%. The terraces are manifested in the Quaternary loess formations and the underlying consolidated Pliocene clay sediments of the Brusartsi Formation (Figure 2-5).



Figure 2-4 Location and boundaries of the Radiana site (on the Google Earth image)

The NDF consists of sixty-six (66) rectangular reinforced concrete disposal cells, situated on three identical disposal platforms, each with a capacity of twenty-two (22) cells. The cells are arranged in two rows of eleven cells each. The capacity of each disposal platform is 6336 reinforced concrete containers (RCC) of radioactive waste and the total capacity of the facility is 19 008 RCC (von Berlepsch et al., 2016).

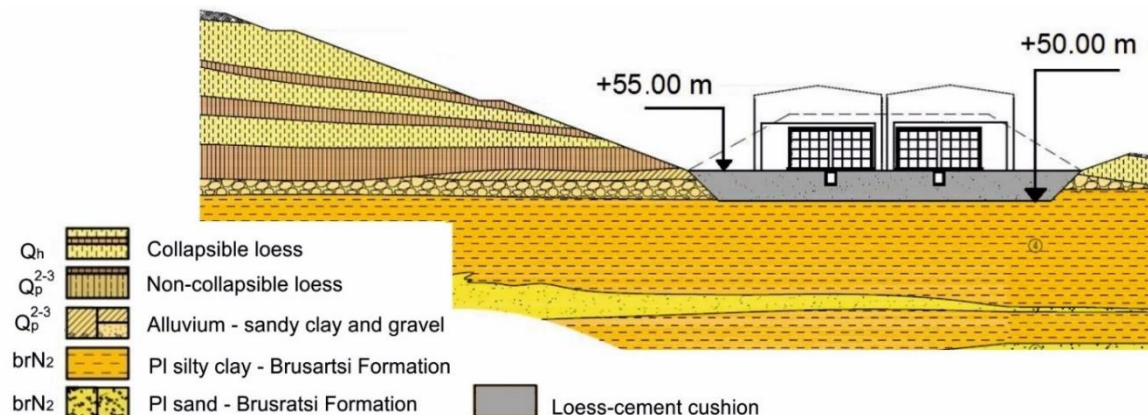


Figure 2-5 Radiana site geological cross-section with NDF foundation

The construction of the facility is planned to be completed in three stages (Figure 2-6). The implementation of the Stage 1 of the facility began in August 2017 and was finalized in the end of 2024 (Figure 2-7). It is expected to start pre-operational activities at the end of 2025 (Stefanova, 2024).

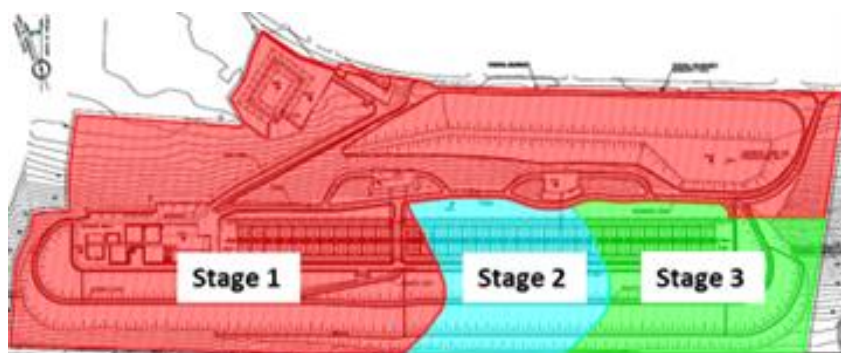


Figure 2-6 Plan of the construction stages of the NDF



Figure 2-7 Overview of the NDF Stage 1

To achieve the safety requirements, the NDF is designed with a system of multiple engineered (Figure 2-8) and natural barriers, which includes:

- **the first engineered barrier** is the waste form itself, forms which are cemented super compacted steel drums.
- **the second engineered barrier** is the RCC in which the waste is placed with the remaining void space being filled with mortar forming a monolithic form.
- **the third engineered barrier** of the disposal facility consists of the disposal cells made of reinforced concrete, their foundation and closure slabs and the filling material.
- **the fourth engineered barrier** consists of the massive loess-cement cushion (with a thickness of 5m) (Nieder-Westermann et al., 2016) and the final multilayer cover (IAEA, 2020).
- **the fifth natural barrier** is provided by the geological media – the vadose zone with at thickness of 24 m and the clayey geo-environment.

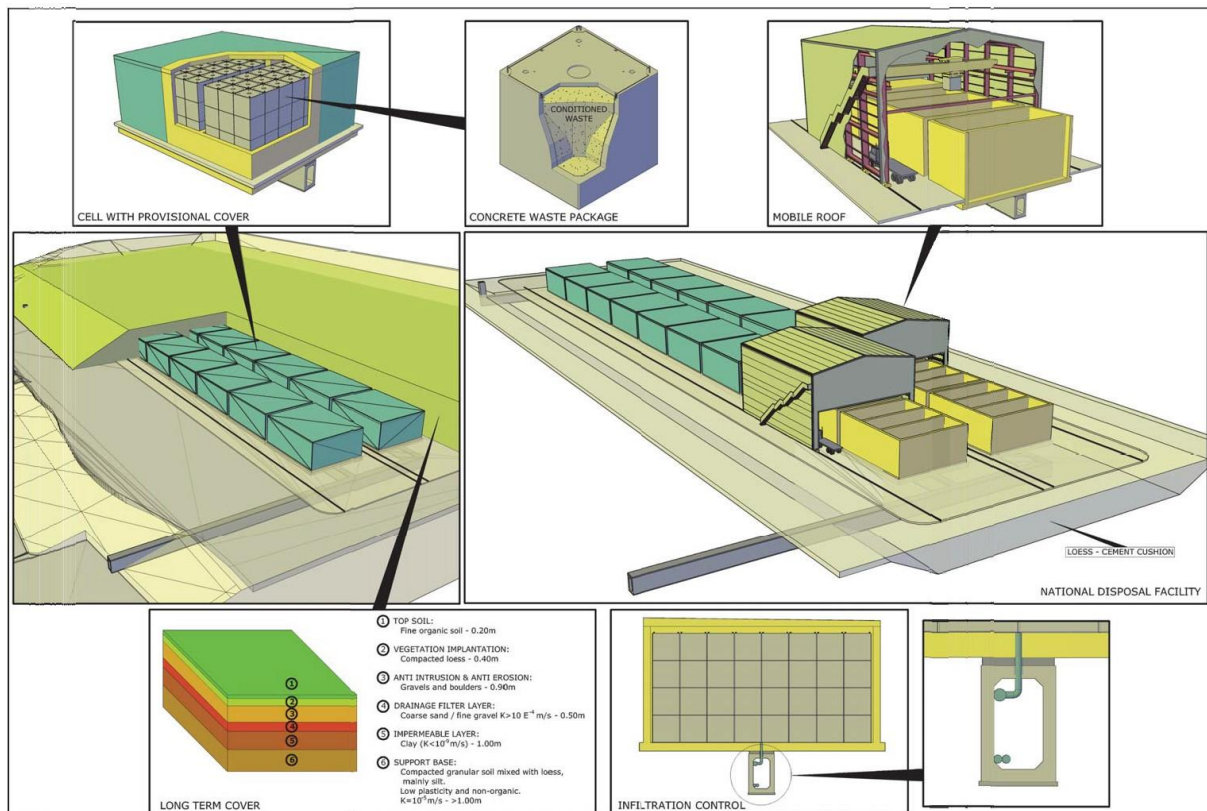


Figure 2-8 Outline of the NDF engineered barrier system

The life cycle of the National Disposal Facility starts with the start of construction and continues until after the end of the Institutional Control Period. It can be subdivided into four major phases, during which the activities at the site and the multiple-barrier containment system will evolve. The phases and their duration are presented in the Figure 2-9 (Biurrun et al., 2016).

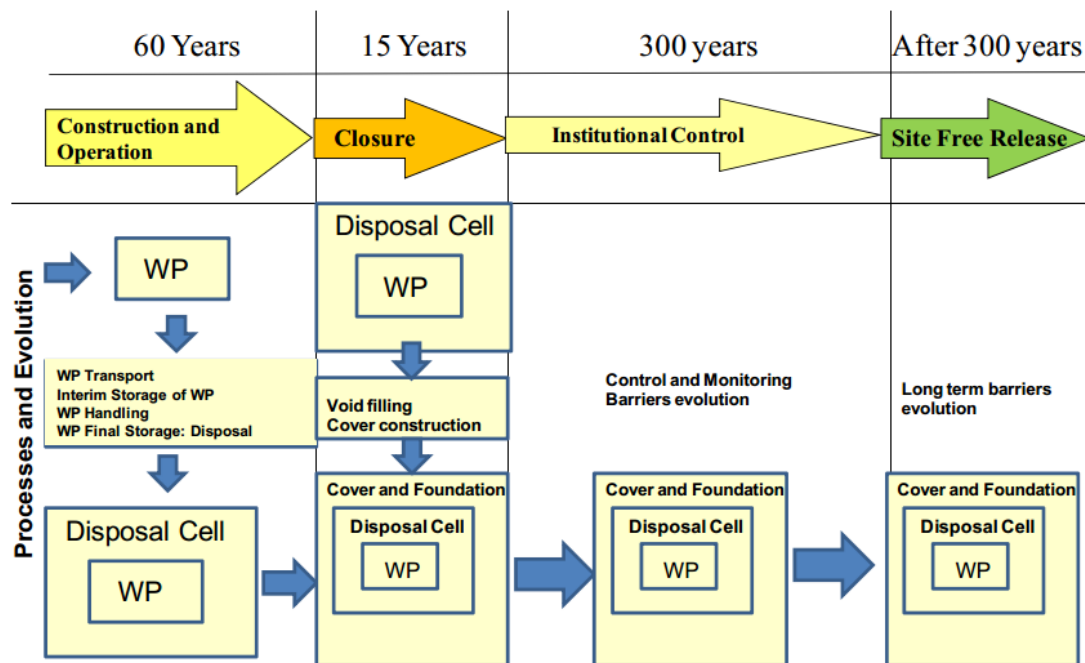


Figure 2-9 Main phases, processes and evolution of the barriers of the NDF (WP: waste package)

2.2.3 Finland

Very low-level waste (VLLW) generated at the Olkiluoto nuclear power plant in Finland will be disposed of in a shallow landfill facility (SLF) located at the nuclear site (Figure 2-10). The selection of the location at the nuclear site involved a comparison of three potential surface locations, alongside an assessment of expanding the existing shallow depth (~50–100 m below sea-level) geological repository currently in use at the site. A comprehensive evaluation of the environmental impact, geological, and hydrogeological conditions, and the potential long-term effects of Finland's climate on the disposal method were completed in 2019 (Keto et al., 2020; TVO, 2021a). Currently, the construction of the SLF is awaiting an operational license from the Finnish Radiation and Nuclear Safety Authority (STUK).

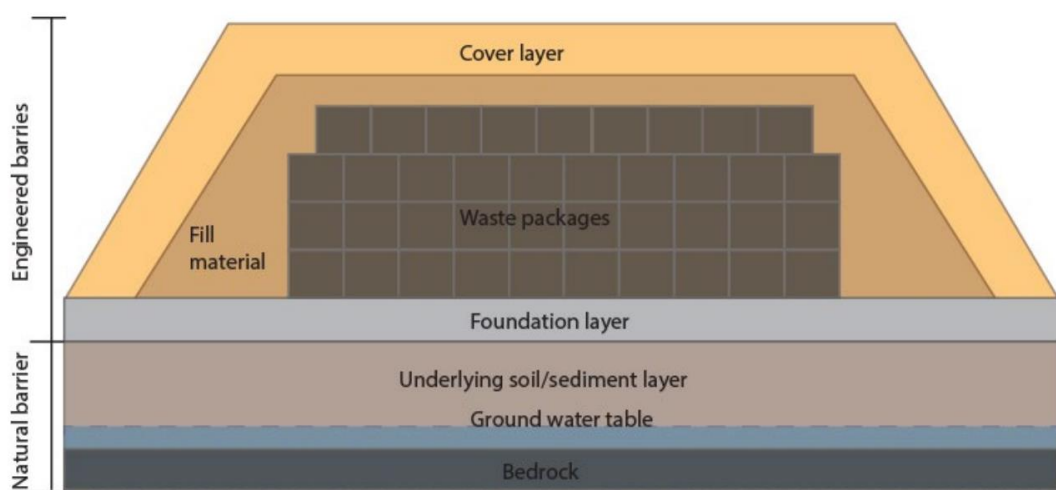


Figure 2-10 Schematic of the TVO's (Teollisuuden Voima Oy) VLLW surface disposal concept (reproduced from Keto et al. (2020)).

The planned SLF will likely be a ‘specialized hazardous material landfill’, located approximately 7 m above sea level, on a part of the nuclear site characterized by moraine till layers, rocks, and gravel. The groundwater at the site is found 1.6 m below the surface, with the bedrock found 5 m below the surface. The repository is designed to accept up to 10,000 m³ of VLLW generated by the Olkiluoto nuclear reactors during their operational period. The wastes will be packed in two types of waste packages: 1 m³ bales wrapped in LDPE film, and standard ISO containers (Figure 2-11) (TVO, 2021a).



Figure 2-11 TVO VLLW waste packages for eventual disposal in a shallow landfill facility (reproduced from TVO (2021b)).

The safety of SLF relies on the combination of natural and engineered barriers. These are divided into foundation layers, and cover layers shown in Figure 2-10. The foundation layer (~1 m) drains water and will contain leachates. Below this, a natural soil layer will distance the repository from regional groundwater. The cover layers (~3.2 m thick) will consist of multiple layers of topsoil, gravel, sand, clay and geotextiles, with a vegetative layer formed on top of the facility (Keto et al., 2021; TVO, 2021a).

The construction of the SLF will begin with the installation of a foundation layer capable of draining water and securely containing the waste. Waste disposal will be conducted in phases, with disposal campaigns planned every 5 to 10 years. During each campaign, the waste accumulated in the interim period will be placed in the repository. At the conclusion of each campaign, the SLF will be temporarily sealed with cover layers. Following the final disposal campaign, the SLF will be permanently sealed, and enter active institutional control for 200–300 years (TVO, 2021a).

2.2.4 Czech Republic

Czech Republic has three operational disposal facilities, each of them designed for dedicated category of radioactive waste: Dukovany repository, an engineered surface facility designed for radioactive waste generated by the country's 6 energetic reactors, Richard repository, located in a former limestone mine and primarily designed for institutional radioactive waste (from medicine, industry, agriculture, and research) and the third repository, located near Jáchymov and dedicated for waste from health, industry and research sectors containing naturally occurring radionuclides. From these three disposal facilities, only Dukovany repository is of interest for SUDOKU experimental and modelling activities.

The Dukovany repository is a surface facility licenced to dispose of the low-level waste generated by the Dukovany and Temelín nuclear power plants. With a disposal capacity of 55,000 m³ (the disposal area occupies a surface of 13,370 m²), Dukovany disposal facility was designed to accommodate all the radioactive waste generated by the NPPs even in case of the extension of their planned lifetimes. The Dukovany disposal facility (Figure 2-12) was put into permanent operation in 1995 (with construction started in 1987) and it is located within the Dukovany NPP complex. It consists of 112 reinforced concrete chambers, with capacity of 1200 drums (200 l) each, arranged in four rows, the first row being filled in 2023.



Figure 2-12 Disposal chamber of Dukovany near-surface disposal facility

After a disposal chamber is filled with waste drums (200 l steel barrels containing radioactive waste conditioned in cement, bitumen or SIAL® matrix) and backfilled with mortar, it is closed by a concrete panel of 0.5 m thick and covered by a waterproof layer made of asphalt. Later, grout application is foreseen to improve the stability and retention capacity of the system. A final cover made of a layer of clay, geotextile and layers of draining materials will be used to close the repository when all disposal chambers will be filled (Konopaskova, 1997).

The safety of Dukovany disposal facility relies both on the natural (the upper unsaturated sandy clay layer) and engineered barriers, and an institutional control of 300 years after closure of the repository (Horyna, 2000).

The engineered barriers mainly comprise of the waste form, waste packages (steel drums), concrete disposal chambers and backfill, drainage system, the concrete slab with the waterproof layer of asphalt (used to close and seal the disposal chambers after filling) and the final cover.

The safety assessment for normal evolution scenario of Dukovany repository assumes that the drums used for waste packaging would last for approximately 50-100 years (Horyna, 2000). After this period the waste form is assumed to be attacked on its surface to produce a degraded waste which if contacted by water would increase the release of radionuclides by an order of magnitude. The release scenario for normal operation allows the water penetration through the cover, water entering in the disposal cell, damaging of the waste drum, leaching of a portion of the radionuclides that are released through the concrete foundation of the disposal vault to the environment (Konopaskova, 1997).

2.2.5 France

Operational disposal solutions exist for very low-level waste (VLLW) and for low- and intermediate-level short-lived waste (LILW-SL). Waste belonging to these categories are emplaced in surface disposal facilities designed in view of their specific radioactivity levels and half-lives. Two surface disposal facilities are currently in operation:

- (i) Cires which is a VLLW disposal facility, and also hosts facilities for the management of non-electronuclear waste (produced outside of NPPs and large nuclear research

facilities), for grouping, sorting, and temporary storing waste. It is located in Morvilliers, in the Aube district.

(ii) CSA which is a short-lived low or intermediate-level radioactive waste disposal facility. It is located in Soulaines-Dhuys and Ville aux Bois (department of Aube), situated about 200 km southeast of Paris.

The CSM facility, which is the first disposal facility built in France for low- and intermediate-level radioactive waste is currently under post-closure monitoring stage. It is located at the very tip of the Cotentin peninsula in Normandy.

The CSA concept will be specifically described in this document. The disposal design benefited from the technical experience accumulated at the first repository, the CSM, where several concepts were tested during the operational phase of the facility life.

CSA concept is based on gradual construction of linear disposal concrete vaults, located above the water table, with a well-identified single water outlet and for a given waste inventory; its flexible architecture and modular configuration allows integration of optimized design features into the reference concept.

The waste disposed at CSA is conditioned in metal and concrete packages which are placed in reinforced concrete repository structures of 25 metres square and 8 metres high. Once they are filled, the structures are closed with a concrete slab and then sealed with an impermeable coat. At the end of operations, a cap formed mainly of clay will be placed over the structures to ensure long-term waste containment. The CSA waste disposal facility will then be monitored for 300 years.

The CSA is situated in the department of Aube on the territory of the communes of Soulaines-Dhuys and Ville aux Bois. The facility borders the northern edge of a 3 000 ha forest, mainly belonging to Soulaines-Dhuys. The CSA covers 95 hectares, 30 of which are dedicated for disposal.

The repository site has been selected in accordance with the requirements of the Safety Authority guidelines. The site is a sedimentary rock outcrop consisting of a semi-permeable layer (the white sands of Aptian) covering an impermeable layer (clays of Aptian). The topography of the site exhibits a gentle slope oriented towards the creek named “Noues d'Amance” draining all the underground flows of the zone.

This rather simple geological configuration facilitates Andra's modelling work in terms of water circulation, localized outlets and radionuclide transfer.

The repository is designed to dispose of one million cubic meters of short-lived low or intermediate-level radioactive waste. Since its launch in 1992, over 393 000 waste packages have been disposed of in the CSA (data of December 2018). Andra can also condition certain waste packages on-site before their disposal, compacting 200 L drums and grouting metal containers of 5 or 10 m³ filled with bulk waste.

Disposal vaults are constructed in batches as operations progress. A batch corresponds to the construction of several rows of vaults (4 to 5 vaults in general per row). Thus, it is possible to anticipate the time and the number of new vaults to be constructed according to the forecast of expected deliveries and to implement, as the case may be, new technologies elaborated on the basis of operational feedback and the acquisition of new technical and scientific knowledge.



Figure 2-13 CSA disposal facility in Aube (France)



Figure 2-14 Disposal vaults at CSA

The CSA facilities include:

- Disposal zone - vaults under construction, vaults in operation and closed vaults;
- Pre-disposal area comprising of:
 - The Waste Conditioning Workshop (ACD) regrouping the industrial processes of compaction and grouting cited above, and a facility dedicated to the quality monitoring of packages;
 - A temporary storage for waste packages (transit building);
 - Other "upstream" facilities necessary for the proper functioning of the CSA such as a service building (cloakrooms, laboratory, etc.), the mechanical building, the warehouse, etc.;
 - Empty container storage area and vehicle parking;
- Guardhouse, the public information building, administrative buildings;
- Storm basin
- Weather station.

A special feature of the CSA is the underground Gravitational Separation System (RSGE) similar to that in service at the CSM. This drainage network aims to collect potentially radioactive liquid seepage that comes mainly from meteoric water infiltrated into the disposal vaults that may have been in contact with

waste packages. Such potentially contaminated water is collected via the pipeline system located in underground tunnels that pass under the vaults. This water is retrieved for control and testing. In addition, two tanks of 250 m³ each able to collect large quantities of water in the monitoring phase are connected to and located under the pipeline system.

Another network of water collection recovers the effluents produced in the technical buildings in the regulated area that are likely to be contaminated (so-called "A effluents"). The water is discharged into the storm basin after radiological control to verify their compliance with authorized release thresholds.

Active liquids that may be present in the waste drums at the time of compaction are not discharged into the environment. Called "radioactive liquid effluents B", they are subject to specialised collection procedure and disposal at an appropriate facility.

Aside these specific drainage and water collection systems, the site is equipped with the standard networks for the management of wastewater and rainwater.

Two types of disposal vaults are used in the CSA:

- So called "perishable" metallic waste packages are disposed of in vaults that are backfilled, layer -by-layer with special concrete;
- Durable waste packages in concrete are disposed of in stacks; when full, such vaults are backfilled by gravel.



Figure 2-15 Metallic waste packages in vault

One row of custom-made vaults is dedicated to the disposal of reactor vessel heads that come from the EDF NPPs - these are large-size waste packages and do not correspond to the standard package dimensions. These vaults are smaller in size and accommodate 12 "vessel head" packages each.

Other "non standard" waste packages, like lateral neutronic shields from Superphénix reactor, were disposed in standard concrete vaults.

The CSA has been operating since January 1992; it has taken over the disposal activity from the La Manche disposal facility CSM where operations ceased in June 1994. Given its currently available capacity and forecast of deliveries, the CSA could be operational for around 50-80 years.

After closure final cap will be built over the vaults, to limit the infiltration of meteoric waters into the vaults. This cover will be installed after backfilling the spaces between the vaults at the end of the operational phase. The detailed design of the final cap is not yet defined.

Currently, the reference concept provides for a composite layer of natural materials (clay, sand...) of an average thickness of 4 m covering the vaults. Following the closure, CSA will enter a 300-year monitoring period.

The waste disposed of in the CSA is classified as LILW-SL, containing mainly radionuclides with half-life of less than 31 years, and the radiological impact of short-lived radioactive waste is negligible after 300 years. However, the LILW-SL waste may also contain long-lived radionuclides in very small quantities. The waste acceptance criteria limit the maximum allowed activity of long-lived radionuclides (C-14, Cl-36 etc.) to ensure a negligible impact in the future.

A CSA disposal vault is intended to receive radioactive waste packaged in containers that can be very different from each other. These packages may have a cylindrical, cubic or parallelepiped shape, variable dimensions (16 types of packages are accepted by Andra to be disposed of in CSA), different container compositions (“Concrete” container is qualified as sustainable or durable whilst “metallic” container is considered perishable) and also different diverse types of emplaced waste (heterogeneous waste, homogeneous waste, steel, concrete, plastic, resin, etc.). Perishable packages consist of metallic drums (100, 200, 450 and 870 l) and boxes (and 10 m³, metal ingots from fusion of metallic waste), while non-perishable packages are considered the various types of concrete drums such as 5 and 10 m³ concrete boxes.

Both in the perishable or non-perishable packages, the homogeneous or heterogeneous waste is always grouted using mortar.

2.2.6 Lithuania

Short-lived low and intermediate level radioactive waste (LILW) in Lithuania will be disposed of in a near-surface repository (NSR) located at Stabatiškė site which is about 1 km south from the Ignalina nuclear power plant (INPP). The site for the NSR was selected from three sites after evaluation of potential impact to environment (RATA, 2007). Investigations of geological structures and their characteristics, hydro-geological and geotechnical properties of the site soils, development of Technical Design, Safety Analysis Report and Repository Monitoring Programme were completed in 2017. The NSR is currently under construction.

The Stabatiškė site is characterized by the moraine till deposits. The upper part contains sporadically distributed sand lenses, however, going down to depth of several meters, permeability is getting lower. The first semi-confined aquifer lies at depth of about 8 meters.

The NSR at Stabatiškė site will be a modular type facility consisting of above ground reinforced concrete vaults arranged in 3 groups of 12 vaults and capable to accommodate up to 100 000 m³ of conditioned radioactive waste generated during operation and decommissioning of INPP. Two types of waste packages are foreseen (see Figure 2-16):

- Concrete containers with either grouted pellets from super compaction or large-size (metallic) items, and
- Concrete containers with grouted drums with cemented spent ion-exchange resins.



Figure 2-16 Containers for waste disposal in Lithuanian NSR (INPP, 2025)

The disposal vaults will be built in three stages, group by group. The vaults in operation will be covered by a shelter to protect the vaults and containers from unfavourable weather conditions. Containers in

the vault will be loaded in layers. After loading of a layer of containers, they will be backfilled with cement-based material. Four layers of containers with backfill interlayers can be disposed of in the vault. After the vault is fully backfilled, it is covered by a reinforced concrete slab. When all 12 vaults of the group are loaded, the shelter will be removed and a final multilayer cover of several layers of clay, gravel, sand, pebble and vegetative ground will be formed over the closed vault group. The total thickness of the cover will be about 6 meters.

Safety of the disposed waste will be ensured by a multiple barrier system as follows: the waste matrix, container, backfill, concrete vault, low permeable embedding clay and other capping layers. The main components of the disposal system are presented in Figure 2-17 and the concept of the NSR during operation and after closure is provided in Figure 2-18.

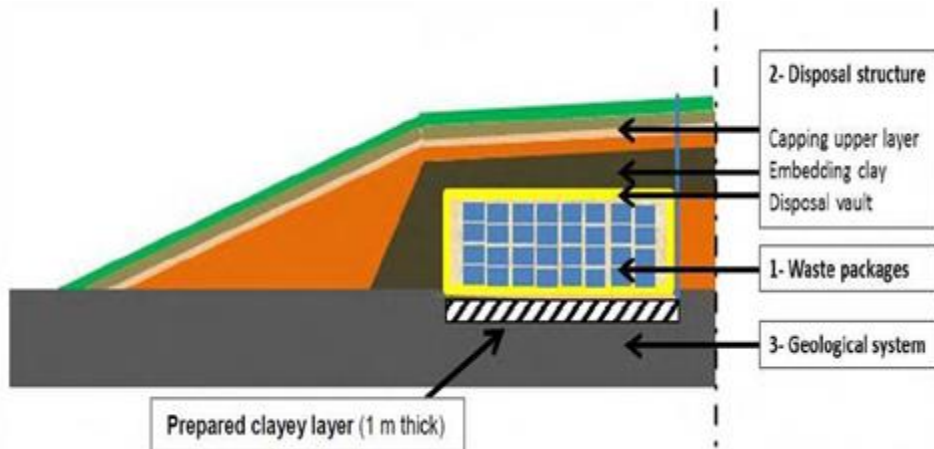


Figure 2-17 Main components of the disposal system at Stabatiškė site (INPP, 2025)

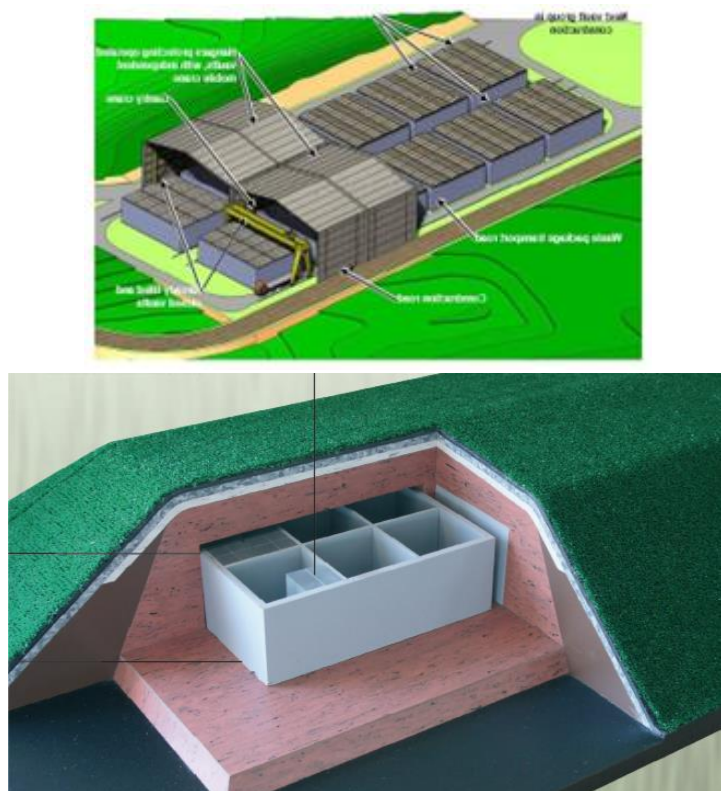


Figure 2-18 Conceptual model of NSR at Stabatiškė site: top – during operation, Bottom – closure

It is foreseen that operation of the NSR will be about 20 years (INPP, 2025). After repository closure, 100 years of the active institutional control will follow with subsequent 200 years of the passive institutional control.

2.2.7 Romania

The disposal concept adopted in Romania for the long-term management of short-lived low- and intermediate-level radioactive waste (SL-LILW) is a near-surface facility with multiple barriers.

Following extensive geological, hydrological, seismological, physical, and chemical investigations carried out during 1992-2006, Saligny site has been declared the preferred site to host the disposal facility. Saligny site is located on Bogdaproste hill (elevation of around 70 meters above the Black Sea level), in the exclusion area of Cernavoda NPP (Figure 2-19). The disposal site is located at around 1.5 km north-east from the Danube-Black Sea Canal and around 4.5 km east from Danube River. At around 3.5 km north from Bogdaproste hill there is the Tibrin Valley, and at 70 km east there is the Black Sea.

From the lithological point of view the Saligny site is composed of four main units: Unit A formed by loess deposits, Unit B formed by red clay deposits, Unit C formed by Aptian deposits and Unit D that is a Carbonate complex (Slavoaca, 2011). Unit A is divided into two layers: silty loess (A1) and clayey loess (A2). According to the position into the unsaturated or saturated zone, the Aptian deposits are divided into unit C1 (unsaturated) and C2 (saturated). The Carbonate complex (Unit D) is formed by oolitic and bioclastic limestones. This unit is a regional aquifer (Beriasian) which is in direct connection with Danube River and Danube-Black Sea Channel (Slavoaca, 2011). Consequently, it is considered the main route for the radionuclides released from unsaturated zone to enter into the biosphere



Figure 2-19 Saligny site position at local scale

The disposal facility for short-lived low and intermediate level waste (DFDSMA) is a multi-barrier facility with disposal cells, designed based on international existing and demonstrated good practices on design, construction and operation of surface repositories (Centre de l'Aube, El Cabril, Dukovany). The disposal facility consists of total 64 disposal cells that will be constructed in stages (8 disposal cells/stage). Conditioned SL-LILW are overpacked in parallelepiped disposal containers (modules) prefabricated from reinforced concrete, ensuring both the long-term radionuclides retention as well as the possibility of extraction and replacement if during operational or active institutional control unexpected releases are detected.

In 2023, the Romanian waste management organization (Nuclear and Radioactive Waste Agency – ANDR) obtained the approval of the a Zonal Urban Plan (PUZ³) and the Local Urban Regulation (RLU⁴) for DFDSMA (Saligny Local Council decision no. 2/16.01.2023). The documentation required by the regulatory body (National Commission for Nuclear Activities Control - CNCAN) for granting the siting and designing licences for DFDSMA (Feasibility Study, Safety Assessment Report, Environmental Impact Report, preliminary WAC etc.) will be updated under a 36 months contract that ANDR recently signed with a private company.

According to the national strategy the facility should be commenced in 2028, but delays are expected.

2.2.8 Slovenia

The Vrbina Low and Intermediate-Level Waste (LILW) Repository in Slovenia is a near-surface disposal facility designed to ensure the long-term isolation of short-lived low- and intermediate-level radioactive waste. The repository is designed to accommodate half of the operational LILW waste from Krško Nuclear Power Plant (NEK), along with all institutional radioactive waste from Slovenia. NEK is a jointly owned facility, with equal ownership (50:50) between Slovenia and Croatia.

The selection of a below-ground silo concept was based on an in-depth comparative analysis, where this configuration provided the highest level of safety, robustness, and feasibility. The silo-based design offers increased resistance to external hazards, such as seismic activity and flooding from the Sava River, while also controlling water infiltration and minimizing radionuclide migration (Duhovnik, 2022). This approach aligns with international best practices, as demonstrated by similar disposal facilities in Sweden (Forsmark), Finland (Olkiluoto), and Japan (Rokkasho), which also use silo-like structures (ARAO, 2019a).

The geological conditions at the Vrbina site play a crucial role in ensuring the safety and long-term stability of the disposal system. The repository is situated within an alluvial plain, characterized by highly permeable upper Quaternary deposits, which exhibit a hydraulic conductivity of approximately 3×10^{-4} m/s. Beneath this, a lower-permeability Plioquaternary layer provides a natural hydraulic barrier with a conductivity of about 10^{-7} m/s at the bottom of the silo (ARAO, 2018). This contrast in permeability ensures that water flow into the disposal zone remains limited, reducing the risk of radionuclide transport. The water table is located relatively shallow, necessitating design adaptations to prevent groundwater intrusion into the disposal area.

The Sava River, flowing south of the repository site, presents a potential flood hazard, particularly during extreme hydrological events. However, hydraulic assessments confirmed that even under probable maximum flood (PMF) conditions, the repository remains protected due to its elevated construction on an anti-flood plateau. Additionally, the region experiences seismic activity, requiring the repository to be designed to withstand ground accelerations of 0.2g, as determined by assessments aligned with those for the nearby NEK (ARAO, 2018).

The silo structure consists of a primary and secondary wall, both crucial to the repository's containment strategy. The primary wall, with a thickness of 1.5 meters, functions as a temporary structural support during excavation and is not classified as a nuclear safety component. The secondary wall, forming the main containment structure, is 1 meter thick and is constructed from reinforced concrete. The bottom

³ [Environmental Report](#) for Zoning Urban Plan (PUZ) (in Romanian) : PUZ is a crucial urban planning document that defines the specific rules and regulations for the development and construction of the radioactive waste repository on that site (Saligny). It's essentially the detailed zoning plan for the facility, which must be approved by the local city council.

It outlines key technical and environmental parameters, including Land Use and Urban Indicators, Infrastructure and Utilities (such as access roads, internal networks, and utility connections, to support the repository's operations).

Obtaining the PUZ is a necessary step in the licensing and authorization process for the facility. It provides the legal framework for the construction and subsequent operation of the repository, as required by Romanian and international nuclear safety regulations.

⁴ **Local Urban Regulation (RLU)** refers to the specific set of legally binding rules that complement the **Zonal Urban Plan (PUZ)**. The RLU provides the detailed, technical, and regulatory framework for how the land within the PUZ's designated area can be used and developed.

structure of the silo is designed as an arched or inverted dome shape to ensure stability against full hydrostatic uplift and ground pressure. In its critical, thinnest section, the floor arch has a thickness of approximately 100 cm and is constructed above a previously installed layer of foundation concrete. (Sinur and Duhovnik, 2020). The bottom of the silo will be a massive reinforced concrete structure, incorporating a permanent drainage basin for collecting any infiltrating water during the operational phase. The silo has an internal diameter of 27.3 meters and a depth of 56 meters, with a total disposal capacity of approximately 12,157 m³ of LILW, corresponding to 990 N2d disposal containers, arranged in 10 layers. Each N2d disposal container has external dimensions of 1.95 m × 1.95 m × 3.30 m, providing a net internal volume of 6.31 m³ and a maximum total mass of 40 tons (ARAO, 2019b). The container walls, made from reinforced concrete, are nominally 20 cm thick, offering additional mechanical and chemical resistance to degradation over time. The proposed lifting technique avoids the possibility of tensile stress in the disposal container concrete when it is being lowered into silo with gantry crane.

The placement of containers within the silo follows a controlled process to maintain structural integrity and limit void spaces, reducing the potential for groundwater accumulation. Once the containers are positioned, the voids between them are filled with backfilling material, which consists of a cementitious grout mixture designed to enhance stability and limit water movement within the disposal zone. Inside the disposal containers, a specialized mortar mix is used to encapsulate radioactive waste, further minimizing the potential for radionuclide migration.

During the operational phase, any water that infiltrates the silo will be collected and managed using a drainage system. This system includes a drainage layer at the bottom of the silo, where water seepage is directed into a controlled collection pool. The collected water will be regularly monitored for radiological contamination before being either pumped out for treatment or safely discharged. This active drainage will remain in operation until the repository is fully sealed.

The final sealing process of the repository includes placing a reinforced concrete slab over the disposal area, followed by a thick clay layer that functions as a low-permeability cap to prevent water infiltration. Above this, a final protective layer of locally sourced soil will be added, ensuring long-term structural stability and natural integration with the surrounding environment. This multi-layered barrier system effectively isolates the waste, forming a monolithic containment structure over time.

The repository will operate in several phases. The construction phase, which began in 2023, includes site preparation, infrastructure development, and installation of security measures. By the end of 2027, the repository will enter a trial operation phase, where final safety assessments will be conducted before full-scale disposal begins in 2028. The repository will continue to accept waste until 2030, after which it will enter a standby phase until 2049 (Mechora and Virsek, 2023). During the standby period, no new waste will be disposed of, but monitoring and maintenance will continue in preparation for the second phase of disposal operations, expected to begin in 2050. This phase will accommodate LILW from the decommissioning of the Krško NPP and its remaining operational LILW, with disposal continuing until 2058 followed by decommissioning of its non-disposal parts. In 2059 the repository will be sealed permanently, transitioning into the post-closure phase. Following closure, the repository will experience gradual water saturation, as groundwater infiltrates the silo over time. However, due to the low permeability of the surrounding geological formations, water ingress will be slow and controlled, ensuring that the chemical conditions within the silo remain stable. The cementitious barriers, grout backfill, and engineered containment system will significantly limit radionuclide migration, keeping potential releases well within regulatory safety limits. The post-closure monitoring period is planned to last 300 years, consisting of 50 years of active monitoring, where water chemistry and structural stability will be closely observed, followed by 250 years of passive monitoring (ARAO, 2019a). After this period, institutional control will be lifted, and the site will be designated for unrestricted use, ensuring that it poses no hazard to future generations.

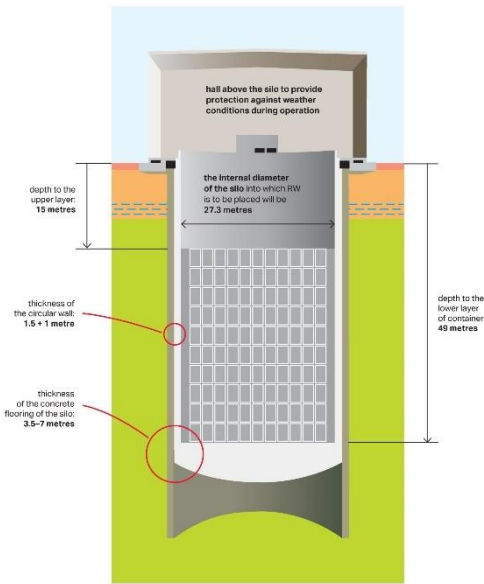


Figure 2-20 Schematic cross-section representation of silo during operation
[\[https://arao.si/en/nacrtovanje-odlagaliska-nsrao/\]](https://arao.si/en/nacrtovanje-odlagaliska-nsrao/)

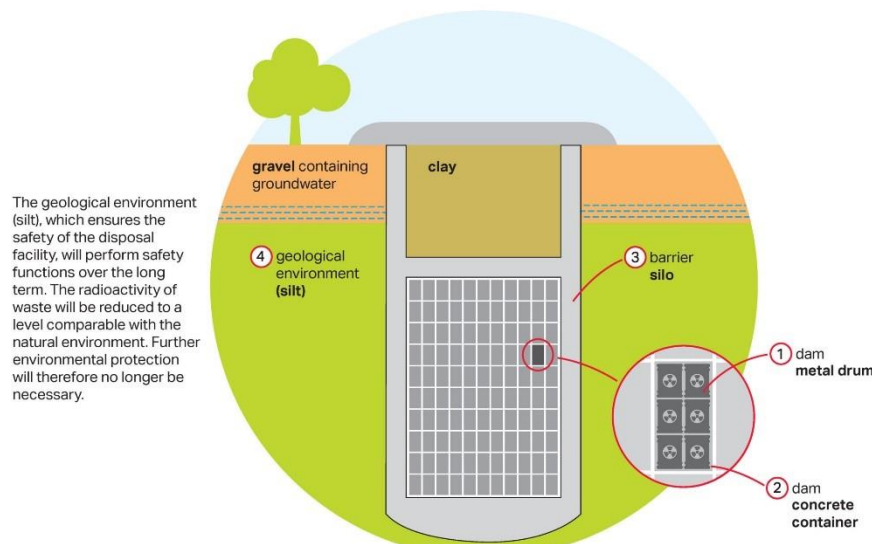


Figure 2-21 Schematic cross-section representation of silo after closure [\[https://arao.si/en/nacrtovanje-odlagaliska-nsrao/\]](https://arao.si/en/nacrtovanje-odlagaliska-nsrao/)

2.2.9 Spain

The “Centro de Almacenamiento de residuos radiactivos sólidos de Sierra Albariana”, more commonly referred to as “El Cabril”, is the Spanish National repository for low and intermediate activity and short-lived radioactive waste (LILW) and very low activity radioactive waste (VLLW). Its main objective is the definitive disposal of these types of wastes in solid form. According to the goals approved by the Seventh General Radioactive Waste Plan, approved by the Government 27 December 2023, it is intended that El Cabril centre will remain operative to accommodate all the LILW and VLLW being generated by the operation and decommissioning of existing nuclear and radioactive installations in the country.

“El Cabril” (Figure 2-22) also has facilities for waste treatment and conditioning, quality verification and characterization, interim storage, and other ancillary equipment. It is in the province of Córdoba in the Southern part of Spain. El Cabril LILW disposal site, in operation since 1992, belongs to the near-surface type of disposal facilities with engineered barriers. It is based on the use of concrete barriers and disposal units. In October 2008, the operation of a new complementary disposal facility for VLLW started at the site which is based on clay and HDPE barriers and different types of disposal units.

“El Cabril” centre has a total surface area of 35 ha. Auxiliary buildings and the LILW disposal area occupy 20 ha, while the remainder is occupied by the VLLW disposal area. The facility has an internal capacity for LILW of 100.000 m³ (corresponding to 50.000 m³ of primary conditioned waste packages, depending on the waste types) and, for VLLW of 130.000 m³.

The disposal area is divided into three platforms, the North and South for LILW, and the East for VLLW. The structures or disposal cells, in which the disposal units are placed, will be buried under a cover layer at the end of the exploitation phase.

The materials disposed of at El Cabril are LILW-SL whose activity is mainly due to the presence of beta or gamma emitting radionuclides of short half-life (less than 30 years) and whose content in long-lived radionuclides is very low and limited by the levels established in the Waste Acceptance Criteria associated to the Exploitation Authorization. The disposal unit-type LILW (LILW-DU) is defined as a set made up by a purposely designed overpack, the LILW conditioned inside primary packages and the blocking/filling material that complies with the limitations of mass activity, requirements and technical conditions established. These units are disposed of in the concrete vaults of the North and South platforms.

Additionally, within LILW it can be distinguished as a subset called very low activity radioactive waste (VLLW). It consists of solid or solidified material that is non-suitable for clearance. If its radioactive content does not exceed a defined limit value in the waste acceptance criteria and it will be disposed of in the disposal units on the East platform of the facility. The disposal-unit-type VLLW (VLLW-DU) is a set consisting of the package, very low activity radioactive waste and stabilization or filling material. Several configurations are used, the most usual are metallic packages that are about 2 m³ boxes, 0,220 m³ drums or 1 m³ big-bags.



Figure 2-22 El Cabril disposal site

2.3 R&D aspects

2.3.1 Belgium

The RD&D programme of ONDRAF/NIRAS aims to address unresolved issues, confirm key hypotheses and parameters from the safety assessment (SA), and further optimise safety. The following RD&D activities are particularly relevant to SUDOKU:

- Measurements of sorption of critical radionuclides on hardened cement paste (HCP) and calcite (and/or degraded cement) to:
 - Verify the validity of the (ranges of) sorption values used in the SA and, if possible, reduce uncertainties; and
 - Evaluate the effect of chlorides and isosaccharinic acid (ISA as a degradation product of cellulose) on this sorption (to investigate the disposability of chloride- and cellulose-containing waste);
- The backfill mortar of the monoliths is a mortar based on a CEM III/C and silica fume. A research programme to quantify the evolution of this binder, its solid phases and its pore water - which can influence the sorption of radionuclides - is in progress.
- As part of the demonstration programme:
 - A damage pattern with cracks was observed on test walls of the modules, which experts believe is probably due to shrinkage. This will be specifically addressed during realisation of the actual modules by a better post-treatment of the concrete;
 - Particular attention will be paid to compliance with the minimum (nominal) reinforcement cover of 40 mm which was not respected everywhere in the demonstration test. The tolerance on the concrete cover will also be re-examined; and
 - Natural concrete carbonation of the walls of the demonstration test will be monitored.
- A fiber-reinforced concrete that allows the impervious top slab placed above the disposal module to be realised with the intended performance has been developed and characterised. Large-scale feasibility will be tested in a multilayer test cover (section 3.2.2.3).
- Specific safety functions/hypotheses and essential parameters of the SA will be followed up. If observations deviate from what is expected, their importance/impact will be evaluated, e.g.:
 - The limitation of water infiltration through the soil layers of the test cover will be evaluated. As part of further optimisation, the feasibility and performance of two alternative cover profiles will be evaluated (section 3.2.2.3).
 - The stability of the earth cover will be evaluated by topographical measurements and physical monitoring. The measurement results will be compared with expected values.
 - The resistance of the earth cover and of concrete components to earthquakes will be evaluated by monitoring the in-situ seismological data and comparing them with design assumptions.
 - Test monoliths and specimens kept in representative conditions will be used to monitor the carbonation front up to the beginning of the closure phase to confirm the assumed carbonation rate, which strongly determines the expected service life of concrete components. It will be verified if no through-going cracks are formed, that no formation of thaumasite and secondary ettringite occurs, and that the corrosion potential and deformations and stresses due to loads and ageing are as expected.

The use of fiber-reinforced concrete for the concrete containers (instead of rebars) could further increase the durability of the monoliths and the overall robustness of the disposal system, because carbonation

and incipient fiber corrosion do not lead to macro-cracks in such concrete and a reinforcement consisting of fibers theoretically possesses a higher resistance to earthquakes. The feasibility of producing containers with the intended performance from fiber-reinforced concrete is being investigated.

2.3.2 Bulgaria

Two main R&D activities are ongoing on the near-surface disposal

Multi-layer test cover

A conceptual multilayer cover for the final closure of the LILW-SL disposal at the Radiana site has been developed within the NDF Technical Design. The layout of the conceptual final cover is shown on Figure 2-23 (IAEA, 2020). The cover includes the three main barriers: *biological, drainage and capillary*, and *impermeable*. These barriers are ensured by seven earth layers (including the support and drainage base layer) and three synthetic sheets. 1-D and 2-D numerical flow models have been developed in order to assess the main functional requirements of the multilayer cover as follows:

- water infiltration through the multilayer cover (i.e. water outflow at the bottom of the cover) to be less than $1.5 \text{ L/m}^2/\text{y}$;
- this infiltration rate shall be kept at least for 300 years, i.e. the durability, stability and integrity of the cover must be ensured for this period.

A field multi-layer test cover is designed considering the requirements of the final multilayer cover of the near-surface disposal facility at the Radiana site. The construction of this test cover will be completed in the next couple of years. The monitoring period will continue at least 15 years.

Cementitious barrier degradation

During the NDF construction (Stage 1) a real size test disposal cell was built at the Radiana site which will be used for monitoring of long-term degradation of the reinforced concrete structure.

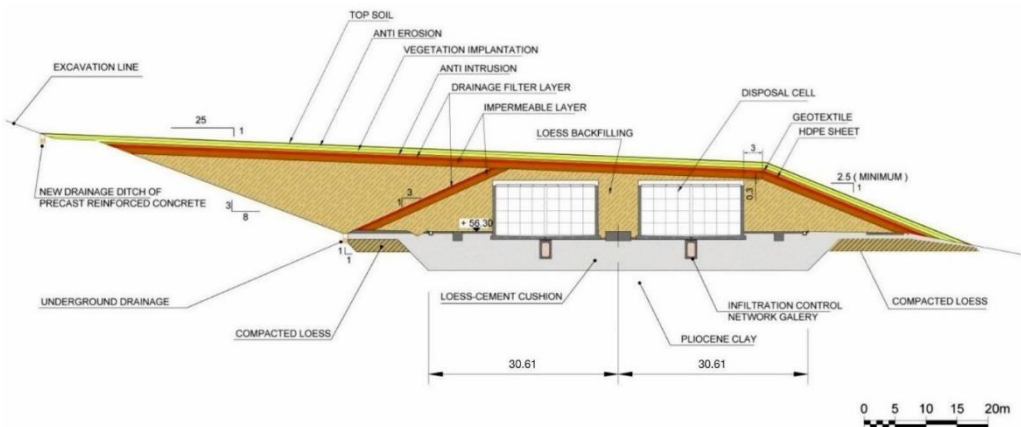


Figure 2-23 Principle design for construction of multi-layer cover of the Bulgarian NDF – Radiana site

2.3.3 Finland

- Preliminary investigation of surface disposal, determining the viability of surface disposal in Finland by investigating geology, hydrology, tectonic stability, and climate impacts on potential sites (Keto et al., 2020).
- Research on the properties of barrier materials to be used in the repository, based on existing international surface disposal designs and determination of safe barrier thickness (Keto et al., 2021).
- Environmental impact assessment to determine both viability and the most suitable location for the disposal site (TVO, 2021a).

- Performance of a SLF in Finland by studying radionuclide transport and retention in barrier materials, biodegradation, and gas generation in waste materials, and modelling long term performance of the repository (TEM, 2023).
- Ongoing research to better understand waste evolution and radionuclide speciation, with focus on waste package evolution, gas generation, radionuclide retention, suitability for decommissioning waste disposal, and assessment of alternative waste form performance – SAFER2028.

2.3.4 France

Many R&D activities were carried out and are still ongoing on the surface repositories and shallow disposal project. These activities are related to the geological sites, the multi-layer cover, the THMC evolution of the components, and the migration of the radionuclide and toxic chemicals (including release, sorption, diffusion, and perturbations by some waste components). Here is a summarized list of the topics investigated in the framework of the R&D activities related to the surface disposals:

- Development of sensors for monitoring the vaults
- Behavior of the cover with time and under meteoric conditions
- Development of hydrogeological models
- Retention of radionuclides and toxic chemicals in the geological and the cement-based barriers (including the degraded cement-based materials and new organic toxic chemicals such as PFAS)
- Effect of the climate change
- Healing of the concretes
- New binders (including the low-carbon cements)
- Effect of the organic perturbation in the radionuclide behavior in sands and cement-based materials
- Effect of the alkaline perturbation (coming from the cementitious barriers) on the migration of radionuclide and toxic chemicals in sands (geological barrier)

2.3.5 Lithuania

Numerous investigations of the Stabatiškė site were performed to gather information on the hydrogeological properties of the site and to confirm its suitability, including:

- Preliminary engineering and geological investigations – identification of general nature on the engineering geological site conditions.
- Site characterization stage – collection of the main information about soil characteristics and geological properties.
- Site confirmation stage – focused on hydro-geological and hydrological research to provide all necessary information for technical support for designing and safety demonstration.
- Site tectonic research – tectonic and seismic investigations.
- Flooding potential in the site.
- Radionuclide sorption – laboratory measurements of sorption coefficients in local soil for radionuclides with the potentially highest impact as identified in the Environmental Impact Assessment report (RATA, 2007).

Several studies on Lithuanian clay were performed in 2004-2006 where properties of three different clayey soils were investigated with the aim to select the most appropriate clay for the NSR barriers, considering assigned safety functions.

In addition to the field and laboratory experiments, modelling work on performance of the top engineered barriers was conducted (RATA, 2003–2005), including:

- Water saturation of the top liner (clay);
- Percolation of the top liner (clay);
- Geotechnical performance (stress/strain) of the clay in the cap.

Numerical modelling to support safety assessment are continuously performed at Lithuanian Energy Institute, Nuclear Engineering Laboratory (Balčiūnas and Grigaliūnienė, 2023; Grigaliūnienė et al., 2016). The most recent investigations concerns modelling of interaction of engineered barriers with the environment and its effect on radionuclide release from the disposal facility and migration in the near field.

The INPP plans to construct a mock-up of the engineered barriers of the NSR. The mock-up will replicate one section of the vault with the protective barriers around it. The aims of this project include demonstration of the ability to erect the top engineered barriers with available construction techniques without affecting the integrity of the underlayers and vault structure; verification of the hydraulic properties of the cap and identification of potential changes in the cap layers over time. The permit for construction is expected in 2026 (INPP, 2025).

2.3.6 Romania

The RD&D program for site selection and characterization was conducted during 1992-2006 and, as on that time Romania did not have designated a responsible organization for radioactive waste management, it was coordinated by the two subsidiaries of RATEN (CITON Bucharest and ICN Pitesti). The results obtained were used in the first safety assessment report finalized by CITON Bucharest and ICN Pitesti in November 2006, report drafted in accordance with the requirements of CNCAN Norms on near-surface disposal (CNCAN Order No. 400/2005) and IAEA recommendations (ISAM/ASAM). This report was revised by the National Agency for Radioactive Waste (ANDRAD, created in 2003, currently ANDR), and peer reviewed by an IAEA international expert team (WATRP Expert Mission during December 2006 – January 2007). Based on revised documentation, CNCAN issued in February 2008 a partial licence for DFDSMA siting on Saligny site.

The studies carried out until 2006 were completed within PHARE Project (PHARE RO 2006/018-411 0303) and based on the updated documentation, in 2018 CNCAN issued a letter of comfort confirming that Saligny site meets the requirements of the national legislation to host the disposal facility.

The ongoing activities carried out in RATEN ICN under R&D program financed by the Ministry of Energy address the CNCAN recommendation regarding the performances and durability of cementitious barriers in conditions relevant for Saligny site. These activities aim to assess the effect of cement degradation on the release of safety relevant radionuclides (C-14, I-129, Tc-99) and are performed in the context of SUDOKU.

2.3.7 Slovenia

The vast majority of past studies are in the form of various tests according to standards, feasibility studies and technical reports. They are written in Slovenian language and less accessible since they were written as a part of larger project founded by Slovenian WMO ARAO.

The studies conducted for the Slovenian repository in Vrbina can be systematically grouped into three main categories relevant to WP SUDOKU: (1) Concrete Material Degradation, (2) Corrosion of Reinforcement Steel, and (3) Numerical Modelling of Hydraulic and Radionuclide Transport Processes.

2.3.7.1 Concrete material degradation studies

Two extensive and more general studies performed by ZAG investigated concrete and mortar degradation processes due to exposure to aggressive groundwater from the Vrbina site:

The first partial study (Legat et al., 2009) involved the preparation of nine different mortar mixtures using various cement types (CEM I, CEM II/B-P, CEM III, CEM V) and mineral additives (microsilica and fly ash). These mortar samples were exposed to a simulated aggressive groundwater solution from Vrbina, containing sulfates, ammonium ions, and chlorides. Researchers assessed dimensional changes, compressive and bending strength, elastic modulus, capillary water absorption, and performed petrographic analyses to detect the formation of ettringite as an indicator of sulfate reaction degradation (Legat et al., 2009). In a follow-up study (Legat et al., 2011), mortar mixtures with cement types (CEM I, CEM III, CEM II/B-P, CEM IV) and mineral additives were again exposed to an aggressive synthetic groundwater solution, this time 50x more concentrated. This work included detailed microstructural analyses via SEM, mercury porosimetry, autogenous shrinkage, and hydration heat measurements. Additional testing involved assessing concrete's resistance to water penetration, freeze-thaw cycling, alkali-silicate reactions, and chemical-transport modelling to simulate concrete degradation due to leaching.

Several studies dealt with concrete for silo secondary wall:

Laboratory and field investigations were performed to determine optimal concrete mixtures for the silo secondary wall concrete, examining both fresh properties such as workability and air content, and hardened properties including strength, elastic modulus, water permeability, chloride diffusion, freeze-thaw resistance, shrinkage, carbonation resistance, and creep (Sustersic and Drolc, 2020). Additionally, studies evaluated key technological parameters affecting the concrete placement process for secondary silo linings, exploring how different construction methods, installation procedures, and environmental conditions influence concrete quality and durability (Ercegovic and Unetic, 2020). The selection of binder components for secondary lining concrete was also systematically investigated, specifically analysing various cement combinations (CEM I and CEM III) supplemented with silica fume to optimize resistance to environmental degradation, minimize thermal development, and enhance concrete longevity (Ipavec, 2020). Further research examined the risks associated with alkali-dolomite reactions in concrete containing dolomite aggregates, seeking to identify and understand potential long-term deterioration due to reactions between aggregates and cement paste, particularly important for repository construction (Bokan-Bosiljkov et al., 2020). Complementary work assessed the carbonation resistance of different concrete mixtures, emphasizing the role of binder type and concrete composition in slowing carbonation rates, thereby ensuring extended service life for cementitious barriers within the repository (Sajna, 2020). The durability assessments involving freeze-thaw testing were conducted to predict the long-term structural performance of concrete mixtures selected for the repository, providing essential data for barrier performance and longevity analyses (Zajc and Polanec, 2020).

The following two studies were devoted to the primary wall/lining (also called diaphragm) concrete:

Recent studies have provided essential insights into the selection, optimization, and practical implementation of tremie concrete for the primary wall (diaphragm wall) LILW repository Vrbina. Laboratory research systematically examined different tremie concrete mixtures intended specifically for the diaphragm wall of the Vrbina repository silo, assessing their workability, pumpability, capability of displacing bentonite slurry, and their fundamental mechanical and durability properties. These laboratory tests aimed at determining optimal concrete formulations capable of ensuring efficient installation and structural performance under repository conditions (Sustersic and Hrtl, 2023). Complementary research established the fundamental performance requirements for tremie concrete used in deep foundations and diaphragm construction at the LILW repository. The study particularly emphasized rheological and fresh-state properties, following established guidelines provided by the European Federation of Foundation Contractors (EFFC) and the Deep Foundations Institute (DFI), thus setting clear standards for concrete quality and performance suitable for repository-specific construction challenges (Bokan-Bosiljkov, 2023). Furthermore, detailed rheological measurements were conducted

on fresh tremie concrete specifically developed for the diaphragm wall of the Vrbina repository. Using rheometers and ultrasonic measurement techniques, these studies evaluated concrete consistency, setting times, and hardening behaviour to optimize concrete mix designs, ensuring they meet required workability and placement conditions necessary for durable, long-term repository performance (Ercegovic et al., 2023).

Lightweight mortars as filling and sealing mortar for disposal containers N2d:

Study by Sustersic and Hertl (2024) specifically investigated the performance of light cement-lime mortar containing expanded vermiculite for use in filling and sealing disposal containers (N2d). The examined properties included fresh mortar workability, air content, water-to-cement ratio, density, setting time, heat release, compressive and tensile strengths, water permeability, capillary absorption, gas permeability, and freeze-thaw durability. They aimed to optimize mortar compositions for long-term durability and sealing efficiency (Sustersic and Hertl, 2024). Ercegovic et al. (2024) carried out experimental filling of disposal containers N2d with lightweight mortar containing expanded vermiculite. Tests evaluated fresh mortar consistency, air content, sorption coefficient, gas permeability, and visual homogeneity assessment after filling. This research aimed at optimizing mortar filling procedures and technology for disposal containers (Ercegovic et al., 2024).

Testing and Certification of Concrete Disposal Container for Vrbina LILW Repository:

The studies and tests (IBE, 2018) conducted on the reinforced concrete disposal container N2d for the Slovenian LILW repository at Vrbina focused on ensuring the container's mechanical strength, durability, structural stability, and barrier functionality. Investigations involved rigorous testing of constituent materials, including cement (CEM I 52.5 N–SR0), aggregates, and mineral additives like microsilica. Extensive characterization of fresh and hardened concrete was carried out, assessing workability, compressive strength, water permeability, shrinkage, freeze-thaw resistance, static modulus of elasticity, carbonation resistance, chloride content, and air and water permeability. Critical tests also included examining the manufactured container's permeability to fluids and gases, ensuring extremely low water permeability ($<10^{-12}$ m/s). Tests related to safety analyses and the European ADR standards were performed, including free-drop tests to validate container integrity during transport. Additionally, load-bearing tests on lifting attachments were executed, ensuring safe handling during transport and placement. Practical testing involved container filling procedures using standard steel drums, assessing the consistency and flow of filling and sealing mortars to verify complete void filling. Final inspections included geometric verification, water and air-tightness testing, concrete strength and homogeneity, concrete cover thickness, and bond strength between filling mortar and container walls. These extensive laboratory and field tests confirm that the container design and materials meet all stringent safety and performance criteria required, and served for granting the Slovenian Technical Approval (Slovensko tehnično soglasje, STS-17/0019).

2.3.7.2 Corrosion of Reinforcement steel

Corrosion studies of reinforcement steel were systematically separated into two specific scenarios: corrosion in simulated solutions and corrosion of steel embedded in concrete. Comprehensive electrochemical corrosion studies, examining several steel reinforcements, including carbon steel and stainless steel alloys, in simulated groundwater solutions from the Vrbina site were conducted at ZAG (Legat et al., 2009). They performed electrochemical impedance spectroscopy (EIS) and potentiodynamic polarization to determine corrosion rates in various aggressive solutions containing sulfates, chlorides, and ammonium ions at different pH values. Concrete specimens, both cracked and uncracked, were prepared with embedded reinforcement to simulate real environmental conditions. These samples underwent direct wetting with aggressive simulated groundwater and cyclic chloride exposure to assess the impact on corrosion initiation and progression. Regular measurements of corrosion potentials and corrosion rates provided essential insights into the relative durability of different steel reinforcements in concrete under aggressive conditions. A follow-up study (Legat et al., 2011) expanded the previous research by continuing electrochemical corrosion assessments in more aggressive synthetic groundwater solutions. Electrochemical measurements, including corrosion

potential monitoring, polarization tests, and electrochemical impedance spectroscopy, were repeated with 50x concentrations of aggressive ions to accelerate corrosion processes and evaluate passive film stability on different reinforcement steels. Additionally, concrete samples containing various types of steel reinforcement and artificially induced cracks were periodically exposed to aggressive simulated groundwater. The corrosion rates were measured using galvanostatic pulse methods, and embedded electrical resistance corrosion sensors were employed for continuous corrosion monitoring. The research highlighted significant differences between the corrosion resistances of stainless steels and carbon steel, particularly noting the enhanced susceptibility of carbon steel and certain ferritic stainless steels (TOP12) to localized corrosion, especially when embedded in cracked concrete under cyclic wetting conditions.

2.3.7.3 Numerical modelling of hydraulic and radionuclide transport processes

Kalin et al. (2011) compared two numerical modelling platforms, Hydrus2D and Alliances, to investigate hydraulic conditions and radionuclide transport for the silo-type Slovenian LILW repository at Vrbina. Their study included simulations of water flow (Darcy velocity fields) and radionuclide transport processes—advection, diffusion, dispersion, sorption, and radioactive decay—considering several key radionuclides. Analyses also evaluated the sensitivity of model predictions to mesh density and computational timestep. Results indicated good agreement between the two codes, validating their suitability for long-term safety predictions. A small part of ZAG study (Legat et al., 2011) tackled also the simulation of the chemical degradation (concrete leaching) of the silo wall at Vrbina over a 300-year period using the Alliances software. The simulations compared concrete degradation exposed to synthetic groundwater with pure water, focusing on chemical processes such as portlandite dissolution, decalcification of calcium silicate hydrate (C-S-H), and ettringite formation due to sulfate attack. Results briefly indicated that aggressive groundwater conditions significantly enhanced concrete degradation, underscoring the need to consider site-specific chemical interactions in predicting long-term barrier performance.

2.3.8 Spain

Enresa is engaged in several research and development (R&D) initiatives focused on engineered barriers. The ongoing work encompasses the following areas:

- Multilayer cover Mock-ups (Tests I and II) at El Cabril, in collaboration with AMPHOS 21: The data collected from the monitoring system are analyzed to evaluate and understand the performance of both cover systems. Predictive models are being developed to assess long-term cover behavior.
- Material Characterization (CARCOB), in collaboration with CIEMAT: Laboratory tests are conducted to determine key parameters and material behavior in the final cover layers. These tests assess the physical, thermal, hydraulic, mechanical, and geochemical properties of materials intended for use in the cover systems of the El Cabril Storage Facility. The results will support the modelling of material performance under construction and operational conditions.
- Construction of a new cover over a LILW Cell at El Cabril: This initiative aims to generate and disseminate practical knowledge and experience regarding the challenges encountered during both the construction phase and subsequent monitoring activities.
- Laboratory-Scale Testing of Cover Layers (CARCOBES), in collaboration with CIEMAT and AMPHOS 21: These tests replicate individual layers or combinations of layers that comprise the cover system. By isolating specific components, the behavior of each barrier can be studied independently. The experiments evaluate the effects of materials with different hydraulic properties, varying layer slopes and thicknesses, and the presence of vegetation. The systems are subjected to simulated precipitation events of varying intensity and duration, alternating with dry periods.
- Study on Vegetation Influence in the Biointrusion Layer (VEBIOCA), in collaboration with CIEMAT: This study analyzes the evolution of vegetation within the biointrusion layer of the

existing multilayer covers at El Cabril. The objective is to assess its impact on key parameters such as infiltration, runoff, erosion, isolation, and evapotranspiration, which influence the overall effectiveness of the isolation barrier.

- Characterization of Barrier Materials for RBMA and RBBA (CARMA), in collaboration with CIEMAT: To improve understanding of cementitious and cover materials and the processes affecting the safety of radioactive waste storage systems, the transport and retention properties of relevant radionuclides are being investigated. The study focuses on tritiated water (HTO) as a conservative tracer and cesium-137 as a representative cation for low- and intermediate-level waste. Mortars prepared with three types of fly ash and one type of concrete (all containing a superplasticizer), along with a clay-based cover material, have been thoroughly characterized from mineralogical and physicochemical perspectives. Retention properties are assessed through sorption isotherms, while transport properties are evaluated using diffusion tests, specifically the through-diffusion technique.

2.4 Safety functions

As mentioned above, the main safety functions are isolation and containment. This section describes how the different SSCs contribute to these safety functions. The concept of the Belgian near-surface repository lacks a safety function of the geosphere; consequently, the engineered barriers play an enormous role in the long-term safety functions. As SUDOKU focusses on the engineered barriers, the description of the Belgian approach is more elaborated in the state-of-the-art report.

2.4.1 Belgium

Both operational and long-term safety is ensured by a combination of barriers and their favourable properties/characteristics, considering normal conditions, incidents and accidents. Safety functions are identified for the operational period and for the post-closure (i.e. long-term) period. The safety concept describes how safety will be ensured by the combination of barriers and safety functions and identifies their intended performance over different timeframes. The safety concept has both an operational and a long-term component (Figure 2-24). Both are essential inputs for the design of the disposal facility.

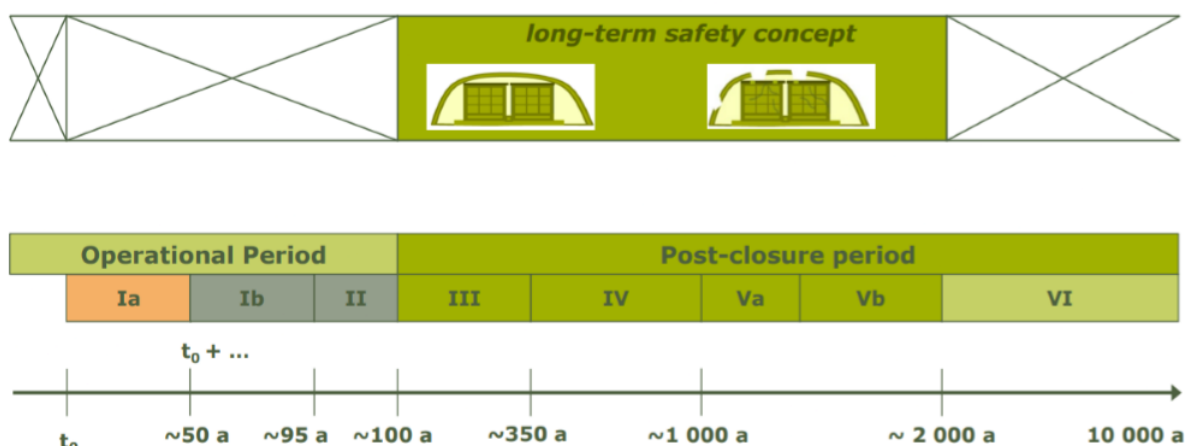


Figure 2-24 Timeframes considered in the Belgian surface disposal programme and period to which the long-term safety concept applies.

In the long-term safety concept, the following safety functions need to be fulfilled by multiple barriers:

- Isolation i.e. limitation of the likelihood and consequences of inadvertent human intrusions;
- Containment of radionuclides (RN):
- Limitation of RN releases from the waste (R1)
- Limitation of water infiltration towards the waste (R2)

- Chemical RN retention (R3)
- Limitation of RN diffusion (R4a)
- Spreading of RN in conductive media (R4b)
- Protection of other safety-relevant components

Isolation of the waste is primarily ensured by the presence of barriers between the waste and human beings and through active controls during 350 years. Because the waste contains mainly short-lived radionuclides, the radiological risk associated with inadvertent intrusion beyond this period is low enough to stop these controls (Figure 2-25).

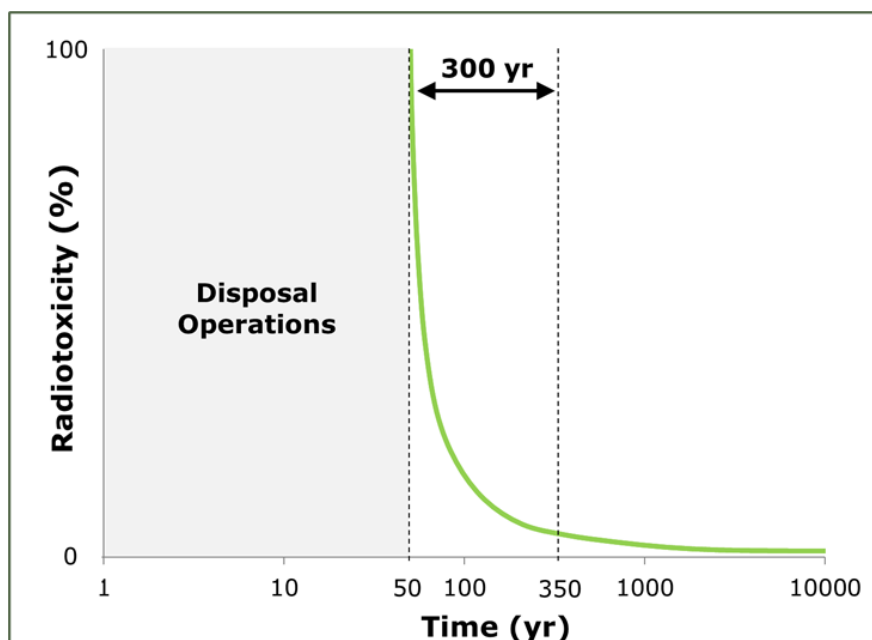


Figure 2-25 Evolution of the radiotoxicity considering that all the radionuclides present in the waste inventory start to decay at the end of the operational phase. The radiotoxicity is calculated by multiplying the activities by the (isotope-specific) dose conversion factor for ingestion.

The containment strategy is based on the evolution of radiotoxicity resulting from radioactive decay (Figure 2-26). It consists in first instance of preventing water infiltration (and hence radionuclide (RN) release) during ~1000 years since short-lived RN will have (almost completely) decayed in the facility after 350 years and a significant part of the small quantity of long-lived RN present in the waste will decay over the centuries following the end of the controls (i.e. after 350 years). However, after ~1000 years, the remaining radiotoxicity decreases very slowly and water infiltration inside the modules can no longer be prevented. Consequently, the strategy associated with the subsequent timeframe consists of limiting and spreading the release of RN over time. This strategy makes it possible to optimise the protection provided by the facility while applying a graded approach whereby the level of protection remains commensurate with the residual risk associated with the waste. It is implemented through a set of complementary and independent safety functions and barriers.

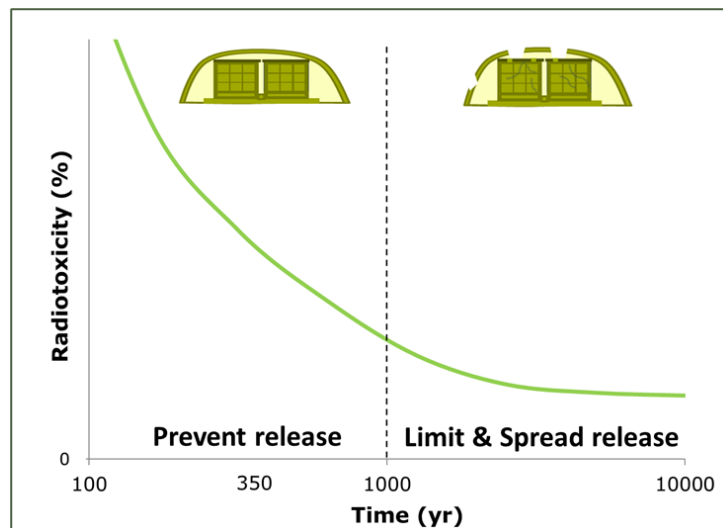


Figure 2-26 Evolution of radiotoxicity and related containment strategy. The radiotoxicity is calculated by multiplying the activities by the (isotope-specific) dose conversion factor for ingestion.

Before \sim 1000 years, the multilayer cover protects the concrete components of the facility and contributes to the isolation of the waste. The release of radionuclides from the facility is prevented by preventing water infiltration into the modules and containing the radionuclides as much as possible within the monoliths (Figure 2-27). Water infiltration into the modules is mainly avoided by different components of the cover performing an R2a function, which sequentially reduce the amount of infiltrating water. Containment within the monoliths is ensured primarily by the slow release of radionuclides from the waste, which is solid or has been solidified. During conditioning, a cementitious matrix is added to the waste, which ensures sorption. Metal waste packaging can form a physical barrier. Sorption onto hardened cement in the monolith and slow diffusion to and within the caisson and to surrounding barriers ensure further containment of radionuclides within the monoliths.

Containment $< \sim 1000$ year Prevent radionuclide release

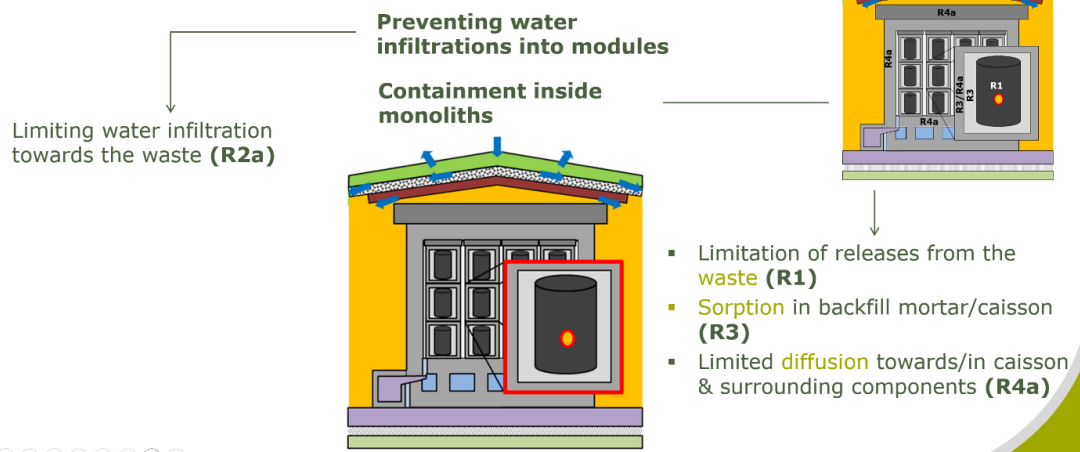


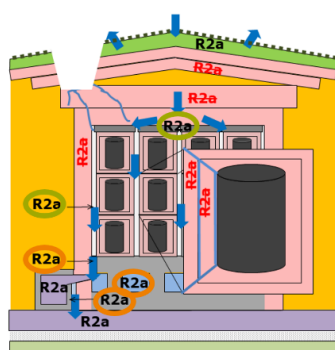
Figure 2-27 Barriers and safety functions contributing to containment between closure and \sim 1000 years.

After 1000 years, the cementitious components of the facility are expected to degrade gradually, and over time they will be completely degraded. Under these conditions, water infiltration into the modules can no longer be avoided (Figure 2-28). Water infiltration will gradually and locally increase as the impervious top slab degrades. As networks of through-going cracks develop in the monoliths, some of this water may come into contact with the waste and accelerate the release of radionuclides from the monoliths. However, several elements continue to contribute to limiting the release of RN from the facility. A first element is the presence of preferential flow paths in the space between the monolith stacks which is filled with gravel. Moreover, slabs placed on top of these stacks, made of fiber-reinforced concrete, divert infiltrated water into the gravel.

Further drainage of water inside the modules is ensured by the presence of an ‘anti-bathtub system’ (ABS) at the bottom of the modules. This prevents the accumulation of water within the modules in the event that no through-going cracks are already present in the module base. The ABS drains infiltrated water through openings in the module floor to the backfill material in the inspection room (a conductive grout) and the connection tunnels between the inspection rooms and gallery, where water is diverted through a joint to the sand-cement embankment (which also has a high conductivity). If the route along that joint is not followed, water flows into the inspection gallery, which is also filled with sand-cement.

Containment > ~1000 year

Limited water infiltration towards the waste (R2a)



- Water infiltration into the modules can no longer be prevented
 - Restricted only through evapotranspiration on earth cover remnants
- Preferential flow in inter-monolith spaces
- Anti-bathtub system
 - Drainage of water infiltrating the modules through openings & porous (cementitious) materials

Figure 2-28 Barriers contributing to the limitation of water infiltration towards the waste after ~1000 years.

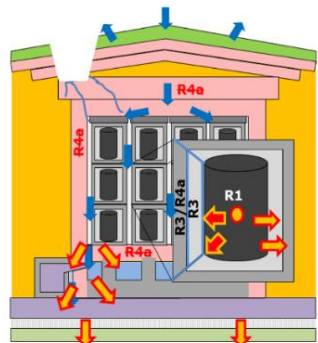
Despite limited water infiltration to the waste, the presence of gradually developing cracks within the monoliths can create preferential pathways for advective radionuclide transport. However, the release of radionuclides to these cracks will be limited and spread over time by (Figure 2-29):

- sorption on the conditioning mortar and in the waste itself (in the case of concrete waste)
- the physical barrier provided by the waste packages
- slow diffusion and sorption in the backfill mortar and concrete containers



Containment > ~1000 year

Containment inside monoliths



Releases from monoliths limited and spread over time by:

- Slow release from the waste (**R1**)
 - Sorption on cement
 - Waste characteristics
- Sorption in backfill mortar and caisson (**R3**)
- Slow diffusion in caisson (**R4a**)

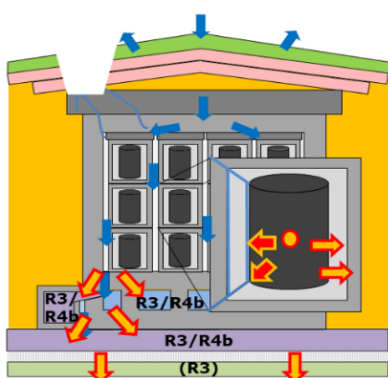
Figure 2-29 Processes contributing to containment inside monoliths after ~1000 years.

When radionuclides enter cracks acting as preferential transport pathways in low-permeability cementitious components, it is assumed that the sorption capacity of these components is bypassed. In these circumstances, a third and final element contributing to containment consists of spreading the radionuclides released from the monoliths in a conductive matrix in which they are transported by advection (Figure 2-30). This role is ensured by the backfill material of the inspection rooms and gallery and the sand-cement embankment at the bottom of the disposal system. Dispersion (safety function R4b) is a necessary condition for the sorption capacity of such materials to be relied upon. These conductive sorbent media are complementary to the cementitious matrices of waste, concrete and backfill mortar of the monoliths limiting releases to cracks.



Containment > ~1000 year

Spreading and retardation outside monoliths



Fractures as preferential transport routes
→ **bypass**

Conductive sorbing media spread the release of radionuclides from the system

- Spreading by **dispersion** in conductive material (**R4b**)
- **Sorption** in conductive material (**R3**)

Figure 2-30 Containment outside monoliths after ~1000 years.

2.4.2 Bulgaria

The main safety objectives of the LILW-SL repository at the Radiana site are:

- to ensure health protection for the personnel and the population and protection of the environment during the full lifetime of the repository, i.e., during operation and after closure;
- to be possible to release the site from regulatory control after the Institutional Control Period for any use without radiological restrictions.

The general safety functions of the NDF can be summarized as:

- Ensuring the isolation of the radionuclides contained in the waste and limiting unavoidable releases so that compliance with regulatory exposure limits is guaranteed;
- Protect the staff and the population from deleterious effects resulting from the repository existence or its operation

The final multi-layer cover is a main part of the fourth safety barriers as described in section 2.2.2. It is designed to reduce infiltration in the disposal cells, prevent bio-intrusion, minimize surface erosion and to maintain proper vegetation. The multi-layer protective cover (Figure 2-23) will be constructed using mainly natural materials as clay, sand, and gravel (Table 2-1), and shall fulfil the following safety functions:

- limit the infiltration of water through the disposal cells;
- serve as a barrier against external intrusion by humans, animals or plants;
- provide protection against long-term erosion agents such as rainfall and wind.

Table 2-1. Conceptual multilayer cover layers and their functions (Bulgaria)

Barrier	Layer No	Description	Function
Biological	1	Vegetation and anti-erosion layer	To reduce hydraulic flow by water storage and evapotranspiration To prevent surface erosion and to limit climatic influence
	2	Coarse sand and gravel layer	To prevent moving down of fine particles from the vegetation layer to anti-intrusion stone layer
	3	Anti-intrusion stone layer	To prevent intrusion of burrowing animals and penetration of deeper roots
Drainage & capillary	4	Coarse sand	To provide capillary barrier To keep humidity of the underlying impermeable clay
Impermeable	5	Compacted clay layer	To limit water inflow into disposal cells
Support & drainage	6	Compacted granular layer	To provide support base of multilayer cover and drainage around the disposal cells

2.4.3 Finland

The SLF design incorporates both natural and engineered barriers. The role of these barriers is to isolate the waste packages from the environment for up to 300 years. This will be done by isolating the waste

packages from environmental factors such as rainfall, whilst also aiming to contain the radionuclides within the SLF. The barriers and their roles are detailed in Table 2-2 (Keto et al., 2021).

Table 2-2 Surface landfill facility barrier materials and their safety functions (I – isolation, C – containment) (Finland)

Barrier	Material	SF	Function	Layer
Vegetation	Grass	I	Prevents erosion, limits water infiltration	Cover layer
Top layer	Soil, moraine till, crushed rock	I, C	Limits water intrusion, protects against erosion, protects from irradiation	
Drainage layer +filter	Coarse gravel, +geomembrane and sand	I	Drains water, limits water intrusion, reduces hydrostatic pressure on sealing layer	
Synthetic geomembrane +filter	HDPE membrane, or bentonite mat +sand	I	Limits water intrusion, filter layer protects membrane	
Mineral sealing layer	Finely crushed rock with up to 6 wt % bentonite	I, C	Radionuclide retention	
Fill material	Finely crushed rock, gravel, sand	C	Radionuclide retention, shapes the repository	
Waste packages	LDPE, Carbon steel	I, C	Waste immobilization, radionuclide retention	
Floor layer	Gravel	I	Flattens the foundation	Foundation layer
Drain layer + piping	Coarse gravel, + plastic pipes	I	Drains water, directs water to collection	
Mineral sealing layer	Finely crushed rock with up to 6 wt % bentonite	C	Radionuclide retention	
Subsoil / sediment	Natural sediment and topsoil	C	Radionuclide retention, Load bearing	Natural barrier

2.4.4 France

Andra's approach to safety is based on the implementation of the functions defined in the Safety Authority guidelines and requirements, and address the following issues:

- Control of nuclear chain reactions;
- The containment of harmful substances (radioactive in particular);
- The protection of man and the environment against radiation.

The function of the control of the thermal power is not retained in the demonstration of CSA nuclear safety, taking into account the relatively low activity levels of the waste received and disposed of. The required level of safety is achieved by the combined properties of three major constituents in the disposal system (Figure 2-31) :

- The waste package (1 in Figure 2-31);
- The disposal facilities (1 in Figure 2-31);
- The geological environment of the site, in particular the Aptian sand layer. The impermeable clay layer covered by a draining layer of sand constitutes a natural barrier (2 and 3 in Figure 2-31).



Figure 2-31 *SSCs contribution to the long term safety at CSA (see text)*

The choice of assumptions and data (parameter values) related to the safety assessment was based on the following considerations:

- The reference situation refers to the best available and substantiated scientific and technical knowledge (models and parameter values described as "best-estimate") ;
- Sensitivity studies correspond to a set of assumptions and data using the conservative limits that can be considered within the normal range of evolution. In most cases (particularly radiological inventories, or sorption parameters of various radionuclides or chemical toxins in sands), the plausible maximum or minimum values were selected ;
- Altered evolution scenarios (or scenarios of unintentional human intrusion), some of which are defined in a "conventional" way, correspond to failures of the different components of the storage system ("defective" packages, "abnormal" cracking of the foundation slab, collapse of the cover at the right of a storage structure, rise in piezometric levels, short circuit of the geological barrier).

Safety assessments begin after the closure of the storage facility. They include a 300-year monitoring phase, followed by a post-monitoring phase that continues up to 50,000 years. The operational phase, estimated to last 70 years, is not included in the assessments. The total inventory progressively stored during operation is considered to be entirely present in the packages at the time of facility closure. Losses due to radioactive decay and migration that has already occurred outside the package during the operational phase are not taken into account.

Timeframe

The mechanical aging of storage structures is partly accounted for by the explicit representation of cracks and shrinkage in the cementitious components. This is compounded by a temporal evolution of the transfer properties in the concrete (permeability, porosity, and diffusion coefficient). The evolution of these transfer properties reflects the transition between different mechanical states: sound, weathered, degraded, and detrital. Chemical aging is reflected in a temporal evolution of sorption properties (partition coefficient), which also reflects the transition between different chemical states: alkali-free, altered, and carbonated.

Barriers

Different cementitious barriers will control the diffusion of radionuclides and toxic chemicals (confinement or limiting factor). These barriers are related to:

- Conditioning matrices
- Waste packages
- Concrete of the vault structures
- Backfilling materials and foundation slab

For each component and its degradation stages, a set of transport parameters is defined in the framework of the safety assessment.

On another hand, the storage facility multi-cover plays a role in limiting the infiltration of rainwater during the monitoring phase. Although not explicitly represented in the model, the cover's role is limited solely by its hydraulic performance and the consideration of an imposed infiltration rate of 5 L/m²/year at the top of the embankments.

From the beginning of the post-monitoring phase, it is assumed that the cover no longer plays its role in limiting the infiltration of rainwater and the water flow imposed on the roof of the embankments becomes 110.5 L/m²/year, a flow representative of the median recharge of the aquifer at the outcrops of the Aptian sands.

The geological surrounding environment

In the CSA hydrogeological model, the Aptian white sands constitute the main aquifer formation at the CSA site. The Albian green sands (overlying the white sands) and the clayey white sands (underlying the white sands) have been homogenized with the main aquifer layer and are therefore not represented in the hydrogeological model as distinct layers. The same applies to:

- the surface weathering formations, the colluvium (present on the slopes of the Pli hill) and the alluvium of the Noues d'Amance, the host formation of the alluvial aquifer;
- the platform fill present on the periphery of the center.

The Tegulines clays that form the natural impermeable cover of the aquifer have not been explicitly modeled, but their extent defines a specific recharge zone. The same is true for the platform waterproofing materials, whose extent also defines a distinct recharge zone.

2.4.5 Lithuania

The concept of the NSR in Lithuania is based on the system of barriers of a natural (geological) origin and engineering artificial (designed) barriers (multiple barriers concept) for containment and isolation of radionuclides to prevent or considerably retard radionuclides migration into the environment.

The safety functions of the different components of the disposal system are presented in Table 2-3 to Table 2-5. Each table identifies the barrier, its material, safety function indicator and assigned functions.

Table 2-3 Multilayer cover materials and safety functions (I – isolation, C – containment, RN – radionuclides) (Lithuania)

Barrier	Material	SF	Assignment
Vegetation	Soil, plants	I	Limit water infiltration, protect against negative climatic impact
Draining layers	Pebbles, sandy gravel, silty sand	I	Limit human intrusion
		C	Drainage, gas escape, limit direct irradiation
Protection against external conditions	Moraine clay	I	Limit human intrusion
		C	Limit direct irradiation
Drainage layer	Gravely sand	C	Drain water
Embedding clay (confining layer)	Clay	I	Limit human intrusion
		C	Limit water infiltration, limit direct irradiation

Table 2-4 Disposal vault components and safety functions (I – isolation, C – containment, RN – radionuclides) (Lithuania)

Barrier	Material	SF	Assignment
Roof (top slab)	Reinforced concrete	I	Limit human intrusion, maintain mechanical stability
		C	Limit water infiltration, limit direct irradiation
Walls	Reinforced concrete	I	Limit human intrusion, maintain mechanical stability
		C	Limit water infiltration, limit direct irradiation
Waste matrix	Cemented waste	I	Waste immobilization, limit human intrusion
		C	Limit water infiltration, retardation of RN, limit direct irradiation
Container	Reinforced concrete	I	Limit human intrusion, maintain mechanical stability
		C	Limit water infiltration, retardation of RN, limit direct irradiation
Backfill	Cementitious material	C	Limit direct irradiation
Bottom slab	Reinforced concrete	I	Maintain mechanical stability
		C	Limit water infiltration, retardation of RN
Foundation mattress	Concrete	C	Limit water infiltration, retardation of RN

Table 2-5 Geological system and its safety functions (I – isolation, C – containment, RN – radionuclides)

Barrier	Material	SF	Assignment
Controlled clay	Moraine clay	C	Limit water infiltration, retardation of RN
Vadose zone	Moraine clay with sand lenses	C	Retardation of RN
	Less permeable moraine clay	C	Retardation of RN

2.4.6 Romania

To minimize the radiological risk for the population and environment, now and in the future, the DFDSMA is designed to ensure the radioactive waste confining for a sufficient long period to allow radionuclides decay, control any releases (during operational and active institutional control period) and minimize the impact of eventually radioactive releases (post closure period).

Both operational and long-term safety is ensured by a combination of barriers and their favourable properties and characteristics, considering normal and alternative evolution scenarios. In the currently considered concept, DFDSMA consists of the following engineered structures:

- disposal cells and modules;
- visiting/collecting galleries and the drainage system;
- mobile hangars covering the disposal cells in operation (to protect the modules against precipitation)
- final multilayer cover

The radioactive wastes are conditioned in standard drums (220 l) to achieve homogeneous waste forms with a minimum mechanical strength of 5 MPa and the drums are placed in concrete modules (reinforced concrete cubic containers). Four standard drums are introduced in a disposal module and the empty

space is backfilled with mortar to form monoliths (Figure 2-32). In the case of compactable waste, the pellets will be also fixed into concrete matrix inside the module. The disposal modules are then placed in the disposal cell with a capacity of 384 modules stacked on 3 levels.

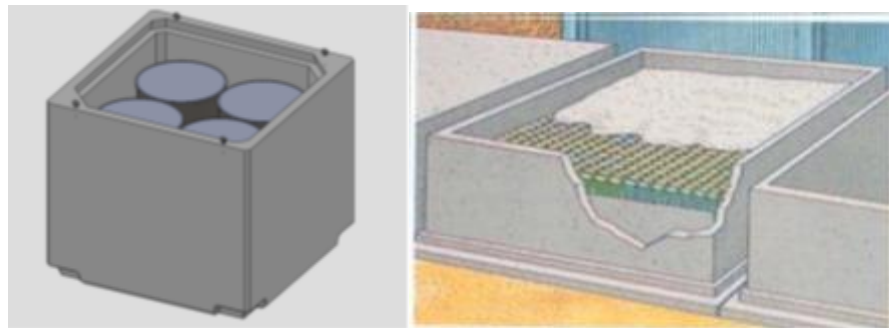


Figure 2-32 Disposal module before backfilling with mortar (left) and disposal cell

Four disposal cells are placed on a common reinforced concrete foundation slab. Because the top layer of the Saligny site is loess which is characterized as a “moisture sensitive soil”, the reinforced concrete foundation slabs will be built on an improved foundation ground.

After filling with disposal modules, the disposal cells are sealed with a concrete slab. When all disposal cells are filled and sealed, a multilayer cover composed of natural (sand, gravel, loess, clay) and artificial materials (waterproofing membranes) will be constructed to restore the natural landscape. The total thickness of the multilayer cover is between 3.2 m - 3.5 m, with slopes allowing rapid evacuation of rainwater. Several combinations of layers are currently considered in the Safety Assessment, and the performances of this engineered barrier need to be studied and final design has to be optimized.

The post-closure period for DFDSMA is divided in three distinct periods:

- *active institutional control period* for 100 years after repository closure - active monitoring is performed and remediation actions are taken if needed
- *passive institutional control period* for the next 200 years - records are kept and also the protective fence is present
- *no control post closure period* after 300 years from repository closure

If in the next stages of the project evolution optimized solutions are identified, these will be evaluated and considered and documented in the safety documentation used for licensing the repository construction phase.

Safety functions are identified for the operational period and for the post-closure period (

Table 2-6). After the institutional control period, a part of the safety functions of the engineered barriers cannot be performed anymore because of their physical and chemical degradation. Nevertheless, the functions determined by chemical characteristics of structural materials (e.g., the pH which influences radionuclide sorption, colloids formation, and actinides precipitation) will be kept a very long period, after repository closure.

Table 2-6 Safety functions allocated to engineered barriers (Romania)

Nr. criteria	Barrier	Operational period	Post-closure period	
			Institutional control period (first 100 years after closure)	Post - institutional control period
1.	Waste form	<ul style="list-style-type: none"> - Stable and inert waste form - Mechanical resistance - Minimization of water infiltration - Radionuclides retention 	<ul style="list-style-type: none"> - Stable and inert waste form - Mechanical resistance - Minimization of water infiltration - Radionuclides retention 	<ul style="list-style-type: none"> - Stable and inert waste form - Mechanical resistance - Minimization of water infiltration - Radionuclides retention
2.	Disposal module	<ul style="list-style-type: none"> - Shielding - Safety during waste transport - Mechanical resistance and stability - Minimization of water infiltration - Radionuclides confinement - Provision for extraction and replacement in unfavourable scenarios 	<ul style="list-style-type: none"> - Mechanical resistance and stability - Minimization of water infiltration - Radionuclides confinement - Provision for extraction and replacement in unfavourable scenarios 	<ul style="list-style-type: none"> - Minimization of water infiltration - Radionuclides confinement
3.	Backfilling material	<ul style="list-style-type: none"> - Filling of empty spaces - Minimization of water infiltration - Precipitation of radionuclides - Control of gases release - Provision for module recovery 	<ul style="list-style-type: none"> - Filling of empty spaces - Minimization of water infiltration - Precipitation of radionuclides - Control of gases release - Provision for module recovery 	<ul style="list-style-type: none"> - Filling of empty spaces - Minimization of water infiltration - Precipitation of radionuclides - Control of gases release
4.	Disposal	<ul style="list-style-type: none"> - Shielding 	<ul style="list-style-type: none"> - Physical stability 	<ul style="list-style-type: none"> - Radionuclides confinement

Nr. criteria	Barrier	Operational period	Post-closure period	
			Institutional control period (first 100 years after closure)	Post - institutional control period
	cells	- Physical stability -Radionuclides confinement - Barrier against intrusion	-Radionuclides confinement -Barrier against intrusion	
5.	Improved foundation ground	- Physical stability -Radionuclides retardation - Minimization of water infiltration	- Physical stability -Radionuclides retardation - Minimization of water infiltration	- Physical stability -Radionuclides retardation - Minimization of water infiltration
6.	Drainage system	- Discharges control -Discharges monitoring	- Discharges control -Discharges monitoring	N/A
7.	Multilayer cover	N/A	- Minimization of water infiltration - Control of gases release - Barrier against intrusion (biological and human) - Barrier against erosion	- Minimization of water infiltration - Control of gases release -Barrier against intrusion (biological and human) - Barrier against erosion

2.4.7 Slovenia

The Vrbina Low and Intermediate Level Waste (LILW) repository has been designed with a robust safety concept to ensure the long-term containment and isolation of radioactive waste. This safety concept is built around a multi-barrier system, combining both engineered barriers and natural geological barriers to prevent the migration of radionuclides into the environment. The concept integrates principles of radiation protection, hydrological isolation, and structural integrity to safeguard human health and the environment over the operational and post-closure phases of the repository, which is expected to last for thousands of years.

The concrete used in the Vrbina LILW repository plays a crucial role as the primary safety element in the multi-barrier system. It provides physical containment and chemical resistance, ensuring that radioactive waste is securely isolated. Concrete serves as the main barrier in both the disposal containers and the secondary silo walls, offering seismic resilience and preventing the migration of radionuclides into the surrounding environment. The low permeability of concrete limits the flow of groundwater and gases, while its alkaline nature helps immobilize certain radionuclides, enhancing chemical isolation.

Most radionuclides have high sorption coefficients in concrete, meaning that concrete effectively binds the radionuclides into its chemical structure, preventing them from spreading into the environment. This

sorption property ensures that even over extended periods, the concrete continues to prevent the release of harmful materials. The clay barrier between the silo and the aquifer shares similar properties, further reinforcing the chemical containment function by binding radionuclides and providing an additional hydrological isolation layer. Together, concrete and the clay barrier ensure the long-term safety of the repository. The multi-barrier system used in the silo consists of several layers, each performing a specific safety function. These barriers include reinforced concrete, backfill materials, steel drums, and the surrounding natural geological formations.

- **Steel Drum** (if used), made of carbon steel, serves as the first layer of containment, preventing direct contact between waste and the external environment during storage and transportation. It provides initial structural support but becomes secondary to other barriers once the repository is operational.
- **Backfill Mortar in the Disposal Container**, provides multiple safety functions:
 - Stabilization - It securely holds the waste in place,
 - Chemical isolation - It isolates waste from external water and gases, minimizing radionuclide migration and
 - Alkaline buffering - It helps immobilize radionuclides by reducing their solubility.
- **Reinforced Concrete Wall of the Disposal Container** that surrounds the steel drum and backfill mortar acts as secondary containment, offering structural support and hydrological isolation. It resists mechanical stresses and chemical degradation, preventing radionuclide migration and providing an alkaline environment that helps immobilize certain radionuclides.
- **Concrete Backfill Filling Voids Between Disposal Containers** is maintaining structural integrity and preventing movement. It also contributes to hydrological isolation, preventing the migration of groundwater.
- **Reinforced Concrete Wall of the Secondary Wall (Silo)** serve as the primary physical barrier. They provide seismic resilience, chemical resistance, and ensure long-term containment by preventing contact with the external environment and resisting groundwater and sulfate exposure.
- **Geological Environment around the Silo** (Natural Geological Barrier), including silt, provide hydrological isolation. These natural barriers have low permeability, ensuring that any potential leakage from the silo is contained within the geological formations.

In accordance with the Rules on radiation and nuclear safety factors (JV5, 2024), safety classification is the classification of (SSCs in line with the required safety functions for ensuring nuclear safety, and classification into safety classes with regard to their importance to nuclear safety. As required by the graded approach and the JV5 rules, which provides that all SSCs should be classified into safety classes, there are two safety classes defined for the LILW repository. These are safety-related (SR) and non-safety-related SSCs (NSR).

The disposal concept is based on a multi-barrier system, where multiple SSCs perform a single function, and multiple safety functions are deployed to achieve safety.

Table 2-7 gives the role of each component in the safety of the repository (ARAO, 2019b).

Table 2-7 Safety functions allocated to engineered barriers (Slovenia)

Description	Safety Function	Safety Classification	Passive (P) or Active (A) Function
Final package	P, C, H, I, S, Sh	SR	P
Backfill	P, C, H, S, Sh	NSR	
Silo	P, C, H, I, S	SR	P
Drainage system	H	SR	A
Barrier between silo and aquifer	P, C, H, I	SR	P
Backfill material at aquifer level	I	NSR	P
Structure for excavation of construction pit	S	NSR	P
Flood protection – embankment	H, Su	SR	P

The abbreviations used in the table represent the following safety functions: Physical Containment (P), Chemical Containment (C), Hydrological Type (H), Intrusion (I), Structural Stability (S), Shielding (Sh), Support Function (Su), and Security (Se).

2.4.8 Spain

The disposal system of El Cabril fulfils three key safety goals:

- Ensuring immediate and deferred protection to people and environment along installation lifespan (operation and long-term).
- Guaranteeing tracking and control of key elements by means of a continued exhaustive and traceable monitoring in those aspects related to radioactive waste, installation, people and environment.
- At the end of surveillance period, verify that disposal operations do not result in an unacceptable radiological impact (human intrusion scenario).

Three basic safety criteria are deducted from the above-mentioned objectives:

- Waste isolation under the conditions and time required:
 - o Engineered barriers system.
 - o Site characteristics.
 - o Operation consideration: shielding, remote operation, controlled ventilation, etc.
 - o Technical and quality related features.
- Establishment of a control and monitoring system over the disposal system, facility itself, affected site and environment.

- Activity limitations: limitation of total activity of radionuclides to be disposed in the facility, as well as the concentration of radionuclides in the waste packages and vaults both guaranteed by the waste acceptance criteria.

The multibarrier system is made up of three barriers (Figure 2-33):

- First barrier to confine the activity.
Waste immobilization matrix made up of package, blocking and sealing mortar and the disposal unit itself
- Second barrier to limit water infiltration and early warning and control any water that may have come into contact with the waste.
Disposal vault, the seepage control network and the long-term coverage.
- Third barrier to limit of the contaminant transport to biosphere.

The geological barrier is the surrounding land which limit the impact of a possible release in the hypothesis of total degradation of the first two barriers.

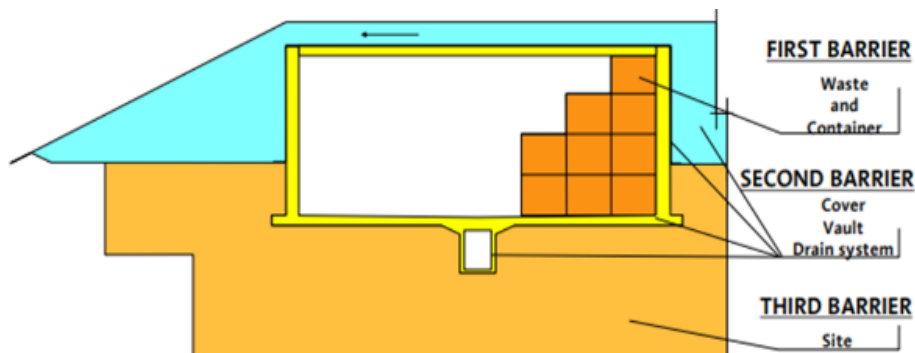


Figure 2-33 Multibarrier system

These three barriers coexist making a strong structure to get their goal.

- The packages, usually 220-litre drums, are placed in disposal units (Figure 2-33). Once the disposal unit is full, the spaces between the drums are filled with grout to immobilize them. The 220 l drums were used for the basic design. Today, there are other types of packages for example drums of 400/480 l or drum of 100 l for ashes resulting from the incineration of organic wastes, which are inserted into 220 l drums with a concrete inner wall.

Different characterization tests are specified for the waste packages to verify if they meet the Waste Acceptance Criteria (WAC) established.

- Disposal units of different sizes are used. Most common is the CE-2a, a block of 2.25 x 2.25 x 2.20 metres in size, where 18 drums are placed. Other kind of disposal unit are CE-2b, a block of half high of CE-2a or Cages for 400/480 l drums.



Figure 2-34 Packages into a disposal unit

The disposal units are placed in vaults (Figure 2-34), each with a capacity for 320 CE-2a disposal units and approximate external dimensions of 24 x 19 x 10 m.



Figure 2-35 Disposal units into a vault

- Vaults are distributed in two platforms. Platform North has 16 vaults and Platform South has 12 vaults. The vaults are placed in two parallel lines in each Platform.

The disposal units are placed in contact with each other; a central cross being left to allow for containers handling or positioning tolerances. The position of each disposal unit is selected according to its radiological activity. Lower activity disposal units will be placed next to vault walls.

For this operation the vault is covered by a mobile roof which protects the disposal unit from atmospheric phenomena and support the disposal unit handling system.

Once each vault has been fully loaded, the central cross is backfilled with gravel and upper closing slab is built.

The structure is then waterproofed with synthetic covering.

A drain at the centre of the bottom slab of the vault collects any seepage water and channels it to a network of pipes located in an accessible gallery beneath the vaults. Each vault is linked to this network through a holding tank; one for each vault. This allows to know from which vault the water came and to take samples to analyse or make reparations. While the vault is empty the rainwater is collected and led to a rainwater pond.

- The long-term cover isolates the disposal system in the long-term and ensure the durability of the disposal units.

The multilayer cover will prevent intrusion of raining water into the disposal system and so prevent contact with waste contained buried and sealed into the disposal vaults and cells themselves. To this end, a series of drainage and sealing layers will be installed, along with anti-intrusion layers and a vegetative cover to enhance long term stability.

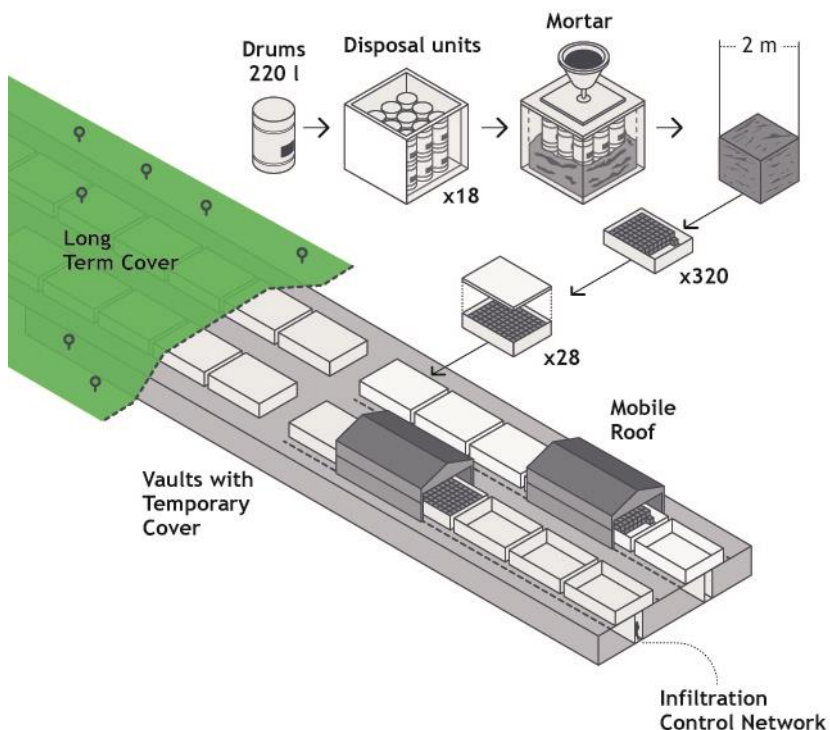


Figure 2-36 Waste disposal diagram

On the other hand, the VLLW multibarrier system is made up for three barriers too:

- Cover that aims to limit the water entry.
- Bottom and intermediate barrier whose function is to confine the activity and control the leakage. These barriers are made up of clay and a leakage collection system.
- Site geology that is the natural barrier that limits the contaminant transport to the biosphere.

VLLW packages are very diverse, including drums, Big-bag or CMT containers disposed on cells without disposal units. They are covered by a provisional removable roof during operation.



Figure 2-37 VLLW Storage



Figure 2-38 VLLW Cells

3 Multi-layer covers

3.1 Processes

3.1.1 Water infiltration and energy balances

Energy balance

Evapotranspiration interferes to the water balance in three ways (Novak and Hlaváčiková, 2019): (i) evaporation of wet surfaces from intercepted water in the vegetation canopy, (ii) evaporation from wet surfaces in the soil-atmosphere continuum, and (ii) transpiration via water evaporation from substomatal cavities of plants in the soil-plant-atmosphere continuum. The potential evapotranspiration is divided between a fraction that reaches the soil/cover surface – the potential evaporation – contributing to the second process, and a fraction used within the canopy and by the vegetation – the potential transpiration – contributing to the first and third process. The partition between potential evaporation and transpiration depends on the leaf area index (LAI) of the vegetation and is mostly described with a light extinction function following Beer's law (Kroes et al., 2008).

Water balance

An important driving factor for water drainage in soils or covers is the precipitation. However, before it reaches the surface of the cover, an initial partition distributes the rainfall into intercepted water by the plant canopy, throughfall, runoff and net precipitation. Description of (soil) water balance processes is available in several textbooks (e.g., (Hillel, 2003; Novak and Hlaváčiková, 2019; Robinson and Ward, 2017)) and reports in the framework of surface disposals (e.g., (Jacques et al., 2010a))

Vegetation interception, and evaporation from plant surfaces

The vegetation on the cover will intercept some precipitation before reaching the surface (either immediately, or after some storage time in the vegetation) (David et al., 2006). Part of the intercepted precipitation will eventually evaporate, and thus never reach the cover surface, is called interception loss (see above). The fraction that eventually reach the cover surface (either without hitting vegetation surfaces (free throughfall), by falling as drops from leaves (drips) and flowing along branches and stems (stemflow)) is called throughfall. Vegetation interception and throughfall can be calculated with a physically-based canopy water balance model (Eliades et al., 2022; Muzylo et al., 2009). Several model formulations exist that follow a water mass balance type of equation, typically indicated as Rutter- or Gash-types of models (Muzylo et al., 2009). The interception loss depends on vegetation characteristics (interception losses will be higher in trees), wind conditions and rainfall characteristics, amongst others (Deng et al., 2025).

Net Infiltration and runoff

At the surface of the cover, the throughfall is divided in runoff and (net) infiltration. This depends on the throughfall intensity, slope characteristics and soil infiltration capacity (function of soil water conditions). The vegetation influence also this process as it has an influence on the amount and timing of throughfall, the energy of the throughfall, and the spatial distribution. Whereas a tree vegetation may funnel water via throughfall and stem flow, a (dense) herbaceous vegetation increases surface roughness through stems and leaves decreasing the velocity of runoff water and thus increasing time for water infiltration (and decreasing erosion) (Löbmann et al., 2020). Note that small depressions (originating from e.g. (bio)turbation) in the surface can temporarily store water before infiltration when the infiltration capacity of the soil is reached (contributing to reducing runoff).

When the throughfall rate is smaller than the soil infiltration capacity (also called infiltrability), infiltration rate equals throughfall rate. This regime of infiltration is also flux- or supply-controlled. It is expected that for a sloped multi-layer cover, this regime occurs most of the time, except during heavy rainfall. The infiltration capacity depends, for a given soil and its general physical properties, on the initial soil water content and will change during infiltration events. As the soil becomes more wet during infiltration and

soil suction gradients decrease, the infiltration capacity decreases which also lowers the infiltration rate until a constant infiltration rate is reached determined by the saturated hydraulic conductivity (in a homogeneous profile). When the infiltration capacity becomes lower than the throughfall rate, infiltration rate equals infiltration capacity. The surplus amount of water will either pond or runoff. This regime is also indicated by the term profile-controlled infiltration (Hillel, 2003).

Moisture redistribution

After infiltration, water will redistribute within the cover profile under gravity, pressure forces and evapotranspiration. When focussing on the layer above the infiltration barrier (typically a thick strongly compacted clay layer) and/or bio-intrusion barrier (typically a stony layer), the main processes are water storage in the cover, water moving back to the atmosphere via evapotranspiration (actual evapotranspiration), and water draining to deeper cover layers.

The actual evapotranspiration is governed by the so-called potential evapotranspiration (linked to the energy balance and vegetation, see above) and water flow processes with the profile. Soil evaporation removes water directly from the surface in different stages: (i) at high soil water content, evaporation is not limited by the soil water conditions, and actual soil evaporation equals the potential evaporation, (ii) due to decreasing water content and lower hydraulic conductivity, the rate of water transport to the evaporating surface decrease resulting in a decreasing evaporation. The actual evaporation will be smaller than potential evaporation. (iii) when a dry layer develops at the surface, evaporation rate is further limited by transport of water through this layer by vapour. Transpiration which is the loss of water from the soil layer by uptake by plant roots and transport through the plant system towards the atmosphere follows roughly also these states. The difference between potential and actual transpiration is again related to the available water in the soil. If it is too wet (at and close to saturation), transpiration is limited due to oxygen deficit. Also, under too dry conditions, water uptake will be limited. Note that also other factors will influence root water uptake such as solute concentration or salt stress (Lu and Fricke, 2023).

Important factors determining the shift from evapotranspiration rates equal to the potential evapotranspiration to lower evapotranspiration rates are related to the water storage (water content and thickness of soil layers) and root depth and distribution. The water storage or water holding capacity is directly related to the soil physical properties, more specifically the texture. When the material has a relative fine texture, water holding capacity will be larger than for a coarse-textured material when both are drying to the same suction. Given also the higher capillary forces and typically lower permeability of fine-textured material, water will retain longer in the top layers. Furthermore, because of the higher capillary forces, more water could be transported upward from deeper layers.

Drainage and subsurface runoff

Ultimately, the water surplus that is not diverted back to the atmosphere via evapotranspiration or that is held in the profile will drain to the underlying layers or structure. The cover of a surface disposal is mostly designed to further divert the water from the underlying radioactive waste by placing an inclined infiltration barrier. An infiltration barrier has a low saturated hydraulic conductivity ($< \sim 10^{-9}$ or 10^{-10} m/s). This low conductivity will divert the largest part of the percolating water in the layer above the infiltration barrier (which should thus be a high-conducting layer).

Under arid or semi-arid climatic conditions, a capillary barrier could also limit deep percolation (Jacques et al., 2010a). Contrary to an infiltration barrier, a fine-textured layer is on top of a coarse-textured layer (Gao et al., 2023). When percolation fluxes are sufficiently low, the unsaturated hydraulic conductivity of the coarse-textured layer will be lower than that of the fine-textured layer and consequently, water is diverted laterally in the fine textured layer. This principle (in combination with a biological layer) has been shown effective for some specific covers (Ward and Gee, 1997). It will not be effective in case percolation rates are too high. When inclined, water will be accumulated down slope until reaching the water-entry in the underlying coarse layer, resulting in infiltration in the coarse-grained layer (Gao et al., 2023). Furthermore, it is better to avoid it when an underlying clayey infiltration barrier is present to keep

the clay layer close to saturation, although performance of a three-layer system (capillary barrier on top of clay layer – note that such configuration is often present in covers for LLIL-SL waste, see section 2.2) has been demonstrated for different conditions (Ng et al., 2015; Wu et al., 2024).

Resistive and capacitive barriers

Given the water flow controlling processes described above, a distinction can be made between two generic types of barriers: resistive or capacitive (or evapotranspirative or alternative cover) covers (Albright et al., 2004). A resistive barrier relies heavily on one or more layers impediment to percolation into the underlying layer. Typically, this is obtained by a layer with low saturated hydraulic conductivity such as a compacted clay layer, or by the presence of geosynthetic membrane. A capacitive cover relies on water storage principle by holding water in the top layers during periods with precipitation surplus, and evapotranspiration during the other periods). The study of Albright et al. (2004), for simple cover designs in the United States, that capacitive barriers are not sufficient in humid climates, but are effective in arid, semiarid and subhumid conditions (according to United States legislation). Cover designs for LLIL-SL waste heavily rely on the low-hydraulic conductivity layer and are thus typically resistive barriers. However, accounting for capacitive aspects may contribute to long-term safety as well, as water storage are typically less sensitive to degradation processes compared to guaranteeing a (very) low hydraulic conductivity at the long term. For example, for the Belgium reference profile, the capacitive properties decrease the infiltration rates to a factor of two of the annual rainfall.

3.1.2 Processes affecting long term performance

The long-term performance of engineered multilayer covers for LILW repositories is governed not only by their initial design but also by slow natural processes that gradually alter their structure and function (Jacques et al., 2010a). Over decades to centuries, mechanisms such as surface erosion, freeze-thaw cycling, desiccation cracking, bioturbation, and material weathering can modify hydraulic properties, compromise barrier integrity, and increase percolation. These processes can significantly influence water balance and contaminant isolation over time. Understanding and anticipating these slow processes is therefore essential for designing resilient covers and ensuring the long-term protection of human health and the environment.

Surface erosion

Raindrop impact, runoff concentration, and wind might remove fines and thin the soil cover; rills can localize water flow and increase erosion in these areas. Long-term average soil loss leads to a thinner water-storage layer which can cause a decrease in the evapotranspiration rate and higher percolation; it could also expose filters/drains/geomembranes. Forensic and modelling studies flag erosion as a primary stressor for multilayer covers (Kumar et al., 2019). To prevent it, most cover designs keep slopes gentle (enough to promote lateral water diversion but not too steep to compromise stability); promote fast native vegetation growth; create a rock-soil admixture and compact the most superficial soil layer; microtopography to spread flow; inspect after extreme storms.

Freeze-thaw cycling

Ice lensing and volumetric strain open cracks and coarsen soil structure, and repeated cycles can increase hydraulic conductivity by ~1–2 orders of magnitude in compacted clays if unprotected. Effects depend on fines, compaction, initial water content, and freezing depth (Othman and Benson, 1993). The impacts of these cracks are the formation of preferential flow paths and the breakdown of the hydraulic barriers. To prevent it, the barrier base should be kept below frost penetration (thermal cover thickness); specify compaction wet-of-optimum; add non-frost-susceptible protection; and monitor seasonal suction/temperature profiles.

Drying-wetting cycles and desiccation

Summer dry periods generate high suction values that could open shrinkage cracks; these might self-heal partially on wetting periods but often persist (Albright et al., 2006). As for the freeze-thaw cycles, cracks could create preferential flow paths and increase percolation. To prevent it, cover designs favour

ET covers with sufficient storage to smooth extremes, specify clays with low shrink–swell, and maintain vegetation to limit bare-soil drying.

Bio-intrusion

The creation of macropores by rooting vegetation and animal burrows significantly affect hydraulic properties of covers within a few years of implementation. Bio-intrusion creates preferential pathways in which water can flow, affects soil structure and permeability and encourages erosion. Certain species burrow deep enough to contact waste, which could be introduced into the environment through castings or ingestion - radon flux. Burrowing activity can be quite high in and around reclaimed cover systems and long-term vegetation succession can introduce deep-rooted species that penetrate barriers. To prevent it, coarse bio-barriers (cobble layers) should be used above liners, maintain a managed plant community (shallow-rooted natives), trap/monitor burrowing activity, and include root-resistant layers if GCLs are used (unprotected GCLs are root-susceptible).

Geosynthetic aging

In the case of geomembranes, geotextiles and drains, antioxidant depletion leads to polymer oxidation and stress cracking. Elevated temperatures (e.g., gas-generating waste) accelerate aging even when buried. Drain geotextiles can clog over decades if fines and biofilms accumulate. All this could derive on loss of liner integrity, reduced drainage and perched water and higher heads on the barrier. To prevent it, resin/additives are often selected, interface temperatures controlled, wrinkles/strain avoided, accessible leak-location zones provided, and filter/drain gradations used to resist clogging (Denis et al., 2012).

Chemical weathering of mineral barriers

Long-term mineralogical changes (e.g., carbonate dissolution/precipitation, sulphate attack) and salt crystallization in arid sites; in bentonite, prolonged exchange with divalent cations plus high ionic strength can reduce swelling/low-k performance. This could lead to increased hydraulic permeability and cracking susceptibility. To prevent it, compatible cover soils must be specified, saline irrigation avoided, porewater chemistry via drainage and soil selection needs to be managed, and periodic mineralogical checks for critical barriers are recommended.

3.2 Experimental studies

3.2.1 Laboratory studies

The long-term performance of multilayer covers is strongly influenced by the factors presented in the previous section. While field-scale studies provide valuable insights into integrated system behaviour under natural conditions, laboratory-scale experiments remain essential for isolating individual mechanisms and quantifying their effects under controlled, repeatable conditions. Such experiments typically expose standardized specimens to accelerated environmental cycles, chemical interactions, or biological activity in order to simulate decades of aging within manageable timeframes. Measurements of hydraulic conductivity, cracking, soil loss, or geosynthetic durability allow for the systematic evaluation of degradation pathways and the identification of critical factors governing barrier resilience. The table below synthesizes representative laboratory approaches used to investigate these slow processes and highlights the key metrics employed to assess their influence on cover integrity.

Process	Typical Specimen	Cycling Protocol	Fluids / Environment	Key Metrics	Representative References
Freeze–thaw	Compacted clay cylinders; GCL coupons	Controlled chamber, -10 °C to +20 °C, 10–50 cycles;	DI water or saline porewater	Hydraulic conductivity (k), suction, crack	(LaPlante and Zimmie, 1992; Othman et al.,

Process	Typical Specimen	Cycling Protocol	Fluids / Environment	Key Metrics	Representative References
	(small specimen cut from the sheet (often 10–30 cm)	sometimes saturated vs. unsaturated		formation, microstructure (SEM/CT)	1994; Othman and Benson, 1993)
Wet-dry / Desiccation	Compacted clay disks or slabs; GCL sheets	Oven or climate chamber cycles: 105 °C drying → saturation; 5–30 cycles	Tap water, saline (CaCl ₂ /NaCl) for chemistry effects	Crack network mapping (image analysis), k, shrink–swell strain, suction	(Albrecht and Benson, 2001; Devapriya and Thyagaraj, 2025; Yesiller et al., 2000)
Erosion (raindrop/rill initiation)	Soil trays (30–100 cm length, controlled slope); cover soil blends	Rainfall simulator, 30–60 mm/h intensity, 30–60 min; repeat with/without vegetation/Erosion Control Products (mats, blankets, geotextiles,etc)	DI water or sediment-laden water	Runoff, sediment mass loss, rill density, infiltration	CEN WG/TC189 rainfall test; erosion control product comparisons (Heili, 2020)
Root intrusion (biointrusion)	GCL specimens (bentonite-based) vs. Geomembrane coupons	Greenhouse or growth-chamber tests: aggressive plant species grown in soil over specimens for weeks–months; sometimes combined with wet-dry cycling	Moist soil or growth medium with controlled irrigation	Root penetration depth (mm), breach occurrence, hydraulic conductivity change	CEN/TS 14416:2014. Geosynthetic barriers—Test method for determining the resistance to roots
Geomembrane aging	HDPE or LLDPE geomembrane coupons (cut from sheets, incl. seams)	Accelerated aging at elevated temperatures (55–85 °C); exposure in air, water, or leachate; long-term oven tests; OIT measurements and Arrhenius extrapolation	Air, deionized water, synthetic landfill leachate; controlled thermal environments	Oxidative Induction Time (OIT), tensile properties, antioxidant depletion curves	(Hsuan and Koerner, 1998; Sangam and Rowe, 2002; Tian et al., 2017)
Chemical weathering of mineral barriers	Compacted clays (kaolinite/illite/bentonite or blends), bentonite-amended soils, cement-treated layers; compacted aggregates at transitions	Batch or flow-through column tests (30–180+ days); isothermal or elevated T (20–60 °C); sequential exposures (acidic ↔ alkaline), sulfate-attack cycles, CO ₂ -enriched atmosphere; ionic-strength and cation-exchange series (Na→Ca/Mg)	Saline solutions (NaCl, CaCl ₂ , MgCl ₂), alkaline cement porewater simulants, elevated CO ₂	Hydraulic conductivity, swelling pressure, Atterberg limits, CEC, mineralogy (XRD/SEM), effluent chemistry	(Pusch and Karnland, 1996)

In the frame of the EURAD2 SUDOKU WP, experiments simulating extreme rainfall events and investigation of erosional patterns and resulting sediment flux output are being carried out by the Mine ParisTech and ANDRA.

3.2.2 In-situ Mock-ups

3.2.2.1 Centre de l'Aube – ANDRA

The Experimental Cover Structure (SEC) of the Centre de l'Aube (CSA) was designed to validate the concept of a multi-layer cover based on Aptian clay, which was proposed for the CSA cover (Figure 3-1).

The objective of the SEC is to test, at full scale, the implementation conditions (practical aspect) and the hydraulic behavior (safety aspect) of the CSA cover concept over several years. In particular, the aim is to confirm, through a representative test of the final cover, that the overall impermeability achieves sufficient performance with regard to the safety function of "protecting waste from meteoric water" in the repository.



Figure 3-1 Picture of the Experimental Cover Structure in 1995

The two cover panels allow the waterproofing performance of a clay layer to be verified by testing two thicknesses for this layer: 0.6 m thick for the left plot (north panel) and 1.5 m for the right plot (south panel) as described by Figure 3-2.

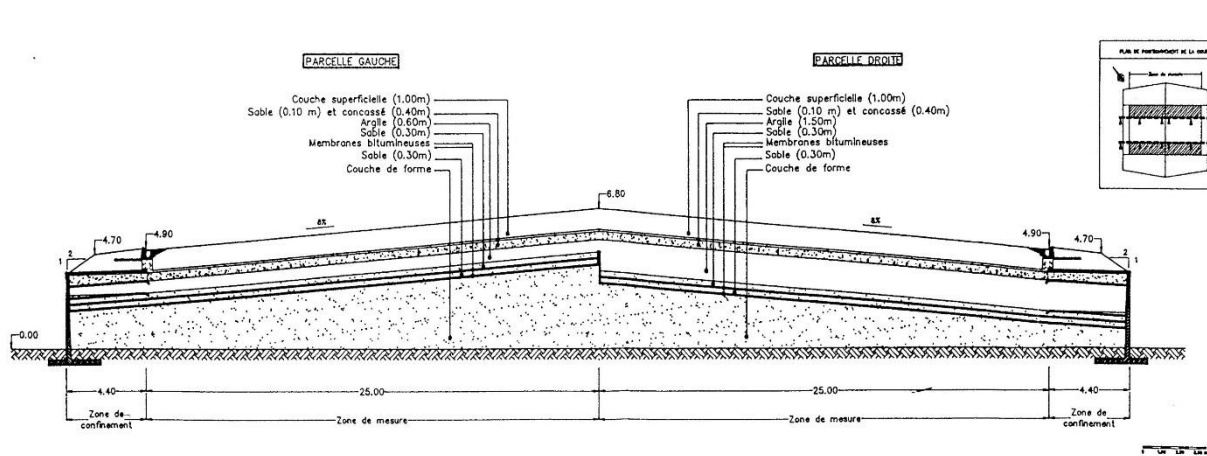


Figure 3-2 Schematic view of the Experimental Cover Structure

The SEC structure is composed of two plots (right and left facing north) that form a double roof with an 8% slope. At the front and rear, this double roof is bordered by side slopes, while at the two lowest points of the roof, it is bordered by retaining walls. On each panel, a central zone allows measurements to be taken without disturbance from edge effects. Indeed, this part is surrounded by protection zones that

protect it from edge effects and allow reliable measurements to be obtained without disturbance from the periphery.

The SEC's instrumentation made it possible to monitor the hydraulic, water, and mechanical behavior of this structure. This experiment was initially monitored for approximately ten years under natural climatic conditions, from 1996 to 2006, in order to obtain an average behavior between years of low, normal, and high rainfall. In the early 2000s, the notion of anthropogenic climate change led to the consideration of the possibility of milder, wetter winters in the future, and drier, hotter summers.

Thus, from 2006 to 2008, this test bed was watered to artificially increase rainfall and increase the flow of water reaching the impermeable barrier (the annual rainfall during these two years was doubled). Then, starting in 2010, a translucent roof (greenhouse) was installed over the SEC to protect it from rain and promote evaporation in order to create conditions of extreme drought. The objective was to verify that the clay of the impermeable barrier was well protected by the biological barrier and allowed it to retain its water content sufficiently to prevent shrinkage cracks from drying out.

On this point, a study on the risk of shrinkage cracks occurring in the event of significant drying out of the clay of the impermeable barrier was conducted in 2000. This study consisted of two phases: (i) estimation of the water content threshold below which cracking is likely to occur, i.e., 26.8% for the clay of the Lower Aptian of the Aube, (ii) simulation of 300 dry years of the 1976 type, based on the hydrodynamic model of the SEC. The results showed that at no time was the critical water content reached, and that the values showed that the water contents always remained above 32%. Subsequently, the hydroclimatic scenario was tightened (drier September and February compared to the reference year 1976), giving almost identical results. Finally, the implementation of the greenhouse in 2010 provided an opportunity to experimentally verify these results.



Figure 3-3 View of the Experimental Cover Structure in 2010

Results

The results of the SEC monitoring since 1996 demonstrate very good performance:

- from 1996 to 2006 under natural climatic conditions, the measured infiltration rate is on average $2.61 \text{ L.m}^{-2}.\text{year}^{-1}$ for the North panel (clay thickness: 0.60 m) and $0.11 \text{ L.m}^{-2}.\text{year}^{-1}$ for the South panel (clay thickness: 1.50 m); the multi-layer cover based on clay and Aptian sand meets the performance objective with infiltration of less than $5 \text{ L.m}^{-2}.\text{year}^{-1}$.
- from 2006 to 2008, the cover maintains good performance even in situations of very intense rainfall (watering during dry periods thus doubling the annual rainfall), with infiltration values always lower than $5 \text{ L.m}^{-2}.\text{year}^{-1}$, with $4.1 \text{ L.m}^{-2}.\text{year}^{-1}$ for the North panel (clay thickness: 0.60 m), and $0.2 \text{ L.m}^{-2}.\text{year}^{-1}$ for the South panel (clay thickness: 1.50 m).
- from 2010 to 2021 in conditions of extreme drought: after more than eleven years without any rain and with high temperatures favoring evapotranspiration, an excavation (Figure 3-4) made it possible to measure the water content of the clay layer of the impermeable barrier and to verify the absence of a desiccation crack.



Figure 3-4 Measurement of the water content in clay layer of the SEC (10/05/2021)

Firstly, the observations made during the excavation confirmed on the one hand the extreme dryness of the surface materials (sand-clay biological barrier), with desiccation cracks descending to the layer of sand located above the crushed rock. On the other hand, the clay located under the crushed rock appeared very wet and plastic, and without any desiccation cracks.

Secondly, the samples showed water contents (by weight) of:

- the biological barrier of around 6%;
- the cover clay:
 - 18% for samples located 10 cm below the crushed rock/clay interface;
 - 20% for samples located 80 cm below the crushed rock/clay interface.

Thus, the water content of the clays in the impermeable barrier is very satisfactory, with water contents of around 18 to 20%, close to those measured when they were installed in 1995. This confirms the protective role of the biological barrier, particularly against desiccation phenomena.

In conclusion, the Experimental Cover Structure demonstrated the effectiveness of this multi-layer cover concept in the face of various climatic conditions: natural conditions, intense rainfall and extreme drought. The measured infiltration remains below the single objective of $5 \text{ L.m}^{-2}.\text{year}^{-1}$, and the risk of shrinkage cracks (desiccation) appearing in the clay of the impermeable barrier is eliminated. This demonstrates the effectiveness and robustness of this cover concept.

3.2.2.2 Spain

The final stage of a near-surface disposal focuses on ensuring there is no impact on the population or the environment, and on achieving its integration into the surrounding landscape. Prior to drawing up the definitive project for the construction of the long-term cover, Enresa decided, in 2008, to initiate two mock up tests to evaluate two previously defined alternatives and to simultaneously acquire construction experience and obtain experimental information for supporting the decisions to be taken in the final detailed long term cover design.

The basic objectives of the cover tests are as follows:

- To acquire construction experience prior to the execution of the long-term cover over the disposal platforms. In this respect, the feedback already obtained has provided very useful information for the implementation of the different materials and for the construction methods to be used on site.

- Analysis of the differences in behaviour and performance of the two test covers, as input to the definition of the detailed design of the final cover.
- Acquisition of quantitative data for El Cabril site on significant variables, basically erosion and seepage rates, which will largely determine the technical options to be implemented.
- Analysis of the thermohydraulic behaviour of each of the test covers, both overall and for each of the constituent parts (a single layer or multiple layers with given functionalities).
- Development of a thermohydraulic model of both cover designs, serving as a support tool for modelling other similar systems with different geometries to be used in design and performance modelling activities.

Basically, four types of activities are performed to verify the operation of the covers:

- Acquisition, analysis, and evaluation of the data obtained from the sensors emplaced in both prototypes. Based on these data and by applying previously established calculation methodologies, it is possible to determine significant system variables, for example the amount of water retained in a layer, seepage rates, rates of evapotranspiration, etc.
- Acquisition of flows drained through certain layers and the system, measured either by passive media (volume of recipients) or using flowmeters.
- Characterization of the materials forming the layers, an activity that supports system modelling and facilitates the interpretation of the acquired data. Special emphasis is laid on the measurement of hydraulic parameters such as conductivity and the retention curves of the materials used.
- System modelling. By using already available thermohydraulic codes, ad hoc developments may be undertaken for modelling of the performance of each of the tests and/or its components.

The basic criteria and requirements that the cover must satisfy are:

- Durability, the cover should last 300 years before degradation.
- Infiltration through the cover 1,5 l/m²/year.
- Erosion reduction (wind and runoff) below 0,5 kg/m²/year.
- Quick rainwater evacuation by means of adequate slopes.
- Bio-intrusion protection to avoid small animals' intrusion and deep-rooted vegetation by means of adequate layering .
- Permeability minimization by means of a clay layer.
- Drainage of infiltration from the top layers of the cover, by means of a granular bed.

Finally, the most immediate application consists of facilitating the detailed design of the long-term cover that is to be built over the LILW disposal platforms. The results obtained will also be of use for the disposal of very low-level waste, since the final covering for this type of disposal cells will in all cases be very similar to those studied.

In the El-Cabril mock-up cove (Figure 3-5), there are two multilayer systems that are separated by a concrete gallery where data acquisition system is place. Test I and II differ in drainage layers (Figure 3-6). The design for Test II features a thick layer of clay over a layer of sand, all under two filter layers (sand and gravel). For Test I, however, a double capillary barrier design is used (two superimposed sequences of clay over a layer of sand). Regarding the biointrusion barrier, the filter layers are relocated on top of the gravel layer, while at the same time, a layer of sand is added between the gravel and clay layers

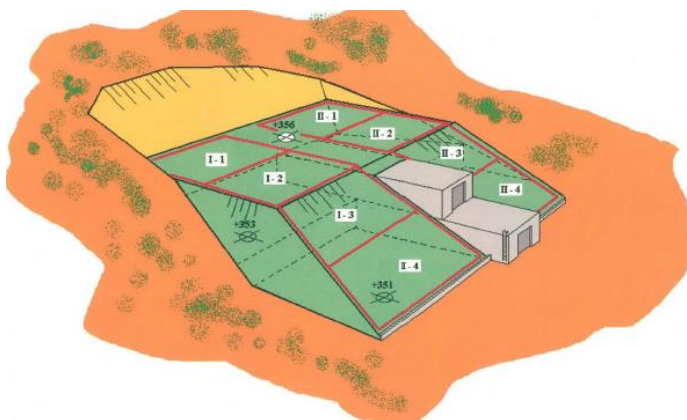


Figure 3-5 General layout of two multilayer systems (Test I and Test II) of the El-Cabril mock-up cover.

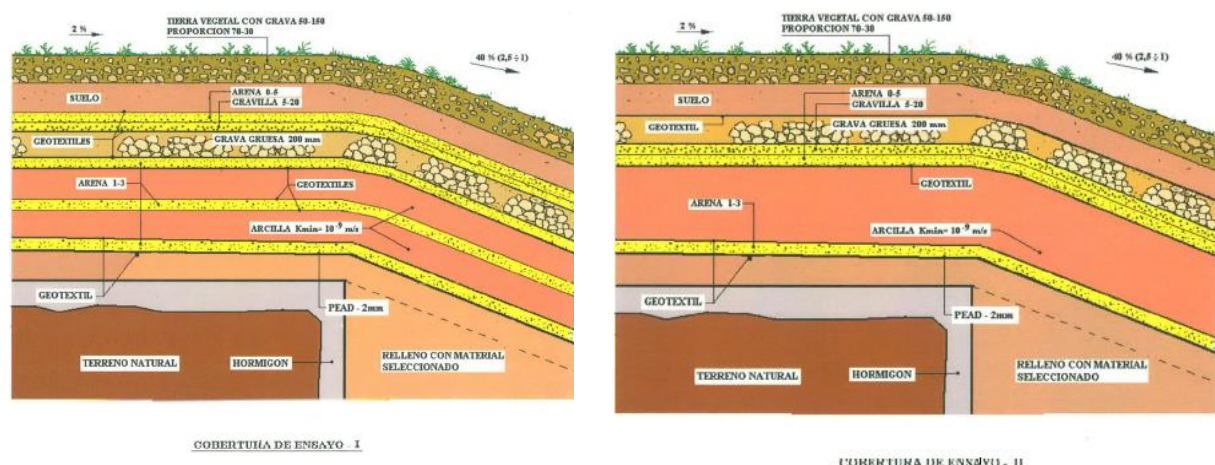


Figure 3-6 Detailed layering of the two multilayer systems of the El-Cabril mock-up cover.

Each multilayer cover design has been instrumented with about 250 sensors to record the evolution of different variables such as temperature and heat flux, capillary pressure and water content. Instrumentation has also been installed to measure some geo-mechanical parameters (geo-referenced levelling milestones and inclinometers) (Figure 3-7). The instrumentation was distributed in four sections per test.

Both Tests have a water collection system along the whole cover that gathers all the infiltrated and superficial water (Figure 3-8).

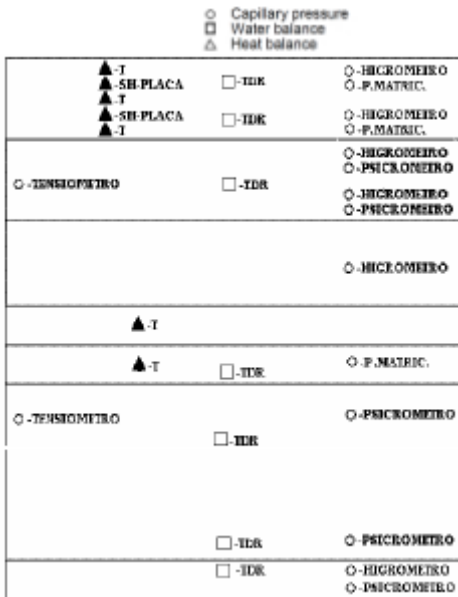


Figure 3-7 Example of sensor types and location in Test I.



Figure 3-8 Details of the drainage water collection system of the El-Cabril mock-up cover.

In addition, a 2D model process has been developed using the CODEBRIGHT Code (Olivella, S. et al., 1996).

The main results of the test up to now are:

- Environmental conditions determine the behaviour of the two upper layers, the temperature oscillation has a remarkable coupling with the atmospheric conditions.
- Wetting and drying cycles occurred in the two upper layers as expected.
- The layer of granular materials placed on the clay layer performs the expected draining function.
- The combination of materials used for filtering and anti-biointrusion layers of Test I (layer of sand and coarse above the larger aggregate) has a better behaviour to avoid the percolation of water.
- The clay layers maintain their initial conditions of placement.
- Two clay layers versus one clay layer do not provide improvements in infiltration performance.
- A temperature attenuation is observed in the concrete wall beneath the cover layers. The annual oscillation range varies between 3 and 5 degrees.

No saturation is observed of the sand layer below the clay in any of the Tests.

3.2.2.3 Belgium – SCK CEN

In the Belgian program for the surface disposal of low- and intermediate-level short-lived radioactive waste at Dessel (Belgium, see section 2.2.1), an experimental cover (“test cover”) will be constructed and monitored for a period of about 30 years. Its design has been developed during the last 15 years, whereas its construction is planned to start in 2026. The test cover will allow to evaluate different safety functions of the final cover including limiting water infiltration, potentially long-term degradation processes (e.g. erosion), to verify assumptions made in the safety assessment (e.g. parameter values) and will contribute to the optimization of the final cover.

The layout and horizontal dimensions are shown in Figure 3-9. The two sides of the test cover will have a different vertical profile (Figure 3-9); one will mainly aim at limiting vertical water movement (resistive barrier), whereas the other will have an enhanced water holding capacity (capacitive barrier, see section 3.1.1).

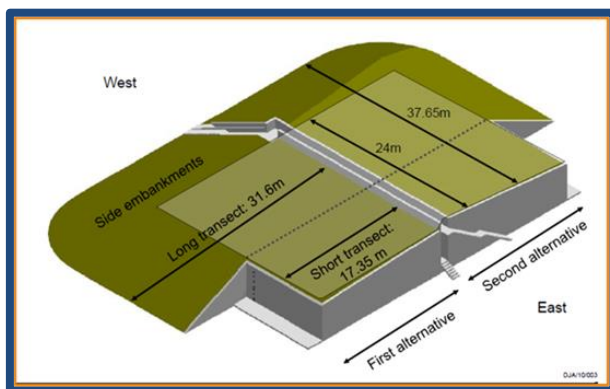


Figure 3-9 Layout of the test cover in the Belgian cAt program.

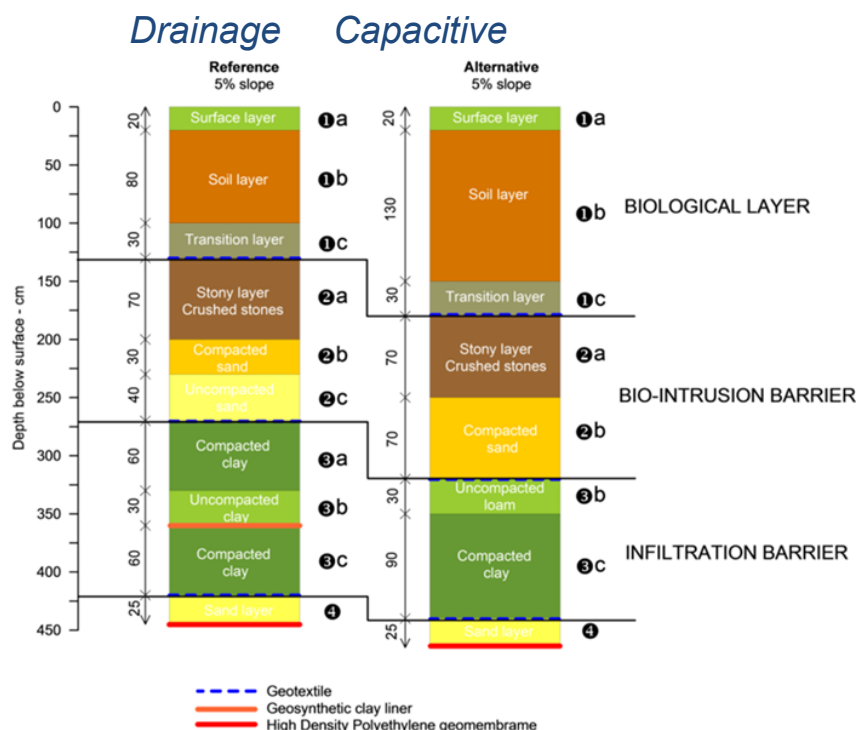


Figure 3-10 The two profiles considered in the test cover of the Belgian cAt program.

Multiple variables will be monitored including meteorological conditions, water content, temperature, moisture potential, surface and subsurface runoff, deep percolation, displacements, pore water composition, oxygen and carbon dioxide content, and mineralogical, hydraulic and mechanical properties. A distributed temperature sensing system will be evaluated as a leak detection system. In addition, several non-destructive methods for monitoring the water balance will be tested such as the ground penetrating radar technique. Besides monitoring and data analyses and interpretation activities, numerical models for water flow and other processes will be developed and applied.

3.3 Modelling

3.3.1 Flow and Energy

Water flow modelling is often based on a continuum approach based on the Darcy-Buckingham law for flow under unsaturated condition (Buckingham, 1907) with the continuity equation, resulting in the so-called Richards' equation (Richards, 1931) – here written for a vertical one-dimensional system (formulation as in Šimůnek and van Genuchten (2008)):

$$\frac{\partial \theta}{\partial t} = \frac{\partial}{\partial z} \left[K(h) \left(\frac{\partial h}{\partial z} \right) + 1 \right] - S$$

where z is the vertical coordinate [L], t is time [T], h is the pressure head [L], θ is the water content [-], K is the unsaturated hydraulic conductivity [$L T^{-1}$] and S is a sink term accounting for root water uptake or any other source or sink [T^{-1}]. Beside initial and boundary conditions, one needs to have the relations between water content and pressure head, and between the unsaturated hydraulic conductivity and pressure head. For modelling purposes, closed-formed functions are the most preferred ones, with the van Genuchten-Mualem model one of the most used functions in (soil) water dynamic modelling (van Genuchten, 1980). However, many other forms exist with extensions towards heterogeneous porous media (e.g., (Durner, 1994; Iden and Durner, 2007; Zumühl and Durner, 1998)) or very dry conditions (e.g. (Iden et al., 2021)). There are ample examples of 1D and 2D simulation efforts based on Richards equation for modelling water flow in (multilayer) covers of (radioactive) waste (e.g., (Guo et al., 2024; Mallants et al., 1999; Ng et al., 2015; Sadek et al., 2007; Zhou et al., 2025)) – only a few dealt also with the integrated multi-layer cover – engineered barrier system in a (near)-surface disposal context (Perko et al., 2017). There are several limitations to the standard formulation of Richards equation. Extensions have been proposed to deal with structured porous media (or soils containing macropores) such as dual-porosity or dual-permeability formulations (Šimůnek and van Genuchten, 2008), and to account for vapor flow. For the latter, formulations as proposed by Saito et al. (2006) can be used or alternatively, multiphase flow models.

Alternatively, modelling water flow is done using data-driven processes. Soil water dynamics predictions based on measured time series have been reported already more than 10 years ago (e.g., (Kornelsen and Coulibaly, 2014); Pan et al. (2012)), but recently, new efforts have been made for prediction of soil water dynamics using data-driven machine learning techniques, e.g. for applications in agriculture (Ali et al., 2015; Azad et al., 2025; Geng et al., 2024; Ivanova, 2025; Manzano et al., 2025; Zhang et al., 2025). We are not aware of any application in the field water flow in multi-layer covers.

The energy balance can be solved simultaneously with the soil water dynamic model. In such case, the atmospheric terms of the energy balance (net radiation, sensible heat flux density, latent heat flux density, surface heat flux density) are taken explicitly into account (e.g., Saito et al. (2006)). Alternatively, models can be used to calculate potential evaporation (e.g. Penman-Monteith model, but other models are available as well, Allen (2013)) as input to the water flow model (potential evaporation as a boundary condition, potential transpiration/root water uptake in the sink term). The actual moisture conditions then dictate the amount of water being evaporated from the surface or taken up the plant roots, leading to predictions of actual evaporation and transpiration.

3.3.2 Degradation processes

There are not many examples of explicit modelling of (multi-)layer covers degradation processes. We limited ourselves here to (i) slope stability analysis, (ii) development of cracks in clays during desiccation, (iii) erosion, and (iv) soil development (bio-intrusion, dissolution of minerals).

Slope stability

Stability modelling of multilayer covers primarily concerns evaluating the potential for movement or failure of the layers within a multilayered cover system. Key factors controlling the stability include: 1) The loadings that the cover may be subjected to such as cover self-weight, equipment during construction, rainfall, snow, erosion, seepage and infiltration, groundwater level, and earthquake or seismic loading; 2) The geometry and materials of the cover: the angle and height of slope, the multilayer materials and geosynthetic layers like geomembrane; 3) Material parameters: the shear strength and constitutive stress-strain behaviour of the multilayer materials and interface materials.

The main methods used for analysis generally include the limit equilibrium methods (LEM), finite element (FE) methods and hybrid methods. LEM divides the slope mass into a number of columns with vertical interfaces and use the conditions for static equilibrium to find the factor of safety (FoS) at vulnerable interfaces (Krahn, 2003; Lam and Fredlund, 1994). The most popular FE tools for slope stability analysis is the strength reduction method (SRM), for which optimization techniques have been successfully used in locating the critical slip line in 2D slopes (Pham and Fredlund, 2003). Hybrid methods, combining the benefits of a FE stress-strain analysis with LEM analyses, were highly recommended by Duncan (1996) and Yu and Batlle (2011).

Development of cracks during desiccation

Several conceptual models are developed to simulate desiccation cracking: energy-based models, stress-controlled cracking model and volume-based model – see Tang et al. (2021), Levatti (2023) and Al-Jeznawi et al. (2025) for reviews. The latter also mentioned models for soil curling – the upward or downward bending of soil surface as a consequence of rearrangement of soil particles during desiccation. Undoubtedly, it is a quite complex modelling approach combining moisture diffusion with fracture mechanics, fracture initiation and propagation. However, several examples of desiccation crack models for clays are available in the literature (Chen et al., 2023; Gui et al., 2016; Yan and Wang, 2025), but mostly limited to clay at the soil surface.

Erosion modelling

Several models are available to estimate erosion losses, also at the scale of a hillslope (applicable for covers as well) (Pandey et al., 2016). Physically based soil erosion and sediment yield models are based on the concept of physics using transfer of mass, momentum, and energy as governing equations (Pandey et al., 2016). Some models are using (variants of the) (Revised) Universal Soil Loss Equation ((R)USLE, Renard et al. (1997); Renard et al. (1991)), applicable for rill and sheet erosion. These models are using also models for overland water flow (kinetic wave equations, Pandey et al. (2016)). Another set of equations are needed for (e.g., Mannings equation for water flow). Jacques et al. (2010a) used the WATEM/SEDEM model (Van Oost et al., 2000) to assess erosion of the multi-layer cover in the Belgian concept (see section 2.2.1). The model consists of two components: (i) calculation of a spatial pattern of mean annual soil erosion rates using the Revised USLE (RUSLE); and (ii) deposition or routing of the eroded sediment to the downslope zone of the cover in function as the transport capacity of each spatial unit. Long-term estimates on average erosion rates (under present day climatic conditions) were obtained. Alternatively, physically based modelling of erosion is possible requiring models for overland flow (including soil water infiltration) and erosion and sediment transport – KINEROS2 is an example of a numerical model (Smith et al., 1995; Smith et al., 1999; Woolhiser et al., 1990). The overland flow can be based on the kinematic wave equation (simplification of the de Saint Venant equations) which is appropriate for most overland flow equations (Morris and Woolhiser, 1980). In addition, a mass balance equation is required for sediment transport with a sink/source term for erosion (accounting for splash

erosion and hydraulic erosion expressing the rate of exchange of sediment between the flowing water and the soil over which it flows). Recently, the interaction with the subsurface has been enhanced by coupling KINEROS2 with a physically based water flow model (HYDRUS-1D, (Chen et al., 2022; Meles et al., 2024)).

Soil development

Several soil forming processes will affect the long-term properties of a multi-layer cover, such as soil organic matter dynamics, bioturbation processes, and mineral dissolution and precipitation. For bioturbation, bio-intrusion potentially creating macropores would affect deep water percolation whereas also bioturbation – movement of soil material by soil fauna – also alters the profile and its properties with time. In the soil research community, mathematical models have been developed for both processes. For bio-intrusion, burrow systems of earthworms have been reproduced (e.g. Bastardie et al. (2002)), and root growth models for bio-intrusion by trees (e.g. Dunbabin et al. (2013); Schnepf et al. (2018)). Bioturbation has been described with a diffusion equation and/or stochastic models (e.g., based on transition matrix theory) (e.g. Michel et al. (2022)). Mechanistic models for soil formation – a slow process over decades or centuries – rely mainly on an integration of flow, solute and heat transport modelling combined with a module for different processes for soil formation (element cycling (surface interaction, soil organic matter dynamics, mineral dynamics), particle transport, mixing (bioturbation) etc.) (Finke, 2024a). In broad sense, coupled reactive transport models can be used for such modelling (Steefel et al., 2015; Steefel et al., 2005), although also specific codes are developed (e.g. SoilGen3, Finke (2024b)). As far as the authors are aware off, none of such models have been used in the framework of degradation modelling of multi-layer covers for radioactive waste management.

4 Durability of cementitious materials under surface disposal condition

Cementitious materials play a fundamental role in the long-term management of radioactive waste, particularly in surface disposal facilities for low and intermediate level waste (LILW). These materials are widely used due to their favourable properties, including high alkalinity, low permeability, mechanical robustness, and capacity to immobilize a wide range of radionuclides through sorption and precipitation mechanisms.

Their role in ensuring containment, both as physical and chemical barriers, is vital over operational and post-closure timescales. However, over time, cement-based materials are exposed to a variety of chemical, physical, and mechanical degradation processes. These processes can gradually alter the microstructure and chemical composition of the cement matrix, thereby influencing key performance indicators such as mechanical integrity, durability, and radionuclide containment efficiency.

In the frame of the EURAD2 SUDOKU WP some of possible degradation processes are evaluated, for their potential effects on the thermo-hydro-mechanical (THM) and chemical (-C) properties of the materials and their possible consequences on radionuclide migration.

In particular, the interest is focused on degradation caused by leaching due to the contact of water containing aggressive ions (e.g., sulphates, nitrates, ...); carbonation which can significantly alter the pH of the cementitious matrix and increase the corrosion of steel rebars used for reinforcing the structures.

Corrosion may produce cracking in the structure deteriorating the mechanical integrity of the material. As new transport pathways are opened, water intrusion is enhanced transitioning from diffusive to increasingly advective regimes, potentially affecting radionuclide mobility.

These degradation mechanisms are often interrelated. Coupled THM-C processes may accelerate degradation, increasing the uncertainties on radionuclide behaviour in the barrier over long timescales. Thus, a comprehensive understanding of degradation processes, their potential interconnections and their implications on material durability and radionuclide transport/retention processes is fundamental to maintain the integrity and safety function of cement-based disposal systems.

This chapter presents an overview of the primary degradation mechanisms affecting cementitious materials in surface disposal systems. Special emphasis is placed on chemical leaching, carbonation, and cracking induced by steel rebar corrosion. The main impact of these processes on the basic properties of the cementitious materials and radionuclide transport is discussed.

4.1 Cementitious materials in disposal systems

Cementitious materials are widely employed in the construction and operation of surface disposal facilities for low and intermediate level radioactive waste (LILW). The most used cementitious material used for construction due to its very high durability is Ordinary Portland Cement (OPC), often blended with supplementary materials such as fly ash, blast furnace slag, or silica fume. These blended cements enhance long-term durability by modifying the hydration products and reducing the permeability of the material.

Cement-based materials are expected to fulfil several critical roles in surface disposal (see also chapter 2) being the structural function the most important, providing mechanical strength and structural integrity to waste packages, vaults, and overpacks, ensuring long-term structural stability. Furthermore, they act as hydraulic barrier, reducing water ingress and controlling the movement of fluids within and around the waste forms. Their effectiveness in fulfilling these roles is linked to key properties as low porosity and permeability that help limiting water movement.

Cement also provides a chemical barrier, buffering the pH at (hyper-)alkaline conditions, which generally improves radionuclide retention through sorption or (co)-precipitation processes, decreasing their mobility.

Nevertheless, all these properties may evolve over time due to environmental factors and different exposure conditions, which causes the onset of various chemical processes, which may cause degradation of the material leading to functional or structural problems (Glasser et al., 2008).

The chemical composition of the hydrated phases of OPC cement (calcium silicate hydrates, C-S-H; portlandite, $\text{Ca}(\text{OH})_2$; hydrated calcium aluminates, AFm and AFt) and their proportions within the matrix, largely determine the chemical stability of the matrix when degrading agents are present. The understanding how these materials can degrade under different attacks and the possible consequences during operational and post-closure conditions is essential for long-term safety assessment.

4.2 Degradation processes

In surface disposal systems, cementitious materials can be exposed to a variety of environmental stressors (atmospheric conditions, soil water or other chemical exposures) that can gradually alter their microstructure, composition, and by consequence their performance.

Within the frame of EURAD2 SUDOKU WP the most significant degradation mechanisms considered are chemical leaching, carbonation, and steel rebar corrosion. Usually, these processes are not isolated as they can act synergistically, accelerating deterioration and reducing the long-term effectiveness of the barriers. Detailed mechanistic studies underscoring the main contributions are needed to a better understanding of their implication on the safety of radioactive waste repositories.

Some of the principal changes expected due to the analysed degradation mechanisms are summarized in Figure 4-1. Some additional information on the discussed degradation mechanisms can be found in Jacques et al. (2021).

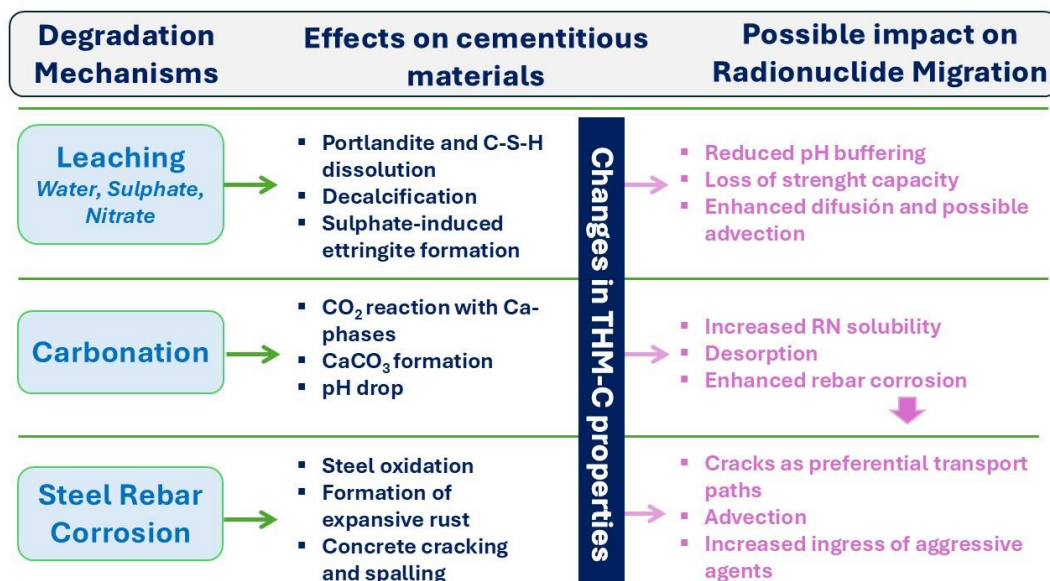


Figure 4-1 Schematic of degradation mechanism effects on cementitious materials and possible impacts

4.2.1 Chemical processes

4.2.1.1 Leaching

Leaching refers to the progressive dissolution and removal of cement hydration products by percolating water or cement in contact with water. The process is mainly controlled by the diffusion of solute ions

within the concrete pore structure and the solubility of different cement phases and the chemical composition of the water. Leaching produces a change of the chemical properties but also on many physical and mechanical properties of cement-based materials such as porosity, elastic modulus, compressive strength, etc (Sellier et al., 2011).

The contact of cement with moisture and water during its time life is unavoidable. The chemical characteristics of the solute are crucial to determine the possible interactions with concrete, as many types of degradation processes can occur which can have different effects on the cementitious materials stability and performance.

In general, the pH is an important parameter. Cement can be degraded when the pH of the solution is less than 7.0, being much more severe as the pH becomes more acid. The role of organic acids, found in some industrial effluents is less studied but can have also an important role in cement stability.

Naturally occurring chlorides, sulphates, nitrates are potentially aggressive ions that can be present in groundwater or in soils porewater. Alteration of rainwater percolating through the multi-layer cover will influence the rate of degradation as well (Jacques et al., 2010b). Natural groundwaters from the Boda formation, Saligny or Dukovany groundwaters will be real cases under study in SUDOKU (Henocq and Missana, 2025).

Finally, the degradation power of the solution depends on the quantity of solute reacting with concrete. Percolating water is expected to cause faster degradation (Chatterjee and Goyns, 2013; Perko et al., 2010).

Pure or low ionic strength water

Ordinary Portland cement (OPC) has highly alkaline porewater, with pH values above 12.5. Pure or low ionic strength waters can attack the material because all the hydrated phases of cement are stable only within a certain range of pH and calcium ions concentration. If these phases enter in contact with solutions with low ion content or low pH, they can start dissolving producing serious changes in material properties (Duchesne and Berton, 2013; Glasser et al., 2008; Kamali et al., 2003; Kamali et al., 2008)

Due to the high concentration gradient, aqueous ions from the external water diffuses into the pore structure and the solid phases (especially the Ca-bearing ones) start dissolving to maintain the water/solid equilibrium.

Portlandite dissolution starts when Ca concentration in solution is lower than approximately 20 mM and the pH lower than 12.5 but the solubility of portlandite is higher at lower temperatures. In degradation processes, preferential dissolution of portlandite is initially observed, followed by ettringite, which start occurring at pH value of 10.7. The decalcification of C-S-H occurs progressively under a wider pH range, after the alteration of portlandite, while the Ca/Si ratio of these hydrates decreases. Thus, the order of dissolution is as follows: Portlandite > AFm > AFt > C–S–H.

These degradation process led to a reduction of the pH of the pore solution and generally to an increase of the porosity, weakening the material over time. Furthermore, this can eventually lead to enhanced permeability and mechanical degradation (Faucon et al., 1998; Faucon et al., 1997).

Sulphates

Sulphate intrusion is one of the most well-known chemical degradation mechanisms in cementitious materials (Ferraris et al., 1997; Glasser, 2009; Menendez et al., 2013; Skalny et al., 1996). It occurs when external sulphates (e.g., from groundwater, seawater, industrial sources or biological activity) react with cement hydration products.

The deterioration of concrete structures due to external sulphate attack is associated with several factors destroying the hydration product forming the backbone of cement paste and binds concrete. As for other solutes, the steps are the following: a) the transport of ions in the inner of the material through its pores; b) the chemical reactions between sulphate ions and cement hydration products; c) formation of

expansive products and stress generation; d) mechanical response of the material to the stress (e.g. cracking).

The aggressiveness of the water to the concrete can be classified depending on the sulphate content. Up to $1000 \text{ mg}\cdot\text{L}^{-1}$, the presence of sulphate is moderated while higher concentrations represent a severe concern, especially if magnesium sulphate is present. The cations associated with sulphate, such as Mg, Ca, or Na, significantly influence the mechanisms of this attack (Brown and Badger, 2000) and must be accounted for.

The extent and kinetics of the degradation process depend on the presence and concentration of other ions as chloride, magnesium or carbonate but also on other factors as the pH of the solution, temperature, and whether the material is subject or not to wet-dry cycles (Mehta and Monteiro, 2000). The characteristic of the material itself as porosity, hydraulic permeability or its composition (C3A or portlandite content) and w/c ratio will also affect the extent of sulphate attack.

Sulphate ions, diffused into the matrix, react with hydration products of tri-calcium aluminate (C3A), hydration products of tetra-calcium ferritealuminate (C4AF) and with calcium hydroxide ($\text{Ca}(\text{OH})_2$), thus forming expansive crystalline products as gypsum, monosulfate (AFm) or ettringite (AFt).

Even ettringite in the first phases of Portland cement hydration contributes to the properties of cement, secondary or delayed ettringite formation can lead to expansive stress, microcracking, and loss of cohesion in the matrix. Expansion resulting from ettringite formation generally causes tensile stresses to develop in the concrete. The increase in porosity due to cracking allows further ingress of sulphate and accelerates the degradation. Sulphates can also react with portlandite to form gypsum ($\text{CaSO}_4\cdot 2\text{H}_2\text{O}$), which can also cause expansion and softening of the cement matrix.

Consequent changes as increased porosity and pores connectivity can compromise the structural and hydraulic barrier functions and loss of the mechanical strength. For analysing the impact of the sulphate attack is important to determine the diffusion coefficients of sulphate in the cementitious matrix, its distribution coefficient in the material; as well as the chemical reactions between the sulphate ions and the impact of cations associated with sulphate ions (Ferraris et al., 2006).

As mentioned, the effect of sulphate can be different according to the original compound from which it comes from. Processes of dissolution and (re)precipitation can both occur but having different relevance. For example, an attack produced by aqueous magnesium sulphate is highly detrimental to the long-term performance of concrete (Santhanam, 2013). In this case, magnesium reacts strongly with the cementitious phases resulting in formation of insoluble substances such as brucite (magnesium hydroxide). While the underlying concrete is protected by the brucite layer formed on the surface –which prevents further entry of the solution, the C-S-H is gradually converted to M-S-H (magnesium silicate hydrate).

Nitrates

The effect of nitrate rich waters on cement degradation is significantly less studied than that of sulphates. Nitrates may be present in some waste streams (fertilizers, sewage, industrial waste) or groundwaters. Even if they are expected to be less aggressive than sulphates, nitrates could also influence cement degradation through different chemical interactions. Nitrate ions can affect the ionic balance of pore solutions and promote the dissolution of calcium phases or alter the chemical buffering capacity of the material (Balonis et al., 2011). Nitrates can also act as an oxidizing agent, accelerating corrosion of embedded steel reinforcement, especially in reinforced concrete structures.

However, it is important mentioning the wide use of ammonium nitrate to accelerate cement degradation (Escadeillas, 2013) in laboratory experiments in respect with pure water. In the highly alkaline environment of concrete, ammonium salts release ammonia gas and hydrogen ions. These ions react with and deplete calcium hydroxide in the concrete, leading to a leaching effect like acid attack. Ammonium nitrate solutions induce a more rapid and severe decalcification of the material relative to

pure water and its effect is variable depending on many experimental conditions (concentration of the solution, w/c ratio, etc.,).

4.2.1.2 Carbonation

Carbonation is a chemical reaction between atmospheric carbon dioxide (CO_2) and the alkaline constituents of cementitious materials, which is known to affect cement microstructure and durability of (reinforced) concrete (Šavija and Luković, 2016). The carbonation process begins when CO_2 diffuses into the porous cement matrix and reacts with hydroxides, for example portlandite, and to a lesser extent C-S-H, producing calcium carbonate (CaCO_3) and releasing water: $\text{Ca}(\text{OH})_2 + \text{CO}_2 \rightarrow \text{CaCO}_3 + \text{H}_2\text{O}$

As it is a diffusion-driven process, carbonation typically occurs slowly. In high-quality concrete, it is estimated to advance at a rate of up to 1.0 mm per year. Carbonation progresses from the concrete surface inward, and the rate depends on cement type and its porosity as well as on external factors as CO_2 concentration, relative humidity and temperature (Liu et al., 2019; Saeki et al., 2025; Xu et al., 2022). Carbonation is strongly influenced by the relative humidity of the concrete. The process is most active when humidity levels are between 50% and 75%. At levels below 25%, carbonation is minimal, while levels above 75% limit carbonation due to moisture in the pores hindering CO_2 penetration (ACI Committee 201, 1992).

The extent of carbonation increases significantly in concrete with a high water-to-cement ratio, low cement content, inadequate curing, low strength, or a highly porous and permeable material.

The consequences of material carbonation are multiple. As far as portlandite is consumed, the pH of the pore solution drops from highly alkaline values (~12.5–13) to below 9. This pH reduction has critical consequences for the durability and containment functions of the material. For example, it can lead to a porosity change in the material. Initially, the precipitation of CaCO_3 can clog pores and reduce permeability. However, long-term processes as the decalcification of C-S-H can increase porosity and promote microcracking. Also, in early stages, slight densification may occur. With progressive carbonation, strength tends to decrease due to the weakening of the C-S-H gel and loss of cohesion.

The most significant concern related to carbonation is the pH drop, which can render radionuclide more mobile and promote steel rebar corrosion, initiating cracking and creating preferential pathways for water and radionuclide transport.

4.2.2 Mechanical processes

As it has been mentioned in the previous sections, the degradation of cementitious materials influences many physical and chemical properties and their overall performance.

The analysed degradation processes (leaching, carbonation, and steel corrosion) affect the THM-C (Thermal, Hydraulic, Mechanical, and Chemical) properties of the materials. Properties as mechanical strength (compressive and tensile strength), modulus of elasticity, can be modified jeopardizing the structural functions of the material. Corrosion-induced cracking (CIC) creates stress concentrations and reduces the load-bearing capacity of structures, leading to early failure. Cracks act as stress concentrators, promoting growth under various loads.

Changes in porosity and mineral composition can also affect thermal properties, such as a decrease in thermal conductivity and variations in thermal expansion, both of which contribute to the development of internal stresses. A non-uniform degradation can also generate internal stresses and lead to the propagation of additional cracks.

It is important to note that degradation processes rarely occur in isolation; instead, they often interact and reinforce one another. For example, leaching increases porosity, which alters thermal conductivity and reduces mechanical strength. Cracking facilitates water ingress, accelerating both leaching and

carbonation—processes that further compromise structural integrity. Additionally, differential thermal responses in degraded areas can induce stress and promote further cracking. These interrelated feedback mechanisms must be considered when evaluating the long-term performance of disposal systems and developing predictive models.

4.2.3 Corrosion

Steel is thermodynamically unstable under typical atmospheric conditions and tends to release energy as it reverts to its natural state—iron oxide, commonly known as rust. This transformation is known as corrosion.

Corrosion of reinforcing steel rebars and other embedded metals is one of the most critical mechanisms of concrete degradation. As steel corrodes, the resulting corrosion products occupy a greater volume than the original metal. This expansion generates internal tensile stresses that can lead to cracking, delamination, and spalling of the concrete.

While steel has a natural tendency to corrode, the highly alkaline environment of concrete (pH 12–13) provides inherent protection. At this pH, a thin passive oxide film forms on the steel surface, significantly reducing the rate of corrosion by preventing metal atoms from dissolving into the surrounding environment. This passive film is not able to stop corrosion completely, but it slows it to an insignificant rate—typically around 0.1 µm per year. Long-term exposure to aggressive agents such as CO₂, chlorides, and moisture can lead to de-passivation and initiation of corrosion, and when the protective layer is consumed, corrosion rates can be more than 1000 times higher (ACI Committee 222, 2001).

Key factors controlling the corrosion rate are the availability of oxygen, the concrete's electrical resistivity and relative humidity, as well as its pH and temperature (Clear, 1976). Once initiated, the corrosion of steel in concrete produces iron oxides and hydroxides (rust), which occupy a larger volume than the original metal—up to 6–10 times more. The expansive pressure generated by corrosion products can exceed the tensile strength of the surrounding concrete, leading to crack initiation around the steel bars or crack propagation toward the surface as well as spalling or delamination of the concrete cover. These cracks not only compromise mechanical performance, but also create preferential pathways for water, gases, and radionuclide transport. Cracking weakens the structure, reduces load-bearing capacity, and increases vulnerability to external stresses.

The immediate consequence of cracking is the enhanced permeability, increasing the diffusion and advection pathways, accelerating leaching, carbonation, and other degradation processes, which in turn can increase corrosion rates. Finally, cracks can significantly reduce the diffusive barrier function of the concrete, especially when connected to macropores or interfaces.

Chlorides

The effect of chlorides in cement degradation is widely described in the literature and many studies have been carried out to determine chloride diffusivities in cementitious materials (Castellote and Andrade, 2006; Castellote et al., 2002; Poulsen and Mejlbø, 2006; Tang and Nilsson, 1993). Chloride ions can be present due to seawater environment, then in conjunction with other salts (e.g. sulphate) (Li et al., 2025) and references therein).

Sea water contains approximately 3.5 wt% of salt. The ionic concentrations of Na and Cl are the highest, typically around 11000 and 20000 mg·L⁻¹ respectively, but it can also contain Mg and sulphate, (around 1500 and 3000 mg·L⁻¹ respectively).

The use of de-icing salts also is a possible source of chloride.

The exposure of reinforced cement to chlorides is considered the most important cause of premature steel corrosion in reinforced materials if oxygen and moisture are also available to sustain the reaction. Chloride ions penetrate concrete and reach the steel reinforcement, breaking down the passive oxide layer that normally protects it – this corrosion process is called pitting corrosion.

4.2.4 Consequences

The described changes can also affect radionuclide mobility. In pristine cementitious systems, radionuclide migration is typically dominated by diffusion, due to low permeability and restricted water flow. Over time, degradation mechanisms alter this balance. Cracking from corrosion opens preferential advective pathways, potentially allowing faster and more localized migration of radionuclides.

Increased porosity and connectivity (from leaching or carbonation) reduce diffusive resistance and allow higher moisture and ion fluxes. Localized zones of altered chemistry (e.g., decalcified fronts) can create heterogeneous transport regimes.

For what concerns adsorption and retardation mechanisms, the cementitious matrices have high pH and under these alkaline conditions many radionuclides present very low solubility being easily retained in the material. Carbonation and leaching can lower the pH fostering desorption or dissolution processes increasing their mobility. The complexation with carbonate species also forms complexes with higher solubility.

Hydrated phases (especially C-S-H) are key sorbent for many radionuclides. Their decalcification / dissolution is expected to modify the adsorption properties.

The presence of chloride, sulphate, nitrate can be competitive for adsorption of anionic species (selenite, technetium etc.,)

These aspects are further elaborated in chapter 5.

4.3 Modelling the degradation processes

Given the extended operational and post-closure periods of surface disposal facilities—often spanning hundreds to thousands of years—predictive modelling is essential for understanding the long-term evolution of cementitious barriers and their influence on radionuclide transport. Such models incorporate experimental data, material characteristics, and degradation kinetics to simulate complex, coupled processes under realistic conditions. Future studies must continue to bridge experimental, modelling, and field-scale data to refine and improve safety assessments.

As far as we aware of, modelling of the mechanical degradation in the context of a near-surface disposal is not well established. As a starting point, Dauzères et al. (2022) and Vidal et al. (2024) provide information on chemo-mechanical modelling of cementitious materials, both for saturated and unsaturated conditions but for conditions representative for geological disposal conditions.

4.3.1 Chemical processes

During the last decades, significant progress has been made in modelling chemical degradation of cementitious systems by developing geochemical tools and databases – see section 4.3.2 in Deissmann et al. (2025). Such modelling is based on thermodynamic modelling of geochemical processes (for cement systems, mainly aqueous speciation and equilibrium mineral precipitation and dissolution including solid solutions – see section 4.1.5 in Deissmann et al. (2025)). Coupling geochemistry with flow and transport models (in so-called coupled reactive transport models, Steefel et al. (2015)) allows for assessing spatial-temporal evolution of degradation in cementitious barriers – the mathematical framework is presented in many reports and books – see also section 4.1 in Deissmann et al. (2025). Examples of such modelling are available for example from the EURAD ACED work package (Jacques et al., 2024), but mainly for saturated conditions in geological repository conditions (in clay or granite). Several examples of geochemical modelling of leaching and/or ingress (of e.g. CO₂, S, Mg) and reactive transport models for leaching are also available in Jacques (2025), but also for saturated conditions.

4.3.1.1 Leaching

Cement degradation is an inevitable process, as infiltrating water interacts with cement materials over time. Understanding the chemical and physical evolution of cement properties and its porewater is

essential for accurately describing repository scenarios, designing experiments, and interpreting data through modelling. Initial thermodynamic models (Berner, 1992) described this degradation process using solubility data for various cement phases. These models laid the foundation for defining degradation stages.

The schematic diagram illustrating the different stages of cement degradation, due to pure water, is presented in Figure 4-2. Cement degradation progresses can be divided in four main stages, each characterized by a gradual decrease in porewater pH. The rate of degradation depends on factors such as temperature, water flow, and cement composition.

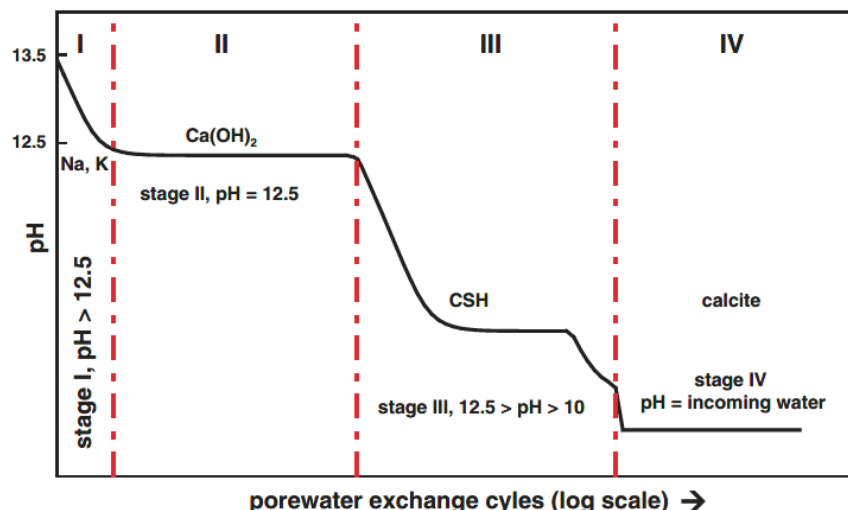


Figure 4-2 Schematic diagram illustrating the evolution of pH in hydrated cement pore fluid as a result of cement degradation (from Ochs et al. (2016)).

In its early interaction with water, cement establishes a hyperalkaline equilibrium with pH values ≥ 13.2 , due to high concentrations of alkali ions (Na and K).

In **Stage I**, the pH is between 13.5 and 12.5. This stage is controlled by the dissolution of soluble alkali salts which releases hydroxyl ions, creating highly alkaline porewater dominated by Na, K, and OH^- . In this pH range, portlandite ($\text{Ca}(\text{OH})_2$) is only sparingly soluble, and calcium release remains limited.

In **Stage II** the pH is around pH 12.5. Once alkalis are depleted, portlandite dissolution governs the system buffering the water with an approximate aqueous concentration of Ca ions of 20 mM. The equilibrium is maintained by the reaction:



The duration of this stage is proportional to the portlandite content of the cement.

In **Stage III**, the pH is between 12.5 and 10. Following portlandite depletion, the pH is buffered by calcium–silicate–hydrate (CSH) phases. Their dissolution depends on the Ca/Si ratio: C-S-H with higher Ca/Si ratios dissolve earlier and buffer at higher pH (e.g., Ca/Si ≈ 1.65 at pH 12.4). As pH decreases, the Ca/Si ratio declines to ≈ 0.80 at pH 11.0 (Atkins and Glasser, 1992). Ultimately, C-S-H dissolution stabilizes the system at pH 10.0.

In **Stage IV**, the pH is lower than 10. Once CSH and other phases are exhausted, porewater chemistry is controlled by calcite dissolution and the composition of infiltrating groundwater, resulting in pH values below 10.

5 Mobility of RN in degraded concrete

5.1 Properties in solution

The properties of the investigated radionuclides in SUDOKU (^{14}C , ^{36}Cl , ^{99}Tc , ^{129}I , and ^{93}Mo) as solute on cementitious waters are evaluated by geochemical modelling according to thermodynamic databases such as Thermochimie (Giffaut et al., 2014), OECD/NEA TDB (Lee et al., 2021), PSI chemical thermodynamic database (Hummel and Thoenen, 2021), Thermoddem (Blanc, 2017), or THEREDA database (Moog et al., 2015). The properties in solution of these elements are characterized by their speciation and their solubility related to a solid phase which is defined from modelling results or expert opinion. For instance, Berner (1999) and Wang (2013) have proposed solubility values and/or speciation for the radionuclides in cementitious environments. It can be remarked here that the concentration in solution for ^{36}Cl , ^{129}I , ^{99}Tc is not limited.

5.2 Sorption properties

Sorption is a generic term, which covers the processes of absorption, physical adsorption and chemical adsorption (Evans, 2008). Sorption mechanisms depend on the chemical speciation of the sorbate, and the chemical and physical properties of the sorbent. As cited by Wieland and Van Loon (2003), who referred to (Cocke and Mollah, 1993) and Gougar et al. (1996) “the immobilization potential of cement originates from its selective binding properties for radioelements. Cation and anion binding by cementitious materials can be classified into particular uptake mechanisms : (i) precipitation or surface precipitation, i.e., the formation of a solid phase of pure or mixed composition without forming a solid solution, (ii) solid-solution formation and co-precipitation, i.e., incorporation of foreign ions in the structure of a solid phase by precipitation with or diffusion into an existing solid phase, and (iii) specific adsorption, i.e., the formation of covalent bonds between the sorbing species and the solid surface (inner-sphere surface complexation) or replacement of one adsorbed, readily exchangeable ion by another (ion exchange, outer-sphere complexation)”.

In general, the radionuclide sorption in cement-based materials is described as the partitioning of a radionuclide between cement pore water and the cementitious material in terms of a distribution ratio, Rd , given by (Wieland & Van Loon, 2002):

$$Rd = \frac{\text{Quantity of a radionuclide sorbed per unit mass cement}}{\text{Equilibrium concentration of the radionuclide in pore water}} \text{ (m}^3 \cdot \text{kg}^{-1}\text{)}$$

The above expression represents the depletion of the radionuclide from solution due to uptake by the solid. The amount of a radionuclide sorbed is determined by the difference between the initial radionuclide concentration and the equilibrium concentration in solution (Allard et al., 1984):

$$Rd = \frac{C_{eq} - C_0}{C_{eq}} \frac{V}{m}$$

Many sorption data of radionuclides in cement-based materials have been produced during the last decades (Evans, 2008). However, this multitude of data is mainly explained by the variety of cementitious systems investigated, i.e. various cement types and materials (HCP, mortars, individual phases). Consequently, as mentioned by (Wieland and Van Loon, 2003), “the large pool of cement sorption data available to date originates from single-point sorption measurements with radionuclides on cementitious systems i.e. hydrated cement, individual cement minerals. At best, the data sets consist of sorption kinetic and isotherm measurements as well as sorption studies conducted at varying pH in the alkaline pH range ($\text{pH} \geq 11$)”.

The Rd approach, mainly consisting of measuring this factor by batch sorption experiments, does not provide any specific information on the sorption mechanism. The latter information can only be obtained based on additional experimental investigations, such as measurements at increasing solute

concentrations (isotherms) and reversibility tests, or spectroscopic investigations on the coordination environment of the sorbate (Wieland, 2014). As seen previously, several mechanisms can be listed to explain the sorption of radionuclides (Evans, 2008), illustrating that the uptake mechanisms in cementitious systems are diverse and intricate, and, in particular, it means that available information on uptake mechanisms is rather limited (Wieland, 2014).

Nevertheless, calcium aluminates (AFm- and AFt-type phases) and calcium silicate hydrates (C-S-H phases) have been identified as prime candidates for cation and anion binding in the cement matrix because of their abundance and appropriate structures (Gougar et al., 1996; Wang and Wang, 2022). Thus, radionuclide uptake by these cement minerals has been specifically studied providing a significant background for understanding the sorption mechanisms (Wieland and Van Loon, 2003).

Most of the Kd values for radionuclide uptake by cement-based materials have been discussed and summarized by Ochs et al. (2016). This work, performed by a scientific committee, aimed to propose Kd values at the different degradation stages of the cement-based materials based on the data in literature (including technical reports and scientific articles).

It can be noted that the uptake of radionuclides depends on the speciation of the species in solution, including the sensitivity to the oxidation degree. Selenium and technetium are clear examples of the influence of the speciation in the case of the cement-based materials i.e. at high pH between 10 and 14. Indeed, several studies have shown a higher sorption of Se(IV) than Se(VI) in cementitious systems such HCP and mortars but also on individual cement hydrates such as C-S-H, AFm, and ettringite (Baur and Johnson, 2003; Bonhoure et al., 2006; Lothenbach et al., 2024; Ochs et al., 2016). However, Grambow et al. (2020) mitigated the gaps between Se(IV) and Se(VI) for Afm and ettringite phases.

These aspects of the properties in solution will be discussed if necessary in the following part where the sorption properties of the radionuclides, studied in the framework of SUDOKU, are specifically presented.

5.2.1 ^{14}C

Carbon-14 is one of the major radionuclides released by the waste because its mobility in the environment, and, consequently, its radiological impact in terms of safety assessment. The case of carbon-14 is specific considering the organic and inorganic forms, and, in addition, the gaseous and solute species. Very few information is available for the gaseous carbon-14, CO_2 or CH_4 . In any case, only solute species will be investigated in SUDOKU, and, this section will focus on $\text{CO}_3^{2-}/\text{HCO}_3^-$ species (inorganic C-14) and low molecular weight organic molecules (organic C-14).

Inorganic carbon-14 can be sorbed by different mechanisms such as electrostatic binding, isotopic exchange or precipitation (Evans, 2008; Grambow et al., 2020). Studies on carbon C-14 have been made in the framework of the European CEBAMA project on CEM I and CEM V cement-based materials at various stages of degradation (Grambow et al., 2020). It has been shown that the $^{14}\text{CO}_3^{2-}$ distribution ratio is greatly affected by the extent of cement degradation, with values ranging between $1600 \pm 268 \text{ L}\cdot\text{kg}^{-1}$ for stage I CEM I HCP, to $120 \pm 36 \text{ L}\cdot\text{kg}^{-1}$ for stage IV. $^{14}\text{CO}_3^{2-}$ uptake on CEM V HCP is significantly higher than on CEM I HCP ($3500 \pm 275 \text{ L}\cdot\text{kg}^{-1}$). The experimental data indicate that ^{14}C adsorption is not attributable solely to isotopic exchange and that precipitation of carbon-14 cannot be excluded. This could explain the results of desorption tests in Figure 5-1. In particular, these results show the effect of the carbonation on carbon-14 sorption, which significantly decreases the Rd value according to the predominance of calcite. The Rd value ($20 \pm 5 \text{ L}\cdot\text{kg}^{-1}$) is then in agreement with Pointeau et al. (2008) cited by Henocq et al. (2018) who measured the ^{14}C uptake on calcite. The results in Figure 5-1(b) show also that there is an irreversible part of the uptake contrary to Figure 5-1 (a) which indicates the contribution of different sorption processes (Grambow et al., 2020).

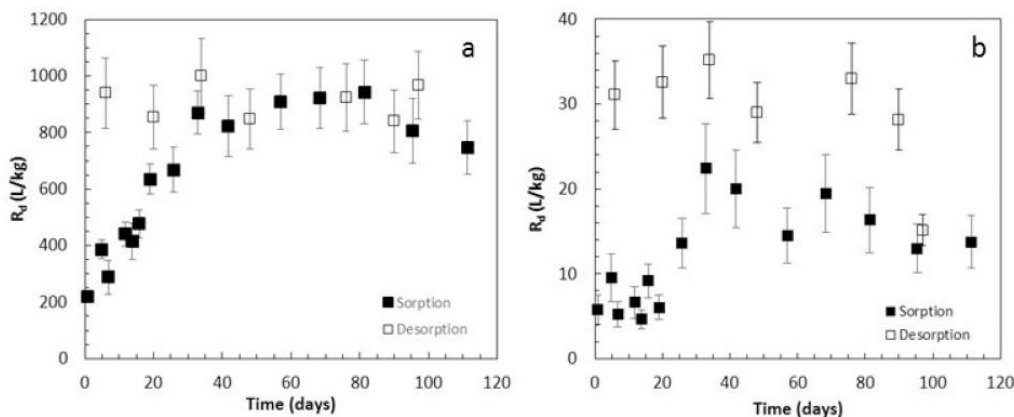


Figure 5-1 Evolution of ^{14}C distribution ratios (R_d) vs time on non-carbonated CEM V HCP (a) and carbonated CEM V HCP (b). Initial ^{14}C concentration is $6 \cdot 10^{-8} \text{ mol.L}^{-1}$ (Grambow et al., 2020).

5.2.2 ^{36}Cl

The retention of chloride by cement-based materials have been extensively studied in the context of civil engineering (Delagrange et al., 1997; Justnes, 1998; Martín-Pérez et al., 2000; Zibara, 2001)). These works demonstrated the chloride binding by the cementitious matrix which depends on the cement composition, especially on the aluminate content. The formation of Friedel's salt is one of the main causes of the chloride uptake with adsorption to the C-S-H surface (Florea and Brouwers, 2012).

Regarding ^{36}Cl , different studies showed a low R_d value which decreases as chloride concentration increases (Jo et al., 2022; Macé et al., 2019) as illustrated by Figure 5-2 and Figure 5-3. Among the anion sorption in cement-based materials, ^{36}Cl has the lower affinity: the affinity order is $^{14}\text{CO}_3^{2-} > ^{75}\text{SeO}_3^{2-} > ^{125}\text{I}^- > ^{36}\text{Cl}^-$ as suggested by Pointeau et al. (2008) (see Figure 5-6(right)).

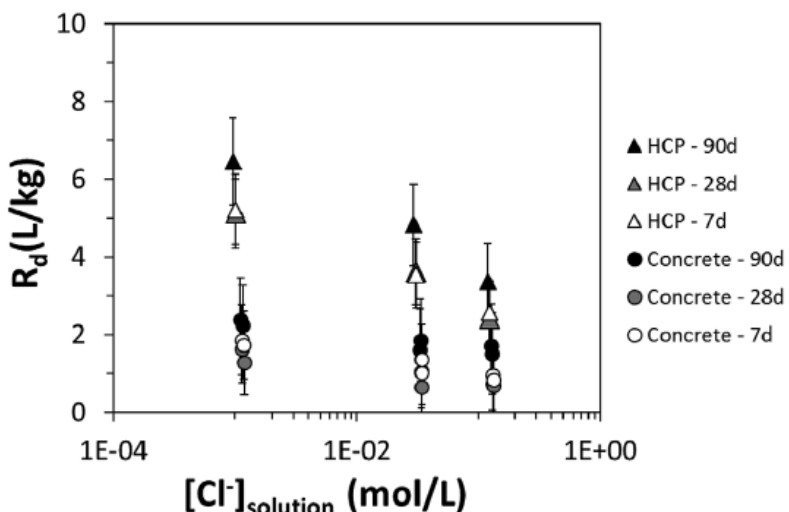


Figure 5-2 Cl-36 distribution ratio, R_d evolution onto HCP and concrete as a function of sorption contact time and chloride concentration in solution (Macé et al., 2019).

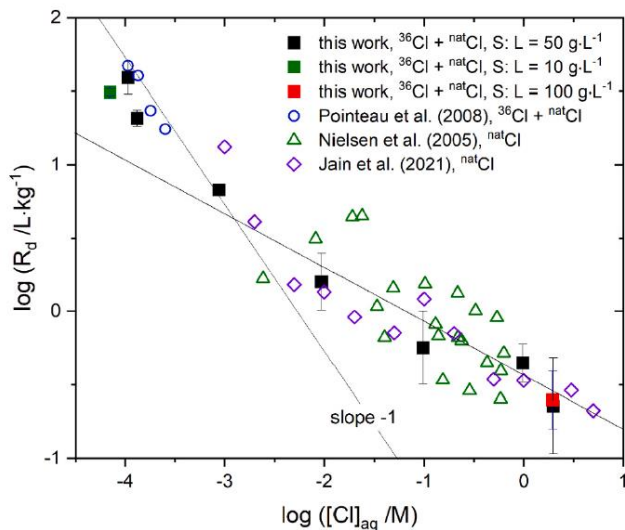


Figure 5-3 Distribution coefficients (R_d) determined in this work (solid symbols) or reported in the literature (empty symbols) for the uptake of Cl by HCP in the degradation stage I (or otherwise at $pH > 12.8$) (Jo et al., 2022)

5.2.3 ^{129}I

Iodine can be sorbed by different mechanisms: (i) Iodide sorption onto cement has been shown to increase with increasing Ca/Si ratios in C–S–H gels suggesting I^- is sorbed electrostatically (Glasser et al., 1989), (Pointeau et al., 2008), and (ii) Aimoz et al. (2012) showed that I^- uptake strongly depends on the anion originally present in the AFm interlayer suggesting an anion exchange between IO_3^- or I^- with SO_4^{2-} groups. Indeed, no I^- uptake was observed in the case of AFm- CO_3 and AFm- Cl_2 , while AFm- SO_4 was found to take up considerable amounts of I^- in its interlayer (Grambow et al., 2020). This observation agrees with the solid solution studies described by Nedyalkova et al. (2021) which measured the I^- sorption by hemicarbonate, monosulfate, and even HS-AFm (Figure 5-4).

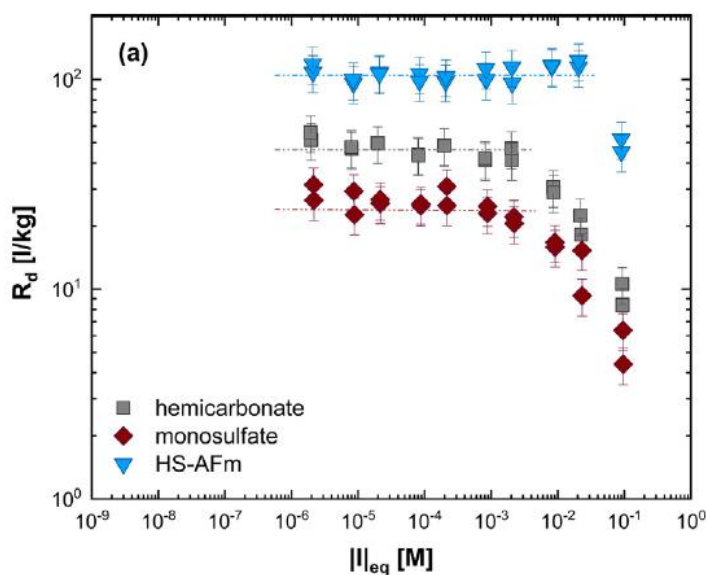


Figure 5-4 R_d values for the sorption of I^- on hemicarbonate, monosulfate and HS-AFm for a S/L ratio of 5.10^{-3} kg/l and $pH 13$ (Nedyalkova et al., 2021)

Grambow et al. (2020) confirmed the dependence of the I^- uptake on the original interlayer occupancy. Structural incorporation of iodide by anion exchange in the interlayer was observed for AFm-SO₄ (Rd $\sim 811 \pm 324 \text{ L}\cdot\text{kg}^{-1}$ at pH 12 and Rd $\sim 30 \pm 5 \text{ L}\cdot\text{kg}^{-1}$ at pH 13) and AFm-CO₃ (Rd $\sim 81 \pm 32 \text{ L}\cdot\text{kg}^{-1}$). The observed decrease of Rd with increasing pH corresponds well to the data of Atkins and Glasser (1992).

Atkins and Glasser (1992) also studied the uptake of iodide and iodate in C-S-H as a function of C/S ratio (*Figure 5-5*) and iodide sorption in HCPs (*Table 5-1*).

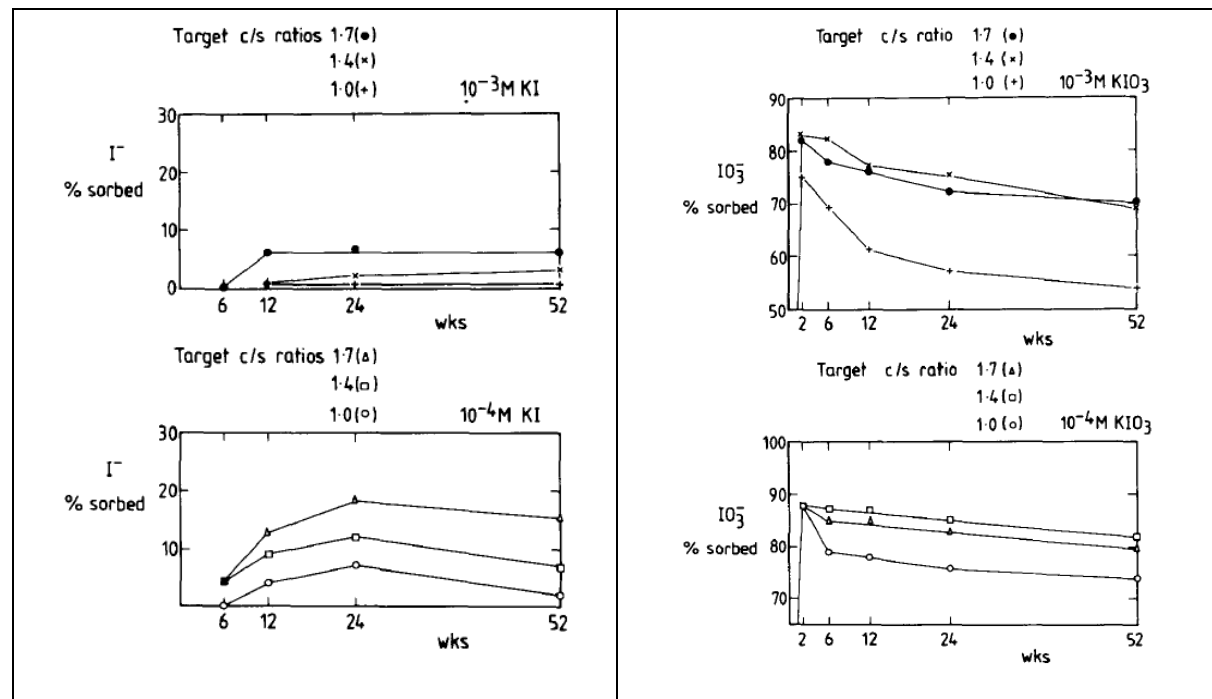


Figure 5-5 Iodide (left) and iodate (right) sorption onto C-S-H as a function of C/S ratio and ageing at 25°C (Atkins and Glasser, 1992).

Table 5-1 Iodide Uptake onto Cement Hydrate Phases (% of Total I Added) (Atkins and Glasser, 1992)

	ca. 10^{-7} M^* (60 d.)	$10^{-3.7} \text{ M}$ (100 d.)	10^{-2} M (100 d.)
OPC	>99	96.5	96
85% BFS	85	77	72

Note. *Initial concentrations.

For I^- uptake in CEM I HCP systems, Pointeau et al. (2008) and Bonhoure et al. (2002) measured Rd values (i) in the range [100; 1000] $\text{L}\cdot\text{kg}^{-1}$ (for degraded HCPs as a function of pH) and (ii) between 20 and 200 $\text{L}\cdot\text{kg}^{-1}$ (for HCP at stage I), respectively (*Figure 5-6*). On the other hand, Grambow et al. (2020) found that iodide and iodate adsorption on crushed CEM I HCP were both adsorbed, with slightly lower sorption of iodide (Rd $\sim 25 \text{ L}\cdot\text{kg}^{-1}$) than iodate (Rd $\sim 140 \text{ L}\cdot\text{kg}^{-1}$).

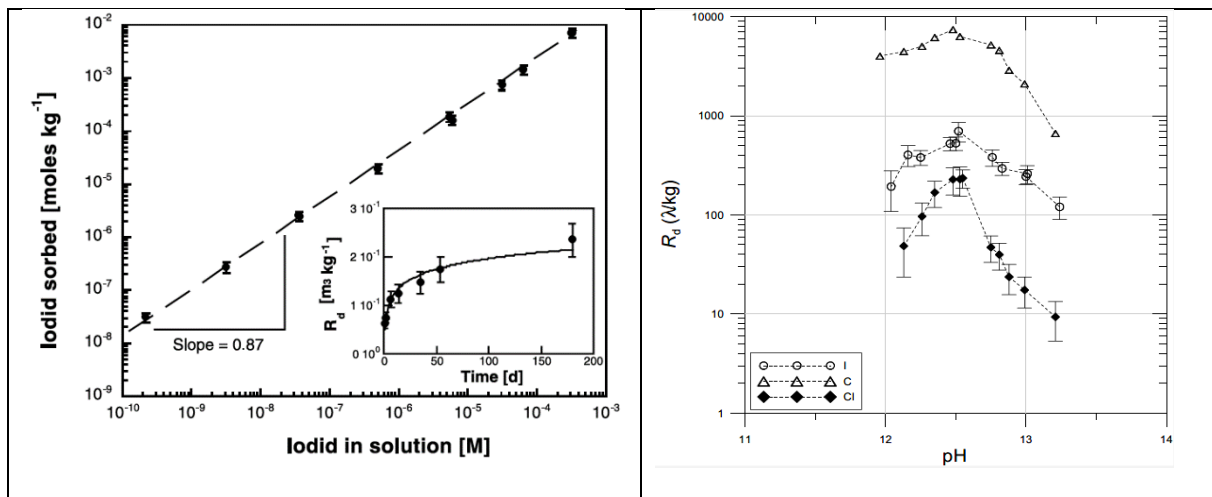
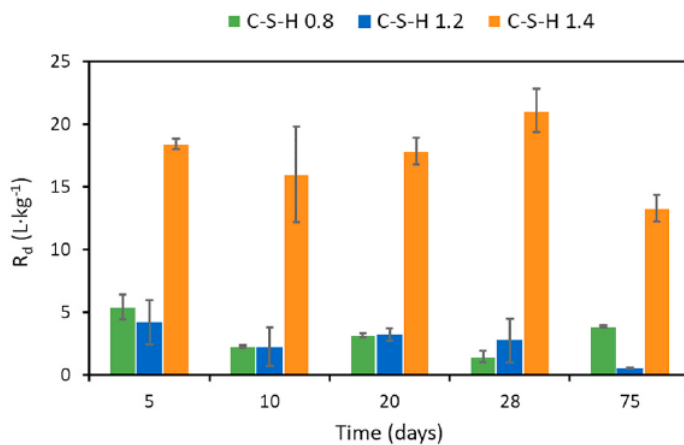


Figure 5-6 Iodide sorption onto HCPs by Bonhoure et al. (2002) (left) and Pointeau et al. (2008) (right)

5.2.4 ⁹³Mo

Molybdenum uptake was studied in HCP (Kindness et al., 1994) and in cement phases such as ettringite by Zhang and Reardon (2003) showing the interaction between the Mo and the cementitious matrix coupled with the formation of CaMoO₄. Ettringite showed a lower anion preference than B(OH)₄⁻, SeO₄²⁻, and CrO₄²⁻. Grambow et al. (2020) presented several studies on molybdate uptake by C-S-H phases and its dependency on the Ca/Si ratio revealing a higher Rd value for high Ca/Si ratios (Figure 5-7). These findings agree with the change in surface charge of C-S-H to positive values at Ca/Si ratios exceeding 1.2 (Churakov et al., 2014), suggesting electrostatic sorption of the molybdate anion on C-S-H.

Figure 5-7 Dependency of MoO₄²⁻ retention on C-S-H phases as function of the Ca/Si ratio and time (Mo initial concentration 10.6 M) (Grambow et al., 2020)

The affinity of Mo with AFm phases has been reported by Grivé and Olmeda (2015), Marty et al. (2018) and Ma et al. (2017) including an incorporation/exchange in the interlayer. Studies on AFt/AFm mixes in CEBAMA project have confirmed the sorption capacity of AFm phases, contrary to ettringite (Grambow et al., 2020). The highest Rd value was observed in AFm phases with values ranging from 1200 to 46400 L·kg⁻¹. On the other hand, Lange et al. (2020) have measured Rd values of Mo by several aluminate phases such as ettringite, AFm and C3AH6 in equilibrium solution (ES) and artificial cement water (ACW) (Figure 5-8(left)). Rd related to AFm phases are slightly lower than Grambow et al. (2020) while ettringite shows higher Rd values. On this latter, it can be noted that ACW has a significant effect

by increasing R_d values by one order of magnitude compared to ES. Lange et al. (2020) have also studied C-S-H phases and calcite (*Figure 5-8(right)*) in ACW and ES. These results agree with those in *Figure 5-7* for ES. ACW also remarkably enhance the sorption of Mo in C-S-H similarly to ettringite. In addition, Caselles et al. (2021) confirmed the results of previous works on Mo in HCP and C-S-H, suggesting that Mo stabilization was mainly controlled by the coprecipitation of powellite (CaMoO_4).

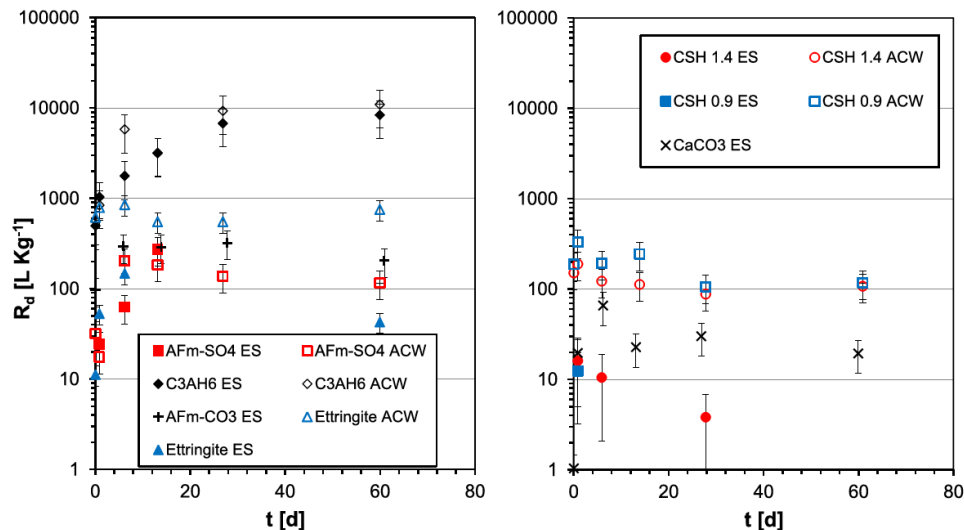


Figure 5-8 Kinetics of the molybdate uptake by various model hydration phases in different solutions: ES for “equilibrium solution”, and ACW for “artificial young cement water (pH 13.3)” (Lange et al., 2020)

5.2.5 ^{99}Tc

^{99}Tc is a redox-sensitive radionuclide, with two main species $\text{Tc}(\text{IV})$ and $\text{Tc}(\text{VII})$. Pertechnetate (TcO_4^-) is the predominant Tc species with the highest oxidation degree. $\text{Tc}(\text{VII})$ has a weak sorption affinity in cement-based materials. In contrast, $\text{Tc}(\text{IV})$ significantly interacts with the cement minerals inducing much higher K_d values compared to the very low K_d values for $\text{Tc}(\text{VII})$ (Ma et al., 2019; Ochs et al., 2016).

The presence of reducing agents in the cement formulation such as blast furnace slag can improve the sorption properties by a partial reduction of pertechnetate anions to the less mobile $\text{Tc}(\text{IV})$ (Allen et al., 1997; Kaplan et al., 2013).

AFm and Aft phases are expected to play a role in the TcO_4^- binding by cementitious matrices (Berner, 1999). Isaacs et al. (2020) have investigated the TcO_4^- retention on several cement individual phases (C-S-H, AFm, Aft, Hydrogarnet, portlandite, calcite). These measurements have confirmed the very low sorption capacity of these minerals with K_d values of TcO_4^- much lower than $10 \text{ L} \cdot \text{kg}^{-1}$ (*Table 5-2*). These results indicate practically no uptake due to exchange for SO_4^{2-} groups (Grambow et al., 2020). On the other hand, K_d values of $\text{Tc}(\text{IV})$ in HCP and C-S-H is greater than $10^3 \text{ L} \cdot \text{kg}^{-1}$ (Ochs et al., 2016).

Table 5-2 Distribution coefficients (R_d) for the uptake of ^{99}Tc by cement hydration phases in various solutions (ES: equilibrium solution; ACW: artificial young cement water (pH 13.3); CH: saturated portlandite solution (pH 12.3)) (Isaacs et al., 2020).

Phase	R_d [$\text{dm}^3 \text{kg}^{-1}$]		
	ES	ACW	CH
C-S-H 0.9	4.5 ± 2.7	4.1 ± 2.7	na
C-S-H 1.4	2.3 ± 2.4	1.9 ± 2.3	na
AFm-SO ₄	4.0 ± 1.9	0.7 ± 1.5	0.6 ± 1.5
AFm-CO ₃	2.3 ± 1.7	na	1.1 ± 1.5
Ettringite	0.6 ± 0.9	0.6 ± 0.9	0.6 ± 0.9
Hydrogarnet C3AH6	0.6 ± 1.6	0.6 ± 1.6	1.0 ± 1.7
Portlandite	na	na	1.0 ± 2.2
Calcite	0.6 ± 2.2	na	0.8 ± 2.2

na – not analysed.

Batch-uptake experiments on crushed HCP were performed in order to study the potential accumulation of reduced Tc on reductive sites such as Fe(II)-bearing phases originating from blast furnace slag (BFS) (Grambow et al., 2020). The uptake experiments conducted for more than 75 days, revealed only minor uptake of TcO_4^- by HCP. As suggested by Grambow et al. (2020), considering the lower content of Fe(II) and/or sulphides, the distribution ratios of HCP based on CEM I tend to be lower ($R_d \sim 2 \text{ L}\cdot\text{kg}^{-1}$) than those obtained for CEBAMA low-pH paste ($R_d \sim 9 \text{ L}\cdot\text{kg}^{-1}$).

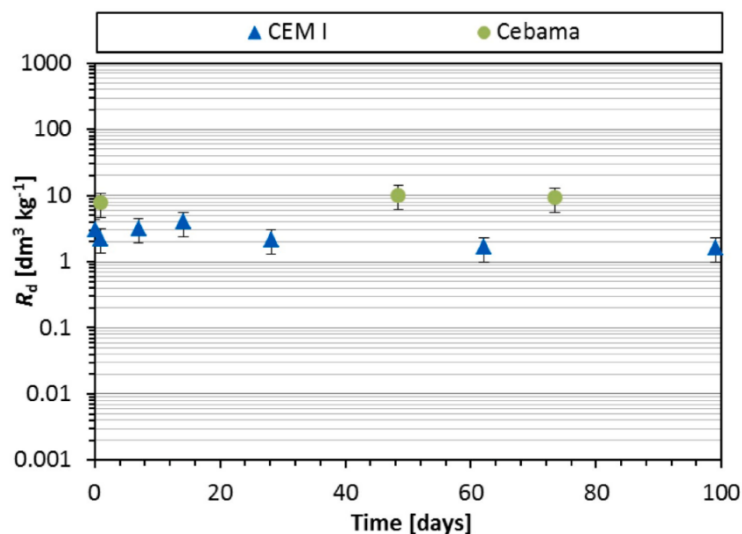


Figure 5-9 Uptake kinetics for $^{99}\text{Tc(VII)}$ by HCP made from CEM I and Cebama reference blend (Isaacs et al., 2020)

The R_d values of the different radionuclides given previously are related on undamaged cement-based materials. Some of the investigated systems were chemically degraded (evolution as a function of pH), but a lack of data is noted for cracked specimens or corroded reinforced materials. A recent Ph.D. work by Marliot (2024) evaluated the diffusion properties through cracked mortars, and consequently a retardation factor was determined. No clear effect of the presence of cracks has been observed on the retardation factor; this work will be also discussed in the following paragraph on diffusion properties.

5.3 Diffusion properties

5.3.1 Introduction

The diffusion properties of cement-based materials were extensively studied during the last decades in the context of civil engineering issues and radioactive waste management. In both cases, it has been shown that the material formulation, especially the water-to-cement ratio (W/C) and cement type, strongly influences the diffusion coefficient. The diffusion coefficient is mainly expressed by the effective diffusion coefficient De which is related to the macroscopic scale; the intrinsic diffusion coefficient at the pore scale (Di or Dp) and the apparent diffusion coefficient Da (which includes the interactions of the tracer with the porous matrix) can also be found in many works (Glaus et al., 2010; Tournassat et al., 2015).

On the other hand, the retardation of the transport is characterised by the rock capacity factor, α , which is related to the porosity ε , the sorption distribution ratio (Rd [$m^3 \cdot kg^{-1}$]), and the dry-bulk density ρ ($[kg \cdot m^{-3}]$), of the porous medium according to the following equation (Glaus et al., 2010)):

$$\alpha = \varepsilon + \rho \cdot R_d$$

The effective diffusion coefficient De and the rock capacity factor α are determined from diffusion experiments performed on tracers in solution; in this part, only works related to radiotracers will be referenced.

Various cement-based materials have been investigated through diffusion tests. The formulations differed with the W/C ratio and the cement type. Consequently, no general trends are available in terms of De values. However, it can be noted that the diffusion coefficient of ternary/quaternary cement mixes is much less than ordinary cement mixes (around a factor 10), and the diffusion coefficient increases as the W/C ratio increases (Richet et al., 2010).

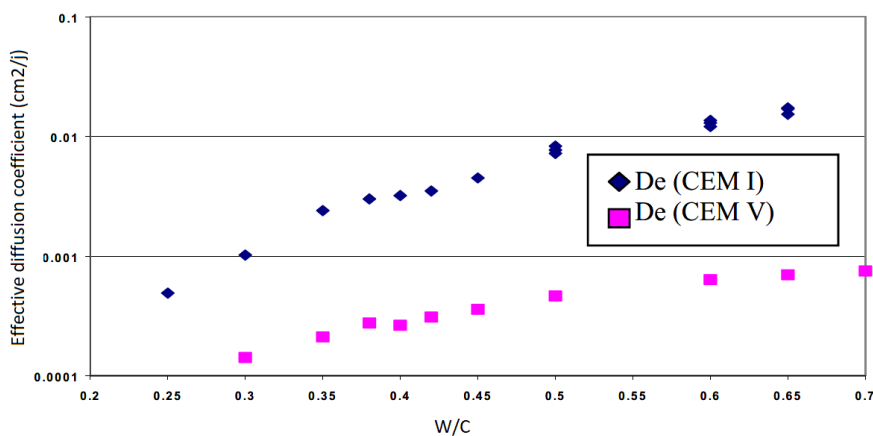


Figure 5-10 Effective diffusion coefficient of tritiated water in CEM I and CEM V HCPs for different W/C ratio (Richet et al., 2010).

5.3.2 Diffusion in cracked samples

The diffusion tests, as presented in Figure 5-10, were mostly performed on sound materials. However, the diffusion of species in solution through damaged cement-based materials is an issue which has been identified since several decades. Nevertheless, due to the experimental challenges for performing diffusion tests on damaged specimens, published studies on this topic are still scarce. Thereafter, some of these references are summarized.

Several works have investigated the influence of the crack width on the diffusion in cracked cementitious samples showing threshold values determining a lower limit from which the diffusion is enhanced by the

cracks, and an upper limit for which the transport properties are equivalent to the diffusion in water (Djerbi et al., 2008; Jang et al., 2010; Kwon et al., 2009; Sahmaran, 2007). Figure 5-11 shows, for various cement-based materials, the linear increase of the diffusion coefficient as a function of the crack width and a plateau when the crack width is higher than $\sim 80 \mu\text{m}$, where the value obtained was the diffusion coefficient in free solution (Djerbi et al., 2008).

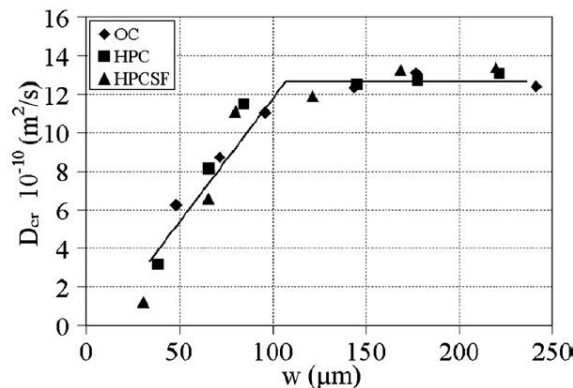


Figure 5-11 Effect of crack width on diffusion coefficient through the crack (Djerbi et al., 2008).

There is a wide range of crack widths where an effect on the diffusion coefficient is observed. That depends on the type of (i) materials, (ii) tracers, (iii) crack generation, and (iv) natural variability. Table 5-3 shows the results of a field investigation where diffusion coefficients have been measured as a function of the crack width; a plateau was not observed for cracks between 0.1 and 0.3 mm (Kwon et al., 2009).

Table 5-3 Results of the field investigation (mean value) (Kwon et al., 2009)

Crack width (mm)	Averaged diffusion coefficient (m^2/s) $\times 10^{-12}$	Surface chloride content (kg/m^3)
Sound concrete	1.46	14.15
0.1	3.02	12.95
0.2	4.27	12.40
0.3	7.82	13.00

Sahmaran (2007) has also shown that the diffusion coefficient of chloride still increases for crack width between 0 and 400 μm (Figure 5-12).

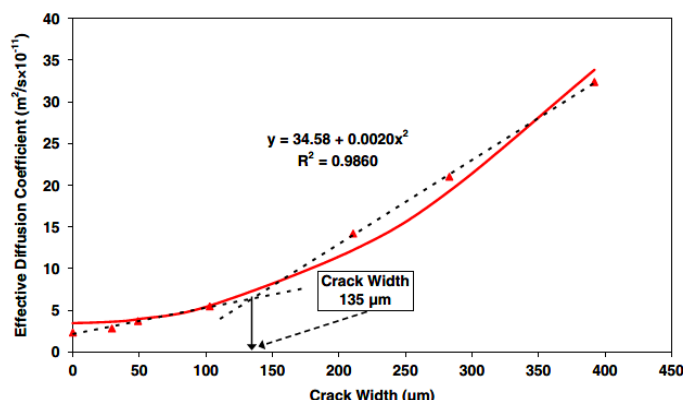


Figure 5-12 Comparison of Diffusion coefficient vs. crack width for mortar deformed under bending load (Sahmaran, 2007)

In addition, the cumulative effect of cracks and leaching was investigated by Tognazzi (1998) revealing the influence of the crack width on the leaching process, and finally, on the diffusion coefficient measured after the leaching time (210 days). For a crack width of 60 μm , the diffusion coefficient increases by 80 % while for a crack width of 350 μm , the increase of the diffusion coefficient is around 500 %.

No overall trend can be highlighted from the published works so far. The impact of the cracks is clear by an enhancement of the solute mobility, but its characterization remains dependent of many factors such as the crack generation and its pattern.

A recent study by Marliot (2024) has investigated the effect of cracks on radionuclide diffusion. In particular, autoradiography imaging has allowed to identify that the radionuclide diffusion was enhanced along the cracks. Figure 5-13 shows the ^{36}Cl diffusion in cracked mortars CEM I and CEM V, indicating that the radiotracer is not localized along the crack but diffuses through the crack surface involving a diffuse zone around the crack.

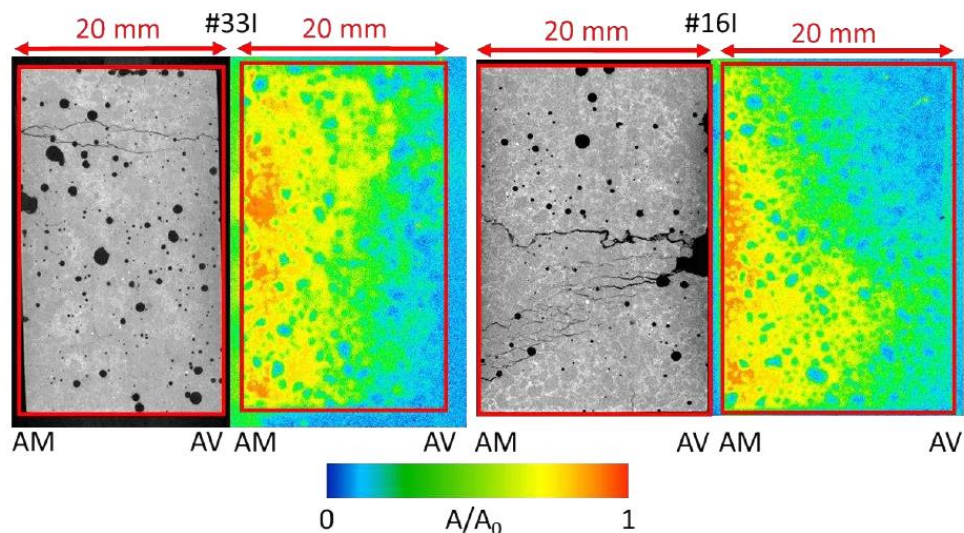


Figure 5-13 ^{36}Cl autoradiographies (colorscale) and tomography images (greyscale) for cracked mortar CEM I (left) and mortar CEM V (right) (Marliot, 2024)

In addition, Marliot (2024) gave results on ^{137}Cs diffusion in cracked mortars CEM I and CEM V which show a similar behaviour than ^{36}Cl for CEM I with a diffuse zone around the crack, but for the mortar CEM V (Figure 5-14(right)), the Cs ingress seems very limited despite the crack revealed by the tomography imaging on the left. For this latter, a self-healing mechanism was assumed. That opens a wide scope on self-healing in damaged cement-based materials and its impact on transport properties (Hou et al., 2022; Jacobsen et al., 1996; Lahmann and Keßler, 2025).

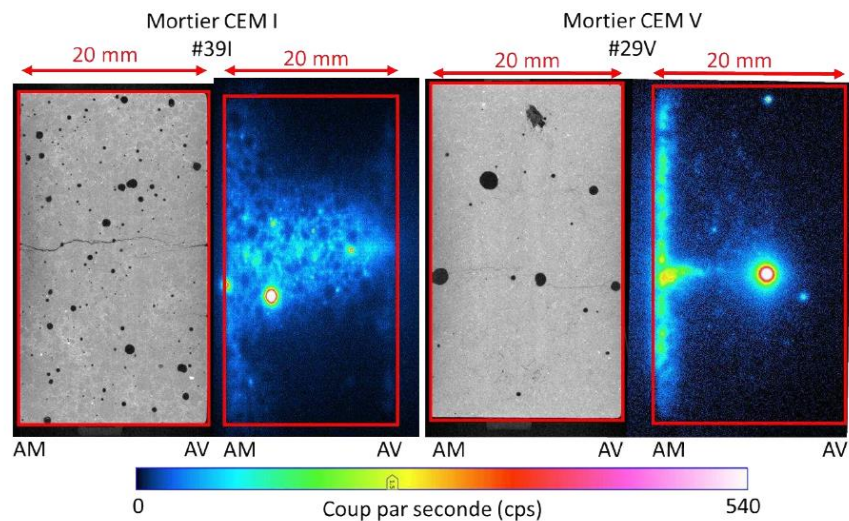


Figure 5-14 ^{137}Cs autoradiographies (colorscale) and tomography images (greyscale) for cracked mortar CEM I (left) and mortar CEM V (right) (Marliot, 2024)

5.3.3 Transport/diffusion in unsaturated conditions

Beside the cement formulation (w/c ratio, cement type), the water-saturation state (characterized by the degree of water saturation S_w or relative humidity RH) will have an effect – a large variation in the relation between water-saturation state and unsaturated diffusion coefficient has been observed between studies (Zhang et al., 2020) – an illustration of this relation is shown in Figure 5-15. In general, one can observe a two-stage decline: first a fast decrease followed by a second more gentle decrease upon the point where the relative diffusivity is zero because there is no connected aqueous pore network. However, the range of saturation degrees between the two stages varies a lot with cement type – the first stage seems to end at saturation degrees between 50-90%, whereas the saturation degree corresponding to a non-connected pore network ranges from 8-52% (Zhang and Zhang, 2014). There is a clear effect of the cement type with factors as water/binding ratio, supplementary material (typically resulting in lower relative diffusivity due to an increase of the volume fraction of small pores) and the interfacial transition zone (typically increasing the relative diffusivity) (Zhang and Zhang, 2014).

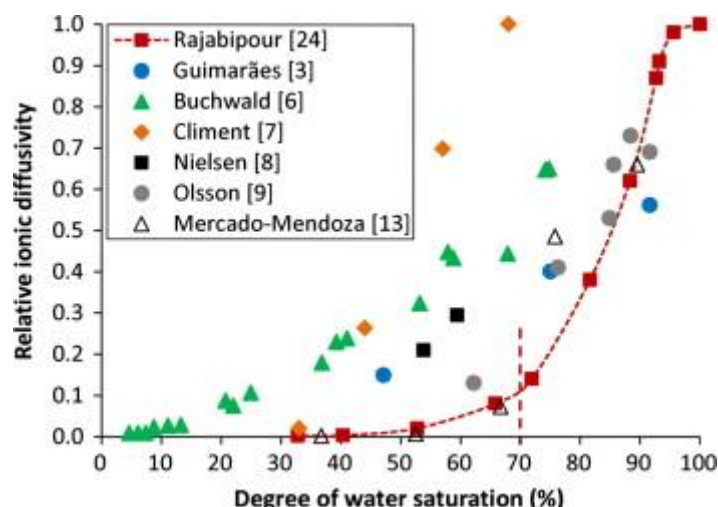


Figure 5-15 – Influence of saturation degree on the relative diffusivity (compared to diffusivity under saturated conditions) in cement-based materials (from Zhang and Zhang (2014) with data from (Rajabipour, 2006), (Buchwald, 2000; Climent et al., 2002; Guimaraes et al., 2011; Nielsen and Geiker, 2003; Olsson et al., 2013)).

There are several models presented in the literature describing these relations, e.g. an S-Shaped curve proposed by Saetta et al. (1993), or an exponential relation by Buchwald (2000). Such relations always have some empirical factor in it, e.g. the relation of Saetta et al. (1993) needs the RH at which the relative diffusivity is 0.5 (can be in a range between ~50-85% from the data in Figure 5-15) or the exponential term in the relation of Buchwald (2000) (reported to be between 3.1 and 4.4 in Olsson et al. (2018) depending on the cement composition).

A further complication is the presence of cracks – in a saturated system, diffusivity through connected cracks will exchange diffusivity (see previous section). However, under unsaturated conditions, cracks will drain quickly – depending on the crack width, the liquid-vapor surface tension and the water density, the matric potential can be calculated below which a crack (fracture) empty spontaneously (Or and Tuller, 2003). However, the fracture will contain still water (i) adsorbed on flat areas, and (ii) in surface irregularities (or pits) both also related to the matric potential. Or and Tuller (2003) proposed a model to calculate the moisture content as a function of matric potential in a (rough) fracture. They also presented a model for the unsaturated hydraulic conductivity of a fracture. Perko et al. (2017) combined a hydraulic model for the matrix domain (cement) accounting for change of hydraulic properties during leaching (via the model of Wissmeier and Barry (2009)) with the model of Or and Tuller (2003) accounted for a variable void aperture (according to a gamma distribution). These models show that, for saturated conditions, the void aperture is the most important parameter; however, the roughness of the voids influences water retention and hydraulic conductivity under unsaturated flow conditions. If under conditions where the multilayer cover is assumed to be degraded, flow conditions in many surface repositories will be mainly under unsaturated conditions. However, it is expected (under equilibrium conditions) that conditions in the matrix domain will be predominantly (close to) saturation, whereas the saturation degree in the fractures can vary many orders of magnitude. Perko et al. (2017) also simulated the flow through a degraded and fractured porous media in an abstracted way using a dual-permeability concept (Gerke and van Genuchten, 1993; Šimůnek and van Genuchten, 2008). The model results indicated a quite complex flow pattern of exchange between the void and matrix domain. Without doubt, unsaturated conditions and fractures/voids will make a physical-based approach for solute transport and diffusion complex. Alternatively, fractures and voids can be represented in an explicit way being with water and solute exchange between the fractures and the surrounding matrix. One example in the framework of (near-)surface disposal is the study of Perko et al. (2015) in which flow and transport in an unsaturated random fracture network within a disposal waste package was simulated.

5.3.4 Diffusion of the studied radiotracers

In this paragraph, the information about the diffusion of the different radiotracers investigated in SUDOKU, i.e. ^{14}C , ^{36}Cl , ^{99}Tc , ^{129}I , and ^{93}Mo , is summarized for sound cement-based materials. This part aims to describe the global behaviour of these radiotracers.

Mattigod et al. (2001) have measured the effective diffusion coefficient of iodine-129 and technetium-99 in concrete formulation waste forms showing much higher values for ^{99}Tc . On the other hand, van Es et al. (2015) compared the diffusion of iodine and chloride in a cementitious backfill pointing out the higher diffusivity of iodine (Figure 5-16). Regarding this latter, it can be noted that cellulose degradation products have an effect on iodine and chloride diffusivity which is remarkable for iodine. These results show that, even if $^{36}\text{Cl}^-$ and $^{129}\text{I}^-$ are chemically close, there are significant differences between iodide and chloride species in terms of transport properties.

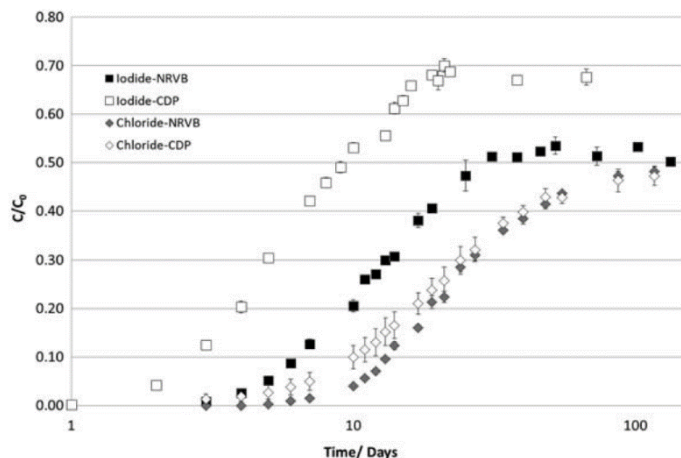


Figure 5-16 Comparison of breakthrough curves for carrier-free ^{36}Cl and ^{125}I in NRVB equilibrated water (van Es et al., 2015)

On the other hand, Atkinson and Nickerson (1988) have shown that the transfer of $^{131}\text{I}^-$ is clearly distinct from $^{137}\text{Cs}^+$ in hydrated cement pastes (Figure 5-17). This kind of outcomes indicates that anions and cations migrate through different pathways within the porous network of cement-based materials, probably due to the charged surfaces of the cement hydrates, independently on their interactions with these minerals.

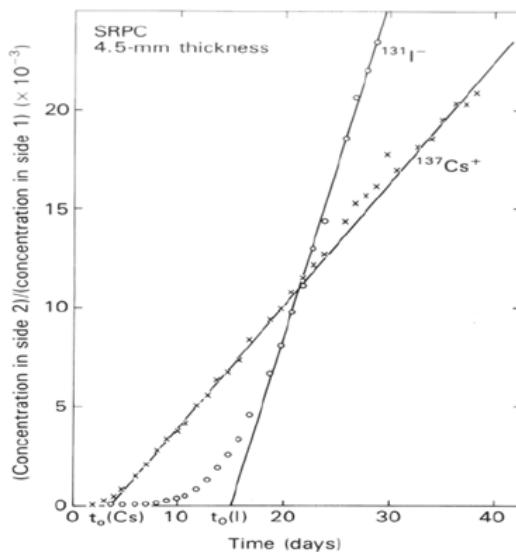


Figure 5-17 Simultaneous diffusion of I^- and Cs^+ through hydrated sulphate resisting Portland cement at 30°C from a maximum concentration (side 1) of 10^{-4} mol/L for each species. The straight lines indicate steady-state diffusion (Atkinson and Nickerson, 1988)

The formulation of the cement-based materials influences the transport properties of the radiotracers. In particular, the type of cement is a significant parameter. Figure 5-18 shows the ^{36}Cl ingress for mortars CEM I and CEM V by ^{36}Cl autoradiography technique (Marliot, 2024). These results confirm for ^{36}Cl the results for HTO given in Figure 5-10, revealing a much deeper ^{36}Cl penetration front in the case of mortar CEM I, inducing a higher diffusion coefficient of chloride for cement CEM I.

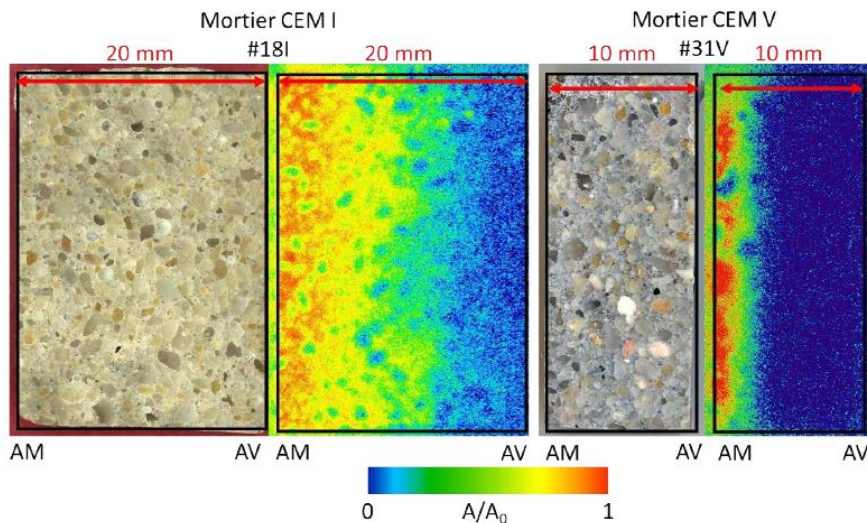


Figure 5-18 ^{36}Cl autoradiographies for mortars CEM I and CEM V compared to microscopic images (Marliot, 2024)

The specific nature of carbon-14 with inorganic and organic speciation has motivated many works on C-14 behaviour in cement-based materials. This existing information on ^{14}C transfer is about (i) diffusion of carbon-14 labelled organic molecules in hardened cement pastes (Wieland et al., 2016), (ii) C-14 inorganic species in solution in unsaturated cement-based-materials (Rasamimanana et al., 2019), and (iii) gaseous diffusion of $^{14}\text{CO}_2$ in cementitious matrices. (Dayal and Reardon, 1994) studied the release of inorganic ^{14}C in solution as $^{14}\text{CO}_3^{2-}$ from cemented waste form showing that inorganic carbon-14 was immobilized by calcium carbonate precipitation and the release came from the dissolved carbon-14 in the pore solution. In addition, (Banba et al., 1992) identified the possible role of colloidal particles in the release process of ^{14}C from such waste form. Consequently, for dissolved inorganic carbon-14, high interactions with the calcium-bearing solid phases and dissolved calcium would highly control its diffusion in cement-based materials, for which no data seem to be available.

Molybdenum diffusion has not been directly investigated through diffusion tests. The mobility of molybdenum has only been studied by leaching tests on hardened cement paste to characterize the behaviour of trace elements initially present in cement (Vollpracht and Brameshuber, 2016). The results of these studies have confirmed the impact of Aft/AFm phases on the Mo behaviour, but the diffusion coefficient of Mo was not determined in such studies.

5.4 Modelling transport of radionuclides in degraded cement

Transport of radionuclides through the cementitious barriers is governed mainly by diffusive processes when water flow in the system is zero or very limited (i.e. when the multi-layer cover and cementitious barriers are not degraded), and by advective-dispersive transport processes when flow rates are larger (under degraded conditions). The most used model to simulate transport of radionuclides in porous media at the continuum scale is the advection-dispersion equation (e.g., Deissmann et al. (2025)). This equation holds for both saturated and unsaturated conditions. However, applicability for radionuclide migration in degraded cement under variable-saturated conditions is complicated due to:

- The effect of unsaturated flow conditions on the effective diffusion coefficient. The tortuosity factor depends on the water saturation with a decrease in tortuosity with decreasing water content (and thus decreasing diffusivity as discussed in section 5.3.3). In soil literature, models exist to quantify this behaviour (e.g. Millington and Quirk (1961) or Moldrup et al. (2000)), but their applicability for cementitious materials (and degraded cementitious materials) has to be tested. Specific models are available for cementitious materials but mostly for saturated

conditions only (e.g., Patel et al. (2016)) potentially capturing the evolution of the tortuosity for saturated conditions during chemical degradation. Water saturation effects could be described by empirical relations as discussed in section 5.3.3).

- A second complication is the presence of cracks. The large effect on diffusion in saturated cracks has been illustrated in section 5.3.2 but under saturated conditions. Under unsaturated conditions, many cracks will be empty (except for some film and water in cavities, see section 5.3.3) and will contribute only minorly to diffusion.
- Hydrodynamic dispersion is typically captured with a dispersivity parameter. Dispersivity is typically viewed as a material parameter, i.e. independent of water saturation degree (although in strongly heterogeneous media, a water content dependency might be present). It is not unlikely that dispersivity will change with degradation state of the cementitious parameters, but the relation is unknown, and models are not available. Pore-scale models can help to elucidate this behaviour.
- A final complication are the geochemical alterations during cement degradation which will affect also the sorption of the radionuclides which has to be taken into account in a dynamic way. One option is to define R_d values for different degradation states (e.g., Ochs et al. (2016)) and define the time scale during which a value should be used. Such approach is used in some studies, but is rather static in nature because of a lack of direct coupling between processes driving the ageing of the cementitious materials and the sorption parameters. Another method is to make a link between cumulative water infiltration, its composition and the R_d value (via geochemical calculations), and integrating this information in the flow and transport model linked by the cumulative water infiltration. An example is the study of Jacques et al. (2014) where a dynamic R_d value was used as a function of the main degradation state (see section 4.3.1.1) and the amount of C-S-H (by a scaling factor). An alternative is to use a fully coupled reactive transport model (Deissmann et al., 2025; Steefel et al., 2015) to model flow, transport and geochemistry. The geochemistry module would address the geochemical changes in the pore water and the solid phase of the cementitious materials and the sorption of radionuclides on the cement hydrates. The modelling of the geochemical changes in cementitious materials is relatively well established; however models for radionuclide sorption (via ion exchange or surface complexation models) on cement hydrates are not yet well established.

6 Concluding remarks

In the last decades, many near-surface repositories for low level and intermediate level short lived radioactive waste are planned, under construction, in operation or even closed. Given the large variety of waste streams, regional settings and national policies, a large variety in near-surface concepts and designs exists. The focus within SUDOKU is on surface or sub-surface (within a few meters) concrete vaults as these concepts are used within the national programs of the different partners. The safety functions, isolation and containment, heavily depend on highly engineered barriers consisting of:

- a multi-layer cover (except the Slovak sub-surface concept) consisting of several, mainly natural, materials, and
- cementitious materials used as conditioning matrix, containers, construction of vaults etc.

In most concepts, also the geological environment contributes to isolation and containment.

SUDOKU aims at improving scientific understanding of the behaviour and evolution of the engineered barriers for increasing the basis for optimisation and implementation.

For the multi-layer cover, the crucial aspects are processes that control infiltration in multilayer covers and to evaluate cover effectiveness and its long-term performance. A main challenge remains to quantify the influence of coupling processes (mainly water movement and energy balance) in a barrier consisting of different materials often with extremely contrasting (hydrological) properties (sometimes even in presence of synthetic geomembranes and/or asphalt layers) on water movement (mainly infiltration) and alteration processes such as erosion, biological effects and soil formation. There is a lack on (i) systematic studies of behaviour/durability of different barrier concepts under controlled conditions relevant for near-surface disposal, (ii) long-term monitoring of multi-layer cover performance under in-situ conditions, and (iii) numerical modelling studies integrating the effect of coupled processes affecting the engineered barriers on radionuclide release from disposal area. Advancements in these three aspects will contribute to further optimisation of multi-layer covers accounting also for possible effects of climate change. As most national programmes of the partners are in the stage of planning, construction or operation, further optimization of the cover is highly relevant.

Cementitious SSCs in a near-surface repository will be subject to degradation related to chemical (leaching, carbonation), mechanical and corrosion processes. Increasing the scientific knowledge on these processes will help to underpin the safety arguments and assessment. Conditions within a (near-)surface repository are significantly different from those in deep geological conditions. Leaching and carbonation are important chemical degradation processes with conditions imposed by the atmosphere and the multi-layer covers. Corrosion of reinforced mortars or concretes could potentially damage the structure by cracks which could have a significant effect on diffusion. Although there exists a large amount of knowledge on these processes, there is a need to study these processes under conditions relevant for near-surface conditions including types of water that are representative for in-situ conditions. Beside the evolution of the geochemistry of the cementitious material, information on the impact on mechanical and transport properties is needed including unsaturated water conditions as well. For the migration of radionuclides, beside water flow and diffusion, retention by sorption is crucial – assessing the sorption capacity of damaged cement-based materials is therefore crucial. Specific data for more mobile radionuclides (^{14}C , ^{36}Cl , ^{129}I , ^{93}Mo , ^{99}Tc) and for a strongly sorbing radionuclide (^{238}Pu) in degraded mortar will be collected. To be useful for safety and performance calculations, numerical tools should be able to capture the combined effects of cementitious material leaching, carbonation and corrosion, changing transport properties and mobility of radionuclides in an integrated way. Ultimately, in combination with models for the cover, this will lead to a more holistic view on the behaviour and evolution of the engineered barriers in a near-surface repository and radionuclide fluxes to the environment.

References

ACI Committee 201 1992 Guide to Durable Concrete, ACI 201.2R-92. American Concrete Institute, Farmington Hills, Michigan.

ACI Committee 222 2001 Protection of Metals in Concrete Against Corrosion, ACI 222R-01. American Concrete Institute, Farmington Hills, Michigan.

Aimoz, L., Wieland, E., Taviot-Guého, C., Vespa, M. and Dähn, R. 2012. Iodine K-Edge Exafs Spectroscopy of Iodine-Bearing AFm-(Cl 2, CO 3, SO 4). Proceedings of the 10th International Congress for Applied Mineralogy (ICAM) (1-7).

Al-Jeznawi, D., Al-Janabi, M.A.Q., Bernardo, L.F.A. and Abbas, H.A. 2025. Modeling and Mechanisms of Desiccation-Induced Cracking and Curling in Clay Soils: A State-of-the-Art Review. Geotechnical and Geological Engineering 43(7), 342.

Albrecht, B.A. and Benson, C.H. 2001. Effect of desiccation on compacted natural clays. Journal of Geotechnical and Geoenvironmental Engineering 127(1), 67–75.

Albright, W.H., Benson, C.H., Gee, G.W., Abichou, T., Tyler, S.W. and Rock, S.A. 2006. Field Performance of Three Compacted Clay Landfill Covers. Vadose Zone Journal 1171, 1157–1171.

Albright, W.H., Benson, C.H., Gee, G.W., Roesler, A.C., Abichou, T., Apiwantragoon, P., Lyles, B.F. and Rock, S.A. 2004. Field Water Balance of Landfill Final Covers. Journal of Environmental Quality 33(6), 2317–2332.

Ali, I., Greifeneder, F., Stamenkovic, J., Neumann, M. and Notarnicola, C. 2015. Review of Machine Learning Approaches for Biomass and Soil Moisture Retrievals from Remote Sensing Data. Remote Sensing 7(12), 16398–16421.

Allard, B., Eliasson, L., Hoglund, S. and Andersson, K. 1984. Sorption of Cs, I and actinides in concrete systems.

Allen, P.G., Siemering, G.S., Shuh, D.K., Bucher, J.J., Edelstein, N.M., Langton, C.A., Clark, S.B., Reich, T. and Denecke, M.A. 1997. Technetium speciation in cement waste forms determined by X-ray absorption fine structure spectroscopy. Radiochimica Acta 76(1-2), 77–86.

Allen, R.G. 2013. REF-ET: REFERENCE EVAPOTRANSPIRATION CALCULATION SOFTWARE for FAO and ASCE Standardized Equations

ARAO 2018. Abstract of the Cross-Border Environmental Impact Assessment, NSRA02-IZV-001-01-ANG, Revision 1.

ARAO 2019a. Draft Safety Analysis Report for the Vrbina Krško LILW Repository: Chapter 2 – General description of the repository. ARAO 02-08-011-004, Revision 5. ARAO, Ljubljana, Slovenia.

ARAO 2019b. Draft Safety Analysis Report for the Vrbina Krško LILW Repository: Chapter 5 – Summary of Design Bases, ARAO 02-08-011-004, Revision 5. ARAO, Ljubljana, Slovenia.

Atkins, M. and Glasser, F.P. 1992. APPLICATION OF PORTLAND CEMENT-BASED MATERIALS TO RADIOACTIVE WASTE IMMOBILIZATION, pp. 105–131.

Atkinson, A. and Nickerson, A.K. 1988. Diffusion and sorption of cesium, strontium and iodine in water-saturated cement. Nuclear Technology 81, 100–113.

Azad, N., Sheikhabaglou, A., Zvomuya, F. and He, H. 2025. Applying LSTM to Model Multi-Depth Soil Moisture Under Various Land Covers, Climates and Soils. European Journal of Soil Science 76(4), e70142.

Balčius, P. and Grigaliūnienė, D. 2023. Analysis of the effect of sorption coefficient in concrete on radionuclide release from a near surface repository. 19th International conference of young scientists on energy and natural sciences issues "CYSENI".

Balonis, M., Mędala, M. and Glasser, F.P. 2011. Influence of calcium nitrate and nitrite on the constitution of AFm and AFt cement hydrates. Advances in Cement Research 23(3), 129–143.

Banba, T., Matsumoto, J. and Muraoka, S. 1992. Leaching Behavior of C-14 Contained in Portland-Cement. Cement and Concrete Research 22(2-3), 381–386.

Bastardie, F., Cannavacciuolo, M., Capowiez, Y., de Dreuzy, J.R., Bellido, A. and Cluzeau, D. 2002. A new simulation for modelling the topology of earthworm burrow systems and their effects on macropore flow in experimental soils. *Biology and Fertility of Soils* 36(2), 161–169.

Baur, I. and Johnson, A.C. 2003. The solubility of selenate-AFt ($3\text{CaO} \cdot \text{Al}_2\text{O}_3 \cdot 3\text{CaSeO}_4 \cdot 7.5\text{H}_2\text{O}$) and selenate-AFm ($3\text{CaO} \cdot \text{Al}_2\text{O}_3 \cdot \text{CaSeO}_4 \cdot x\text{H}_2\text{O}$), pp. 1741–1748.

Beattie, T.M., Andersson, J., Bruggeman, C., Chapman, N.A., Grambow, B., Knuuti, T., Theodon, L. and Zuidema, P. 2021. EURAD Roadmap, extended with Competence Matrix. Final version as of 27.09.2021 deliverable D1.7 of the HORIZON 2020 project EURAD. EC Grant agreement no: 847593.

Bergström, U., Pers, K. and Almen, Y. 2011. International perspective on repositories for low level waste. R-11-16. SKB International AB, Sweden.

Berner, U. 1999. Concentration limits in the cement based Swiss repository for long-lived, intermediate-level radioactive wastes (LMA) PSI-99-10. PSI, Villigen, Switzerland.

Berner, U.R. 1992. Evolution of pore water chemistry during degradation of cement in a radioactive waste repository environment, pp. 201–219.

Biurrun, E., Stefanova, I. and Gonzalez Herranz, E. 2016. Realization of the National Disposal Facility for Radioactive Waste in Bulgaria Annual Waste Management Symposium.

Blanc, P. 2017. Thermoddem: Update for the 2017 version. Report BRGM/RP-66811-FR.

Bokan-Bosiljkov, V. 2023. Osnovne značilnosti kontraktorskega betona (Essential characteristics of tremie concrete). 29. slovenski kolokvij o betonih (29th Slovenian colloquium on concrete): Kontraktorski beton za globoko temeljenje (Tremie concrete for deep foundation), 33–50.

Bokan-Bosiljkov, V., Stukovnik, P. and Marinsek, M. 2020. Alkalna-dolomitna reakcija v betonu (Alkaline-dolomite reaction in concrete). 27. slovenski kolokvij o betonih (27th Slovenian colloquium on concrete): Beton sekundarne obloge silosa odlagališča nizko in srednje radioaktivnih odpadkov (Concrete of the secondary lining of the disposal silo for low and intermediate level radioactive waste), 102–116.

Bonhoure, I., Baur, I., Wieland, E., Johnson, C.A. and Scheidegger, A.M. 2006. Uptake of Se(IV/VI) oxyanions by hardened cement paste and cement minerals: An X-ray absorption spectroscopy study. *Cement and Concrete Research* 36(1), 91–98.

Bonhoure, I., Scheidegger, A.M., Wieland, E. and Dohn, R. 2002. Iodine species uptake by cement and CSH studied by I K-edge X-ray absorption spectroscopy, pp. 647–651.

Brown, P.W. and Badger, S. 2000. The distributions of bound sulfates and chlorides in concrete subjected to mixed NaCl, MgSO₄, Na₂SO₄ attack. *Cement and Concrete Research* 30(10), 1535–1542.

Buchwald, A. 2000. Determination of the ion diffusion coefficient in moisture and salt loaded masonry materials by impedance spectroscopy. Proceedings of the 3rd international PhD symposium, 475–482.

Buckingham, E. 1907. Studies on the movement of soil moisture., USDA Bureau of Soils, Washington DC.

Caselles, L.D., Roosz, C., Hot, J., Blotevogel, S. and Cyr, M. 2021. Immobilization of molybdenum by alternative cementitious binders and synthetic C-S-H: An experimental and numerical study. *Science of the Total Environment* 789.

Castellote, M. and Andrade, C. 2006. Round-Robin Test on methods for determining chloride transport parameters in concrete. *Materials and Structures* 39(10), 955–990.

Castellote, M., Andrade, C. and Alonso, C. 2002. Accelerated simultaneous determination of the chloride depassivation threshold and of the non-stationary diffusion coefficient values. *Corrosion Science* 44(11), 2409–2424.

Chatterjee, A. and Goyns, A. (2013) Cementitious Materials Performance in Aggressive Aqueous Environments – Engineering Perspectives Alexander, M., Berton, A. and De Belie, N. (eds), Springer.

Chen, L., Šimůnek, J., Bradford, S.A., Ajami, H. and Meles, M.B. 2022. A computationally efficient hydrologic modeling framework to simulate surface-subsurface hydrological processes at the hillslope scale. *Journal of Hydrology* 614, 128539.

Chen, R., Lindqwister, W., Wu, F., Mielniczuk, B., Hueckel, T. and Veveakis, M. 2023. The physics of desiccation cracks 2: Modeling and prediction of the crack patterns. *Geomechanics for Energy and the Environment* 35, 100489.

Churakov, S.V., Labbez, C., Pegado, L. and Sulpizi, M. 2014. Intrinsic Acidity of Surface Sites in Calcium Silicate Hydrates and Its Implication to Their Electrokinetic Properties. *J Phys Chem C* 118(22), 11752–11762.

Clear, K.C. 1976 Time-to-Corrosion of Reinforcing Steel in Concrete Slabs. PB 258 446. Federal Highway Administration.

Climent, M.A., de Vera, G., López, J.F., Viqueira, E. and Andrade, C. 2002. A test method for measuring chloride diffusion coefficients through nonsaturated concrete - Part I. The instantaneous plane source diffusion case. *Cement and Concrete Research* 32(7), 1113–1123.

Cocke, D.L. and Mollah, M.Y.A. (1993) Chemistry and microstructure of solidified waste forms. Spence, R.D. (ed), pp. 187–242, Lewis Publisher, Boca Raton.

Dauzères, A., Helson, O., Churakov, S., Montoya, V., Zghondi, J., Neeft, E., Shao, J., Cherkouk, A., Mijnendonckx, K., Sellier, A., Deissmann, G., Arnold, T., Lacarrière, L., Griffa, M., Vidal, T., Neji, M., Bourbon, X., Ibrahim, L., Seigneur, N., Poyet, S., Bary, B., Linard, Y., Le Duc, T., Hlavackova, V., Pasteau, A., Jantschik, K., Middelhoff, M., Perko, J., Tri Phung, Q., Seetharam, S., Shan, W., Singh, A., Lloyd, J. and Vilarrasa, V. 2022 Initial State of the Art on the chemo-mechanical evolution of cementitious materials in disposal conditions. Final version as of 09/11/2022 of deliverable D16.1 of the HORIZON 2020 project EURAD. EC Grant agreement no: 847593.

David, T.S., Gash, J.H.C., Valente, F., Pereira, J.S., Ferreira, M.I. and David, J.S. 2006. Rainfall interception by an isolated evergreen oak tree in a Mediterranean savannah. *Hydrological Processes* 20(13), 2713–2726.

Dayal, R. and Reardon, E.J. 1994. C-14 Behavior in a Cement-Dominated Environment - Implications for Spent Candu Resin Waste-Disposal. *Waste Management* 14(5), 457–466.

Deissmann, G., Neeft, E. and Jacques, D. 2025. EURAD State-of-the-Art Report: Assessment of the chemical evolution at the disposal cell scale – part II – gaining insights into the geochemical evolution. *Frontiers in Nuclear Engineering* 3.

Delagrave, A., Marchand, J., Ollivier, J.P., Julien, S. and Hazrati, K. 1997. Chloride binding capacity of various hydrated cement paste systems. *Advanced Cement Based Materials* 6(1), 28–35.

Deng, Z., Lan, H., Li, L. and Sun, W. 2025. Vegetation-induced modifications in hydrological processes and the consequential dynamic effects of slope stability. *CATENA* 251, 108793.

Denis, R., Tan, D. and Cao, D. 2012 A literature review on lifetime prediction of thin HDPE geomembranes in the exposed environment.

Devapriya, A.S. and Thyagaraj, T. 2025 Hydraulic Conductivity of Compacted Clay Liners Subjected to Alternate Wet-Dry Cycles. Thyagaraj, T., Ravichandran, P.T., Janardhanan, G., Bhuvaneshwari, S., Muttharam, M. and Maji, V.B. (eds), pp. 179–186, Springer Nature Singapore, Singapore.

Djerbi, A., Bonnet, S., Khelidj, A. and Baroghel-Bouny, V. 2008. Influence of traversing crack on chloride diffusion into concrete. *Cement and Concrete Research* 38(6), 877–883.

Duchesne, J. and Berton, A. (2013) Performance of Cement-Based Materials in Aggressive Aqueous Environments, State-of-the-Art Report. Alexander, M., Berton, A. and De Belie, N. (eds), RILEM.

Duhovnik, B. 2022. Development of the Vrbina LILW Repository Design. 31st International Conference Nuclear Energy for New Europe : NENE 2022.

Dunbabin, V.M., Postma, J.A., Schnepf, A., Pagès, L., Javaux, M., Wu, L., Leitner, D., Chen, Y.L., Rengel, Z. and Diggle, A.J. 2013. Modelling root–soil interactions using three-dimensional models of root growth, architecture and function. *Plant and Soil* 372(1), 93–124.

Duncan, J.M. 1996. State of the art: Limit equilibrium and finite-element analysis of slopes. *J Geotech Eng-Asce* 122(7), 577–596.

Durner, W. 1994. Hydraulic conductivity estimation for soils with heterogeneous pore structure. *Water Resources Research* 30(2), 211–223.

EIA 2015 Non-technical summary of EIA report “Construction of National Disposal facility for disposal of low and intermediate level radioactive waste – NDF”. <https://www.moew.government.bg/static/media/ups/tiny/file/Industry/EIA/2015>.

Eliades, M., Bruggeman, A., Djuma, H., Christou, A., Rovanias, K. and Lubczynski, M.W. 2022. Testing three rainfall interception models and different parameterization methods with data from an open Mediterranean pine forest. *Agricultural and Forest Meteorology* 313, 108755.

Ercegovic, R., Drolc, S. and Sustersic, J. 2024. Poskusno polnjenje odlagalnih zaboljnikov N2d z lahko malto (Experimental filling of disposal containers N2d with lightweight mortar). 31. slovenski kolokvij o betonih (31th Slovenian colloquium on concrete): lahki betoni in malte (lightweight concretes and mortars), 31–48.

Ercegovic, R., Drolc, S., Trtnik, G. and Hocevar, A. 2023. Reološke meritve svežega kontraktorskega betona v okviru projekta DIAFRAGMA NSRAO (Rheological measurements of fresh tremie concrete in the framework of the LILW diaphragm project). 29. slovenski kolokvij o betonih (29th Slovenian colloquium on concrete): Kontraktorski beton za globoko temeljenje (Tremie concrete for deep foundation), 51–70.

Ercegovic, R. and Unetic, A. 2020. Osnovni tehnološki parametri izvedbe sekundarne amiranobetonske obloge silosa odlagališča NSRAO = Basic technological parameters of the execution of the secondary reinforced concrete lining of the NSRAO disposal silo. 27. slovenski kolokvij o betonih (27th Slovenian colloquium on concrete): Beton sekundarne obloge silosa odlagališča nizko in srednje radioaktivnih odpadkov (Concrete of the secondary lining of the disposal silo for low and intermediate level radioactive waste), 79–92.

Escadeillas, G. (2013) Performance of Cement-Based Materials in Aggressive Aqueous Environments, State-of-the-Art Report. Alexander, M., Berton, A. and De Belie, N. (eds), RILEM.

Evans, N.D.M. 2008. Binding mechanisms of radionuclides to cement. *Cement and Concrete Research* 38(4), 543–553.

Faucon, P., Adenot, F., Jacquinot, J.F., Petit, J.C., Cabrillac, R. and Jorda, M. 1998. Long-term behaviour of cement pastes used for nuclear waste disposal: Review of physico-chemical mechanisms of water degradation. *Cement and Concrete Research* 28(6), 847–857.

Faucon, P., Adenot, F., Jorda, M. and Cabrillac, R. 1997. Behaviour of crystallised phases of Portland cement upon water attack, pp. 480–485.

Ferraris, C.F., Clifton, J.R., Stutzman, P.E. and Garboczi, E.J. (1997) Mechanisms of Chemical Degradation of Cement-Based Systems. Scrivener, K. and Young, J.F. (eds), pp. 185–192, Spon Press, London.

Ferraris, C.F., Stutzman, P.E. and Snyder, K. 2006. Sulfate resistance of concrete: a new approach. PCA R&D Serial Number 2486.

Finke, P. (2024a) Modelling Soil Development Under Global Change, Springer Cham.

Finke, P. 2024b SoilGen3.8 model (code, executable, supporting software and cases), Zenodo, <https://doi.org/10.5281/zenodo.13934823>.

Finster, M. and Kamboj, S. 2011 International Low Level Waste Disposal Practices and Facilities. ANL-FCT-324. Argonne National Laboratory.

Florea, M.V.A. and Brouwers, H.J.H. 2012. Chloride binding related to hydration products Part I: Ordinary Portland Cement. *Cement and Concrete Research* 42(2), 282–290.

Gao, C., Ye, W.-M., Lu, P.-H., Liu, Z.-R., Wang, Q. and Chen, Y.-G. 2023. An infiltration model for inclined covers with consideration of capillary barrier effect. *Engineering Geology* 326, 107318.

Garamszeghy, M. 2021 Disposal of Low- and Intermediate-Level Waste: International experience, Report prepared for the Nuclear Waste Management Organization (Canada).

Geng, Q., Yan, S., Li, Q. and Zhang, C. 2024. Enhancing data-driven soil moisture modeling with physically-guided LSTM networks. *Frontiers in Forests and Global Change* Volume 7 - 2024.

Gerke, H.H. and van Genuchten, M.T. 1993. A dual-porosity model for simulating the preferential movement of water and solutes in structured porous media. *Water Resources Research* 29(2), 305–319.

Giffaut, E., Grive, M., Blanc, P., Vieillard, P., Colas, E., Gailhanou, H., Gaboreau, S., Marty, N., Made, B. and Duro, L. 2014. Andra thermodynamic database for performance assessment: ThermoChimie. *Applied Geochemistry* 49, 225–236.

Glasser, F., Macphee, D., Atkins, M., Pointer, C., Cowie, J., Wilding, C.R. and Evans, P.A. 1989 Immobilisation of radwaste in cement based matrices. DOE-RW-89.058. Department of the Environment, London (UK).

Glasser, F.P. 2009 The thermodynamics of attack on Portland cement with special reference to sulfate, concrete in aggressive aqueous environments, performance, testing and modeling. Alexander, M. and Bertron, A. (eds), pp. 3–17, Toulouse.

Glasser, F.P., Marchand, J. and Samson, E. 2008. Durability of concrete - Degradation phenomena involving detrimental chemical reactions. *Cement and Concrete Research* 38(2), 226–246.

Glaus, M.A., Frick, S., Rossé, R. and Van Loon, L.R. 2010. Comparative study of tracer diffusion of HTO, Na and Cl in compacted kaolinite, illite and montmorillonite. *Geochimica Et Cosmochimica Acta* 74(7), 1999–2010.

Gougar, M.L.D., Scheetz, B.E. and Roy, D.M. 1996. Ettringite and C-S-H Portland cement phases for waste ion immobilization: A review. *Waste Management* 16(4), 295–303.

Grambow, B., López-García, M., Olmeda, J., Grivé, M., Marty, N.C.M., Grangeon, S., Claret, F., Lange, S., Deissmann, G., Klinkenberg, M., Bosbach, D., Bucur, C., Florea, I., Dobrin, R., Isaacs, M., Read, D., Kittnerová, J., Drtinová, B., Vopálka, D., Cevirim-Papaioannou, N., Ait-Mouheb, N., Gaona, X., Altmaier, M., Nedyalkova, L., Lothenbach, B., Tits, J., Landesman, C., Rasamimanana, S. and Ribet, S. 2020. Retention and diffusion of radioactive and toxic species on cementitious systems: Main outcome of the CEBAMA project. *Applied Geochemistry* 112, 104480.

Grigaliūnienė, D., Poškas, P. and Kilda, R. 2016 Waste zone conceptual model effect on predicted radionuclide flux from near surface repository, pp. 38–41, IAEA, Vienna, Austria.

Grivé, M. and Olmeda, J. (2015) Cebama project Deliverable 2.03 WP2: State of the Art Report (initial), pp. 32–66.

Gui, Y.L., Zhao, Z.Y., Kodikara, J., Bui, H.H. and Yang, S.Q. 2016. Numerical modelling of laboratory soil desiccation cracking using UDEC with a mix-mode cohesive fracture model. *Engineering Geology* 202, 14–23.

Guimaraes, A.T.C., Climent, M.A., de Vera, G., Vicente, F.J., Rodrigues, F.T. and Andrade, C. 2011. Determination of chloride diffusivity through partially saturated Portland cement concrete by a simplified procedure. *Construction and Building Materials* 25(2), 785–790.

Guo, H., Ng, C.W.W., Zhang, Q., Qu, C. and Hu, L. 2024. Modelling the water diversion of a sustainable cover system under humid climates. *Journal of Rock Mechanics and Geotechnical Engineering* 16(7), 2429–2440.

Heili, V. 2020 Lab-scale tests of erosion control on slopes with rainfall simulator according to Fpr CEN/TS 17445:2019.

Henocq, P. and Missana, T. 2025 Work Package 14 (SUDOKU) Milestone 14: Agreed degradation protocols to study the chemo-mechanical evolution of reinforced and unreinforced cementitious barriers and for preparing the degraded mortar/concrete samples for diffusion experiments.

Henocq, P., Robinet, J.C., Perraud, D., Munier, I., Wendling, J., Treille, E. and Schumacher, S. 2018 Integration of CAST results to safety assessment: Contribution from Andra to D6.3. Cast project report CAST-2018-D6.3.

Hillel, D. (2003) Introduction to Environmental Soil Physics, Elsevier Science & Technology, San Diego, UNITED STATES.

Horyna, J. 2000. Dukovany Radioactive Waste Repository. WM'00 Conference.

Hou, S.L., Li, K., Wu, Z.M., Li, F.M. and Shi, C.J. 2022. Quantitative evaluation on self-healing capacity of cracked concrete by water permeability test-A review. *Cement Concrete Comp* 127.

Hsuan, Y.G. and Koerner, R.M. 1998. Antioxidant depletion lifetime in high density polyethylene geomembranes. *Journal of Geotechnical and Geoenvironmental Engineering* 124(6), 532–541.

Hummel, W. and Thoenen, T. 2021. The PSI chemical thermodynamic database 2020. Nagra Technical Report NTB 21-03. NAGRA, Wettingen, Switzerland.

IAEA 2020. Design Principles and Approaches for Radioactive Waste Repositories. No. NW-T-1.27. IAEA.

IBE 2018. Izdelava prototipa in certificiranje odlagalnega zabojnika za odlaganje NSRAO: STS za Odlagalni zabojnik NSRAO (NRVB---5G/17) (Prototype Development and Certification of a Disposal Container for LILW Disposal: STA for the LILW Disposal Container). IBE, Ljubljana, Slovenia.

Iden, S.C., Blöcher, J.R., Diamantopoulos, E. and Durner, W. 2021. Capillary, Film, and Vapor Flow in Transient Bare Soil Evaporation (1): Identifiability Analysis of Hydraulic Conductivity in the Medium to Dry Moisture Range. *Water Resources Research* 57(5), e2020WR028513.

Iden, S.C. and Durner, W. 2007. Free-form estimation of the unsaturated soil hydraulic properties by inverse modeling using global optimization. 43, 1–12.

INPP 2025. Ignalina Nuclear Power Plant website.

Ipavec, A. 2020. Vezivna komponenta betona sekundarne obloge silosa odlagališča NSRAO (Binding component of the secondary lining concrete of the NSRAO disposal silo). 27. slovenski kolokvij o betonih (27th Slovenian colloquium on concrete): Beton sekundarne obloge silosa odlagališča nizko in srednje radioaktivnih odpadkov (Concrete of the secondary lining of the disposal silo for low and intermediate level radioactive waste), 93–101.

Isaacs, M., Lange, S., Deissmann, G., Bosbach, D., Milodowski, A.E. and Read, D. 2020. Retention of technetium-99 by grout and backfill cements: Implications for the safe disposal of radioactive waste. *Applied Geochemistry* 116.

Ivanova, I. 2025. Soil moisture forecasting from sensors-based soil moisture, weather and irrigation observations: A systematic review. *Smart Agricultural Technology* 10, 100692.

Jacobsen, S., Marchand, J. and Boisvert, L. 1996. Effect of cracking and healing on chloride transport in OPC concrete. *Cement and Concrete Research* 26(6), 869–881.

Jacques, D. 2025. ThermoChimie Benchmark – Evolution of a cementitious engineered barrier system in an argillaceous environment. ER-1440. SCK CEN.

Jacques, D., Leterme, B., Beerten, K., Schneider, S., Finke, P. and Mallants, D. 2010a. Long-term evolution of the multi-layer cover Project near surface disposal of category A waste at Dessel. pp. NIROND-TR 2010–2003 E September 2010.

Jacques, D., Neeft, E. and Deissmann, G. 2024. Updated State of the Art on the assessment of the chemical evolution of ILW and HLW disposal cells. Final version as of 15.05.2024 of deliverable D2.2 of the HORIZON 2020 project EURAD. EC Grant agreement no: 847593.

Jacques, D., Perko, J., Seetharam, S.C. and Mallants, D. 2014. A cement degradation model for evaluating the evolution of retardation factors in radionuclide leaching models. *Applied Geochemistry* 49, 143–158.

Jacques, D., Wang, L., Martens, E. and Mallants, D. 2010b. Modelling chemical degradation of concrete during leaching with rain and soil water types. *Cement and Concrete Research* 40(8), 1306–1313.

Jacques, D., Yu, L., Ferreira, M. and Oey, T. 2021. Overview of state-of-the-art knowledge for the quantitative assessment of the ageing/deterioration of concrete in nuclear power plant systems, structures, and components. Deliverable 1.1 in ACES project (<https://aces-h2020.eu/deliverables/>).

Jang, S.Y., Kim, B.S. and Oh, B.H. 2010. Effect of crack width on chloride diffusion coefficients of concrete by steady-state migration tests, pp. 9–19.

Jo, Y., Androniuk, I., Çevirim-Papaioannou, N., de Blochouse, B., Altmaier, M. and Gaona, X. 2022. Uptake of chloride and iso-saccharinic acid by cement: Sorption and molecular dynamics studies on HCP (CEM I) and C-S-H phases. *Cement and Concrete Research* 157.

Justnes, H. 1998. A review of chloride binding in cementitious systems. *Nordic Concrete Research-Publications* 21, 48–63.

JV5 2024 Rules on radiation and nuclear safety factors (JV5). Official Gazette of the Republic of Slovenia, 56/2024.

Kalin, J., Petkovsek, B., Montarnal, P., Genty, A., Deville, E., Krivic, J. and Ratej, J. 2011. Comparison of two numerical modelling codes for hydraulic and transport calculations in the near-field. *Nuclear Engineering and Design* 241(4), 1225–1232.

Kamali, S., Gérard, B. and Moranville, M. 2003. Modelling the leaching kinetics of cement-based materials—fluence of materials and environment. *Cement and Concrete Composites* 25(4), 451–458.

Kamali, S., Moranville, M. and Leclercq, S. 2008. Material and environmental parameter effects on the leaching of cement pastes: Experiments and modelling. *Cement and Concrete Research* 38(4), 575–585.

Kaplan, D.I., Estes, S.L., Arai, Y. and Powell, B.A. 2013. Technetium Sorption by Cementitious Materials Under Reducing Conditions SRNL-STI-2011-00716-R1. Savannah River Site (SRS), Aiken, SC (United States).

Keto, P., Gharbieh, H., Carpen, L., Ferreira, R.M., Somervuori, M., Rinta-Hiilo, V., Laikari, A., Jafari, S. and Vikman, M. 2020. KYT SURFACE: Near Surface Repositories in Finland. VTT-R-00124-20. VTT, Finland.

Keto, P., Kivkoski, H., Rinta-Hiilo, V., Schatz, T. and Gharaibeh, M. 2021. KYT SURFACE: Performance of a Landfill-Type Near Surface Repository. VTT-R-00016-21. VTT, Finland.

Kindness, A., Lachowski, E.E., Minocha, A.K. and Glasser, F.P. 1994. IMMOBILISATION AND FIXATION OF MOLYBDENUM (VI) BY PORTLAND CEMENT. *Waste Management* 14, 97–102.

Konopaskova, S. 1997. Safety Assessment of the Dukovany Repository and Waste Acceptance Evaluation. International symposium on experience in the planning and operation of low level waste disposal facilities, , 383–394.

Kornelsen, K.C. and Coulibaly, P. 2014. Root-zone soil moisture estimation using data-driven methods. *Water Resources Research* 50(4), 2946–2962.

Krahn, J. 2003. The 2001 R.M. Hardy Lecture: The limits of limit equilibrium analyses. *Canadian Geotechnical Journal* 40(3), 643–660.

Kroes, J.G., van Dam, J.C., Groenendijk, P., Hendriks, R.F.A. and Jacobs, C.M.J. 2008. SWAP version 3.2. Theory description and user manual. Alterra Report1649(02).

Kwon, S.J., Na, U.J., Park, S.S. and Jung, S.H. 2009. Service life prediction of concrete wharves with early-aged crack: Probabilistic approach for chloride diffusion. *Structural Safety* 31(1), 75–83.

Lahmann, D. and Keßler, S. 2025. Reactive transport modelling of autogenous self-healing in cracked concrete. *Cement and Concrete Research* 187, 107733.

Lam, L. and Fredlund, D.G. 1994. General Limit Equilibrium-Model for 3-Dimensional Slope Stability Analysis - Reply. *Canadian Geotechnical Journal* 31(5), 795–796.

Lange, S., Klinkenberg, M., Barthel, J., Bosbach, D. and Deissmann, G. 2020. Uptake and retention of molybdenum in cementitious systems. *Applied Geochemistry* 119.

LaPlante, C.M. and Zimmie, T.F. 1992. Freeze/Thaw Effects on the Hydraulic Conductivity of Compacted Clays. *Transportation Research (Record 1369)*, 126–129.

Lee, J.Y., Park, S.J. and Ahn, S. 2021. Impact of Updated OECD/NEA Thermodynamic Database on the Safety Assessment of Radioactive Waste Repository Studied Using RESRAD-OFFSITE Code. *Appl Sci-Basel* 11(16).

Legat, A., Sajna, A., Mladenovic, A., Strupi-Suput, J., Bernard, J., Kuhar, V., Gartner, N., Kosec, T., Cesen, A., Kranjc, A., skerl, M. and Bras, V. 2011. *Metodologija Spremljanja Stanja in Razvoja Poškodb Armiranobetonskih Pregrad in Kovinskih Zabojnikov Za Najverjetnejši Tip Odlagališča NSRAO: Identifikacija Ključnih Parametrov in Osnovni Opis Degradacijskih Procesov Armiranobetonskih Pregrad in Kovinskih Zabojnikov Za Najverjetnejši Tip Odlagališča NSRAO, 3. Faza: Projektna Naloga: Končno Poročilo Po Reviziji* (Project study: Methodology for Monitoring the Condition and Development of Damage to Reinforced Concrete Barriers and Metal Containers for the Most Likely Type of LILW Repository: Identification of Key Parameters and Basic Description of Degradation Processes of Reinforced Concrete Barriers and Metal Containers for the Most Likely Type of LILW Repository, Phase 3). ZAG, Slovenia.

Legat, A., Sajna, A., Mladenovic, A., Strupi-Suput, J., Kuhar, V., Gartner, N. and Kosec, T. 2009. *Ocena in Spremljanje Degradacijskih Procesov Inženirskih Pregrad Odlagališča NSRAO: Identifikacija Ključnih Parametrov in Osnovni Opis Degradacijskih Procesov Armiranobetonskih Pregrad in Kovinskih Zabojnikov Za Najverjetnejši Tip Odlagališča NSRAO: Projektna Naloga* (Project study: Assessment and Monitoring of Degradation Processes of Engineered Barriers of the LILW Repository: Identification of Key Parameters and Basic Description of Degradation Processes of Reinforced Concrete Barriers and Metal Containers for the Most Likely Type of LILW Repository). ZAG, Slovenia.

Levatti, H.U. 2023. Review of Methods to Solve Desiccation Cracks in Clayey Soils. *Geotechnics* 3(3), 808–828.

Li, X., Jiang, G., Wang, Y., Cheng, Z., Li, J. and Chen, B. 2025. Effect of chlorides on the deterioration of mechanical properties and microstructural evolution of cement-based materials subjected to sulphate attack. *Case Studies in Construction Materials* 22, e04235.

Liu, W., Li, Y.-Q., Tang, L.-P. and Dong, Z.-J. 2019. XRD and ^{29}Si MAS NMR study on carbonated cement paste under accelerated carbonation using different concentration of CO₂. *Materials Today Communications* 19, 464–470.

Löbmann, M.T., Geitner, C., Wellstein, C. and Zerbe, S. 2020. The influence of herbaceous vegetation on slope stability – A review. *Earth-Science Reviews* 209, 103328.

Lothenbach, B., Nedyalkova, L., Wieland, E., Mäder, U., Rojo, H. and Tits, J. 2024. Sorption of Se(VI) and Se(IV) on AFm phases. *Applied Geochemistry* 175.

Lu, Y. and Fricke, W. 2023. Salt Stress-Regulation of Root Water Uptake in a Whole-Plant and Diurnal Context. *Int J Mol Sci* 24(9).

Ma, B., Charlet, L., Fernandez-Martinez, A., Kang, M.L. and Madé, B. 2019. A review of the retention mechanisms of redox-sensitive radionuclides in multi-barrier systems. *Applied Geochemistry* 100, 414–431.

Ma, B., Fernandez-Martinez, A., Grangeon, S., Tournassat, C., Findling, N., Claret, F., Koishi, A., Marty, N.C.M., Tisserand, D., Bureau, S., Salas-Colera, E., Elkaïm, E., Marini, C. and Charlet, L. 2017. Evidence of multiple sorption modes in layered double hydroxides using Mo ss structural probe. *Environ. Sci. Technol.* 51(10), 5531.

Macé, N., Fichet, P., Savoye, S., Radwan, J., Lim, C., Lefèvre, S., Page, J. and Henocq, P. 2019. Use of quantitative digital autoradiography technique to investigate the chlorine-36-labelled radiotracer transport in concrete. *Applied Geochemistry* 100, 326–334.

Mallants, D., Volckaert, G. and Marivoet, J. 1999. Sensitivity of protective barrier performance to changes in rainfall rate. *Waste Management* 19, 467–475.

Manzano, J.M., Orihuela, L., Pacheco, E. and Pereira, M. 2025. Data-driven spatio-temporal estimation of soil moisture and temperature based on Lipschitz interpolation. *ISA Transactions* 156, 535–550.

Marliot, J. (2024) Impact de la fissuration sur le transfert des radionucléides dans les matériaux cimentaires, Université de Poitiers.

Martín-Pérez, B., Zibara, H., Hooton, R.D. and Thomas, M.D.A. 2000. A study of the effect of chloride binding on service life predictions. *Cement and Concrete Research* 30(8), 1215–1223.

Marty, N.C.M., Grangeon, S., Elkaïm, E., Tournassat, C., Fauchet, C. and Claret, F. 2018. Thermodynamic and crystallographic model for anion uptake by hydrated calcium aluminate (AFm): an example of molybdenum. *Scientific Reports* 8.

Mattigod, S.V., Whyatt, G.A., Serne, R.J., Schwab, K.E. and Wood, M.I. 2001 Diffusion and leaching of selected radionuclides (Iodine-129, Technetium-99, and Uranium) through category 3 waste encasement concrete and soil fill material. Pacific Northwest National Lab.(PNNL), Richland, WA (United States).

Mechora, S. and Virsek, S. 2023. Updates on LILW Disposal Facility in Slovenia. 32nd International Conference Nuclear Energy for New Europe NENE.

Mehta, P.K. and Monteiro, P.J.M. (2000) Concrete: Microstructure, Properties, and Materials (3rd ed.), McGraw-Hill.

Meles, M.B., Chen, L., Unkrich, C., Ajami, H., Bradford, S.A., Šimunek, J. and Goodrich, D.C. 2024. Computationally efficient Watershed-Scale hydrological Modeling: Integrating HYDRUS-1D and KINEROS2 for coupled Surface-Subsurface analysis. *Journal of Hydrology* 640, 131621.

Menendez, E., Matschei, T. and Glasser, F.P. (2013) Performance of Cement-Based Materials in Aggressive Aqueous Environments, State-of-the-Art Report. Alexander, M., Berton, A. and De Belie, N. (eds), RILEM.

Michel, E., Néel, M.-C., Capowiez, Y., Sammartino, S., Lafolie, F., Renault, P. and Pelosi, C. 2022. Making Waves: Modeling bioturbation in soils – are we burrowing in the right direction? *Water Research* 216, 118342.

Millington, R.J. and Quirk, J.P. 1961. Permeability of porous solids. *Transactions of the Faraday Society* 57, 1200–1206.

Moldrup, P., Olesen, T., Gamst, J., Schjonning, P., Yamaguchi, T. and Rolston, D.E. 2000. Predicting the gas diffusion coefficient in repacked soil: Water-induced linear reduction model. *Soil Science Society of America Journal* 64(5), 1588–1594.

Moog, H.C., Bok, F., Marquardt, C.M. and Brendler, V. 2015. Disposal of nuclear waste in host rock formations featuring high-saline solutions – Implementation of a thermodynamic reference database (THEREDA). *Applied Geochemistry* 55, 72–84.

Morris, E.M. and Woolhiser, D.A. 1980. Unsteady One-Dimensional Flow over a Plane - Partial Equilibrium and Recession Hydrographs. *Water Resources Research* 16(2), 355–360.

Muzylo, A., Llorens, P., Valente, F., Keizer, J.J., Domingo, F. and Gash, J.H.C. 2009. A review of rainfall interception modelling. *Journal of Hydrology* 370(1-4), 191–206.

Nedyalkova, L., Tits, J., Bernard, E., Wieland, E. and Mäder, U. 2021. Sorption Experiments with HTO, 36-Cl, 125-I and 14-C Labeled Formate on Aged Cement Matrices Retrieved from Long-term In-situ Rock Laboratory Experiments. *J Adv Concr Technol* 19(7), 811–829.

Ng, C.W.W., Liu, J., Chen, R. and Xu, J. 2015. Physical and numerical modeling of an inclined three-layer (silt/gravelly sand/clay) capillary barrier cover system under extreme rainfall. *Waste Management* 38, 210–221.

Nieder-Westermann, G., Haverkamp, B., Biurrun, E., Moraleda Gamero, F., Gonzalez Herranz, E., Jordanov, M. and Stefanova, I. 2016 Design and Construction of a Loess-Cement Cushion as an Integral Component of an SL-LILW Repository. OSTI ID:22837978.

Nielsen, E.P. and Geiker, M.R. 2003. Chloride diffusion in partially saturated cementitious material. *Cement and Concrete Research* 33(1), 133–138.

NIRAS 2019a Het veiligheidsdossier - Mijlpaal voor de veilige oppervlakteberging van het laag- en middelactieve kortlevende afval in België. .

NIRAS 2019b Hoofdstuk 1 uit het veiligheidsrapport voor de oppervlaktebergingsinrichting van categorie A-afval in Dessel - Organisatie van het dossier en algemene informatie, Versie 1.

NIRAS 2019c Hoofdstuk 2 uit het veiligheidsrapport voor de oppervlaktebergingsinrichting van categorie A-afval in Dessel - Veiligheidsbeleid, -strategie, en -concept, Versie 3. .

NIRAS 2019d Hoofdstuk 14 uit het veiligheidsrapport voor de oppervlaktebergingsinrichting van categorie A-afval in Dessel - Veiligheidsevaluatie – Langetermijnveiligheid, Versie 3. .

Novak, V. and Hlaváčiková, H. (2019) Applied Soil Hydrology, Springer.

Ochs, M., Mallants, D. and Wang, L. (2016) Radionuclide and Metal Sorption on Cement and Concrete, Springer.

Olsson, N., Baroghel-Bouny, V., Nilsson, L.O. and Thiery, M. 2013. Non-saturated ion diffusion in concrete - A new approach to evaluate conductivity measurements. *Cement Concrete Comp* 40, 40–47.

Olsson, N., Lothenbach, B., Baroghel-Bouny, V. and Nilsson, L.-O. 2018. Unsaturated ion diffusion in cementitious materials – The effect of slag and silica fume. *Cement and Concrete Research* 108, 31–37.

Or, D. and Tuller, M. 2003. Hydraulic conductivity of partially saturated fractured porous media: flow in a cross-section. *Advances in Water Resources* 26(8), 883–898.

Ormai, P. 2018 A fresh stocktaking on L/ILW disposal practice: Past experience, key achievements and future challenges.

Ormai, P. (2024) Nuclear Waste Management Facilities. Rahman, R.O.A. (ed), pp. 431–462, Academic Press.

Othman, M., Benson, C., Chamberlain, E., Zimmie, T., Daniel, D. and Trautwein, S. (1994) Hydraulic Conductivity and Waste Contaminant Transport in Soil, p. 0, ASTM International.

Othman, M.A. and Benson, C.H. 1993. Effect of freeze–thaw on the hydraulic conductivity and morphology of compacted clay. *Canadian Geotechnical Journal* 30(2), 236–246.

Pan, F., Pachepsky, Y., Jacques, D., Guber, A. and Hill, R.L. 2012. Data Assimilation with Soil Water Content Sensors and Pedotransfer Functions in Soil Water Flow Modeling. *Soil Science Society of America Journal* 76(3), 829–829.

Pandey, A., Himanshu, S.K., Mishra, S.K. and Singh, V.P. 2016. Physically based soil erosion and sediment yield models revisited. *CATENA* 147, 595–620.

Patel, R., Phung, Q.T., Seetharam, S.C., Perko, J., Jacques, D., Maes, N., De Schutter, G., Ye, G. and van Breugel, K. 2016. Diffusivity of saturated ordinary Portland cement- based materials: A critical review of experimental and analytical modelling approaches. *Cement and Concrete Research* 90, 52–72.

Perko, J., Jacques, D. and Govaerts, J. 2017 Water saturation and flow in a surface disposal facility - Numerical study for the Dessel repository. SCK•CEN ER-0355. SCK•CEN, Mol, Belgium.

Perko, J., Jacques, D. and Seetharam, S. 2015 Solute transport in cracked concrete systems under unsaturated conditions. (Unpublished results). SCK CEN.

Perko, J., Jacques, D., Seetharam, S.C. and Mallants, D. 2010 Long-term evolution of the near surface disposal facility at Dessel. NIROND-TR 2010–04 E. ONDRAF/NIRAS.

Pham, H.T.V. and Fredlund, D.G. 2003. The application of dynamic programming to slope stability analysis. *Canadian Geotechnical Journal* 40(4), 830–847.

Pointeau, I., Coreau, N. and Reiller, P.E. 2008. Uptake of anionic radionuclides onto degraded cement pastes and competing effect of organic ligands. 96(6), 367–374.

Poulsen, E. and Mejlbø, L. (2006) Diffusion of Chloride in Concrete, Taylor & Francis, London.

Pusch, R. and Karnland, O. 1996. Physico chemical stability of smectite clays. *Engineering Geology* 41(1-4), 73–85.

Rajabipour, F. (2006) In situ electrical sensing and material health monitoring of concrete structures, Purdue University, USA.

Rasamimanana, S., Perrigaud, K., Ribet, S., Bessaguet, N., Grambow, B. and Landesman, C. 2019. Radionuclide through-diffusion experiments in partially saturated carbonated and non-

carbonated hardened cement paste using the osmotic technique. Proceedings of the second workshop of the HORIZON 2020 CEBAMA project.

RATA 2003–2005 Selection of a Site for a Near-Surface Disposal Facility: A Joint Report on Characterization of Sites. Submitted for IAEA Peer Review.

RATA 2007 Environmental Impact Assessment Report for Construction of a Near-surface Repository for Radioactive Wastes. Revision 3-2 (in Lithuanian).

Renard, K.G., Foster, G.R., Weesies, G.A., McCool, D.K. and Yoder, D.C. 1997 PREDICTING SOIL EROSION BY WATER: A GUIDE TO CONSERVATION PLANNING WITH THE REVISED UNIVERSAL SOIL LOSS EQUATION (RUSLE).

Renard, K.G., Foster, G.R., Weesies, G.A. and Porter, J.P. 1991. RUSLE: Revised universal soil loss equation. *J Soil Water Conserv* 46(1), 30–33.

Richards, L.A. 1931. Capillary conduction of liquids through porous mediums. *Physics* 1, 377–386.

Richet, C., Galle, C., Le Bescop, P., Peycelon, H., Bejaoui, S., Tovena, I., Pointeau, I., L'Hostis, V. and Lovera, P. 2010 Synthesis of knowledge on the long-term behaviour of concretes. Applications to cemented waste packages. CEA-R-6050. CEA, Saclay, France.

Robinson, M. and Ward, R.C. (2017) *Hydrology: Principles and Processes*, IWA Publishing.

Sadek, S., Ghanimeh, S. and El-Fadel, M. 2007. Predicted performance of clay-barrier landfill covers in arid and semi-arid environments. *Waste Management* 27(4), 572–583.

Saeki, N., Kurihara, R., Ohkubo, T., Teramoto, A., Suda, Y., Kitagaki, R. and Maruyama, I. 2025. Semi-dry natural carbonation at different relative humidities: Degree of carbonation and reaction kinetics of calcium hydrates in cement paste. *Cement and Concrete Research* 189, 107777.

Saetta, A.V., Scotta, R.V. and Vitaliani, R.V. 1993. Analysis of Chloride Diffusion into Partially Saturated Concrete. *Aci Materials Journal* 90(5), 441–451.

Sahmaran, M. 2007. Effect of flexure induced transverse crack and self-healing on chloride diffusivity of reinforced mortar. *Journal of Materials Science* 42(22), 9131–9136.

Saito, H., Simunek, J. and Mohanty, B.P. 2006. Numerical analysis of coupled water, vapor, and heat transport in the vadose zone. *Vadose Zone Journal* 5, 784–800.

Sajna, A. 2020. Odpornost betona proti karbonatizaciji (Concrete resistance to carbonation). 27. slovenski kolokvij o betonih (27th Slovenian colloquium on concrete): Beton sekundarne obloge silosa odlagališča nizko in srednje radioaktivnih odpadkov (Concrete of the secondary lining of the disposal silo for low and intermediate level radioactive waste), 117–126.

Sangam, H.O. and Rowe, R.K. 2002. Effects of exposure conditions on the depletion of antioxidants from high-density polyethylene (HDPE) geomembranes. *Canadian Geotechnical Journal* 39(6), 1221–1230.

Santhanam, M. (2013) *Performance of Cement-Based Materials in Aggressive Aqueous Environments, State-of-the-Art Report*. Alexander, M., Berton, A. and De Belie, N. (eds).

Šavija, B. and Luković, M. 2016. Carbonation of cement paste: Understanding, challenges, and opportunities. *Construction and Building Materials* 117, 285–301.

Schnepf, A., Leitner, D., Landl, M., Lobet, G., Mai, T.H., Morandage, S., Sheng, C., Zörner, M., Vanderborght, J. and Vereecken, H. 2018. CRootBox: a structural–functional modelling framework for root systems. *Annals of Botany* 121(5), 1033–1053.

Sellier, A., Buffo-Lacarrière, L., El Gonnouni, M. and Bourbon, X. 2011. Behavior of HPC nuclear waste disposal structures in leaching environment. *Nuclear Engineering and Design* 241(1), 402–414.

Šimunek, J. and van Genuchten, M.T. 2008. Modeling Nonequilibrium Flow and Transport Processes Using HYDRUS. *Vadose Zone Journal* 7, 782–797.

Sinur, F. and Duhovnik, B. 2020. Odlagališče nizko in srednje radioaktivnih odpadkov = Low and intermediate level waste repository. 27th slovenski kolokvij o betonih (27th Slovenian colloquium on concrete): Beton sekundarne obloge silosa odlagališča nizko in srednje radioaktivnih odpadkov (Concrete of the secondary lining of the disposal silo for low and intermediate level radioactive waste), 41–47.

Skalny, J., Johansen, V., Thaulow, N. and Palomo, A. 1996. DEF: As a form of sulfate attack. *Materials de Construcción* 46(244), 5–29.

Slavoaca, D.C. 2011. Saligny site unsaturated zone hydrology. Proceedings of International Simposion of Nuclear Energy, Bucharest, Romania.

Smith, R., Goodrich, D., Woolhiser, D. and Unkrich, C. 1995. KINEROS-a kinematic runoff and erosion model.

Smith, R.E., Goodrich, D.C. and Unkrich, C.L. 1999. Simulation of selected events on the Catsop catchment by KINEROS2. A report for the GCTE conference on catchment scale erosion models. *Catena* 37(3-4), 457–475.

Steefel, C.I., Appelo, C.A.J., Arora, B., Jacques, D., Kalbacher, T., Kolditz, O., Lagneau, V., Lichtner, P.C., Mayer, K.U., Meeussen, J.C.L., Molins, S., Moulton, D., Shao, H., Šimůnek, J., Spycher, N., Yabusaki, S.B. and Yeh, G.T. 2015. Reactive transport codes for subsurface environmental simulation. *Computational Geosciences* 19, 445–478.

Steefel, C.I., DePaolo, D.J. and Lichtner, P.C. 2005. Reactive transport modeling: An essential tool and a new research approach for the Earth sciences. *Earth and Planetary Science Letters* 240, 539–558.

Stefanova, I. 2024. Challenges in completing the construction and commissioning of the NDF. Bulatom Conference.

Sustersic, J. and Drolc, S. 2020. Predstavitev projekta Študija proizvodnje, vgradljivosti in karakteristik končnih betonskih mešanic za izvedbo sekundarne armiranobetonske obloge silosa odlagališča NSRAO (Presentation of the project Study on the production, workability, and characteristics of final concrete mixtures for the construction of the secondary reinforced concrete lining of the NSRAO disposal silo). 27. slovenski kolokvij o betonih (27th Slovenian colloquium on concrete): Beton sekundarne obloge silosa odlagališča nizko in srednje radioaktivnih odpadkov (Concrete of the secondary lining of the disposal silo for low and intermediate level radioactive waste), 49–78.

Sustersic, J. and Hertl, B. 2023. Študija proizvodnje, vgradljivosti in karakteristik končnih mešanic kontraktorskega betona za izvedbo diafragme – primarne obloge silosa odlagališča NSRAO (DIAFRAGMA NSRAO) (Presentation of the project Study on the production, workability and characteristics of the final mixes of tremie concrete for the diaphragm - primary lining of the silo of the LILW repository (LILW DIAPHRAGM)). 29. slovenski kolokvij o betonih (29th Slovenian colloquium on concrete): Kontraktorski beton za globoko temeljenje (Tremie concrete for deep foundation), 15–32.

Sustersic, J. and Hertl, B. 2024. Lahka malta z ekspandiranim vermiculitom kot polnilna in tesnilna malta odlagalnih zabožnikov N2d (Lightweight mortar with expanded vermiculite as a filling and sealing mortar for disposal containers N2d). 31. slovenski kolokvij o betonih (31th Slovenian colloquium on concrete): Lahki betoni in malte (lightweight concretes and mortars), 13–30.

Tang, C.-S., Zhu, C., Cheng, Q., Zeng, H., Xu, J.-J., Tian, B.-G. and Shi, B. 2021. Desiccation cracking of soils: A review of investigation approaches, underlying mechanisms, and influencing factors. *Earth-Science Reviews* 216, 103586.

Tang, L.P. and Nilsson, L.O. 1993. Chloride Binding-Capacity and Binding Isotherms of Opc Pastes and Mortars. *Cement and Concrete Research* 23(2), 247–253.

TEM 2023 KYT2022 Finnish Research Programme on Nuclear Waste Management 2019–2022:Final Report.

Tian, K., Benson, C.H., Tinjum, J.M. and Edil, T.B. 2017. Antioxidant Depletion and Service Life Prediction for HDPE Geomembranes Exposed to Low-Level Radioactive Waste Leachate. *Journal of Geotechnical and Geoenvironmental Engineering* 143(6).

Tognazzi, C. 1998. Coupling between cracking and chemical degradation in cement based materials: characterisation and modelling Institut National des Sciences Appliquées (INSA).

Tournassat, C., Steefel, C., Bourg, I.C. and Bergaya, F. (2015) Natural and engineered clay barriers Elsevier.

TVO 2021a Maaperälloppusijoitus Ympäristövaikutusten arvointi (public event).

TVO 2021b Ympäristövaikutusten arvointimenettely hyvin matala-aktiivisen ydinjätteen loppusijoituksesta Olkiluodon ydinvoimalaitosalueella [accessed 16.3.2025].

van Es, E., Hinchliff, J., Felipe-Sotelo, M., Milodowski, A.E., Field, L.P., Evans, N.D.M. and Read, D. 2015. Retention of chlorine-36 by a cementitious backfill. *Mineralogical Magazine* 79(6), 1297–1305.

van Genuchten, M.T. 1980. Closed-form Equation for Predicting the Hydraulic Conductivity of Unsaturated Soils. *Soil Science Society America Journal* 44, 892–898.

Van Oost, K., Govers, G. and Desmet, P. 2000. Evaluating the effects of changes in landscape structure on soil erosion by water and tillage. *Landscape Ecol* 15(6), 577–589.

Vidal, T., Rougelot, T., Jantschik, K., Middelhoff, M., Kulenkampff, J., Hausmannová, L., Vasicek, R., Hlavackova, V., Le Duc, T., Griffa, M., Ma, B., S., C., Phung, T.Q., Neeft, E., Deissmann, G., Mijnendonckx, K., Helson, O., Večerník, P., Černoušek, T., Němeček, J., Singh, A., Engelberg, D., Evan, E., Boothman, C., Morris, K., Shaw, S., Lloyd, J.R., Wei, T.-S., Cherkouk, A., Dewitte, C. and Neji, M. 2024 Report on bio-chemical processes controlling the evolution of the microstructure and mechanical properties of cementitious materials. Final version as of 30/06/2024 of deliverable D16.4 and D16.6, of the HORIZON 2020 project EURAD. EC Grant agreement no: 847593.

Vollpracht, A. and Brameshuber, W. 2016. Binding and leaching of trace elements in Portland cement pastes. *Cement and Concrete Research* 79, 76–92.

von Berlepsch, T., Gonzalez Herranz, E., Stefanova, I., Haverkamp, B. and Nieder-Westermann, G. 2016 The National Disposal Facility for Radioactive Waste in Bulgaria, Vienna, Austria.

Wang, D.Q. and Wang, Q. 2022. Clarifying and quantifying the immobilization capacity of cement pastes on heavy metals. *Cement and Concrete Research* 161.

Wang, L. 2013 Solubility of radionuclides in Supercontainer concrete. Transferability document: Use of solubility determined within the category A (cAt) project in the B&C waste disposal assessment.

Ward, A.L. and Gee, G.W. 1997. Performance evaluation of a field-scale surface barrier. *Journal of Environmental Quality* 26(3), 694–705.

Wieland, E. 2014 Sorption data base for the cementitious near-field of L/ILW and ILW repositories for provisional safety analyses for SGT-E2 NTB--14-08. Paul Scherrer Institute Villigen, Switzerland.

Wieland, E., Jakob, A., Tits, J., Lothenbach, B. and Kunz, D. 2016. Sorption and diffusion studies with low molecular weight organic compounds in cementitious systems. *Applied Geochemistry* 67, 101–117.

Wieland, E. and Van Loon, L.R. 2003 Cementitious Near-Field Sorption Data Base for Performance Assessment of an ILW Repository in Opalinus Clay.

Wissmeier, L. and Barry, D.a. 2009. Effect of mineral reactions on the hydraulic properties of unsaturated soils: Model development and application. *Advances in Water Resources* 32(8), 1241–1254.

Woolhiser, D.A., Smith, R.E. and Goodrich, D.C. 1990. KINEROS: a kinematic runoff and erosion model: documentation and user manual.

Wu, Y., Ren, J. and Liu, J. 2024. Field Investigation of Water Infiltration into a Three-Layer Capillary Barrier Landfill Cover System Using Local Soils and Construction Waste. *Buildings* 14(1), 139.

Xu, Z.H., Zhang, Z.X., Huang, J.S., Yu, K.F., Zhong, G.M., Chen, F.Z., Chen, X.Y., Yang, W.E. and Wang, Y.C. 2022. Effects of temperature, humidity and CO₂ concentration on carbonation of cement-based materials: A review. *Construction and Building Materials* 346.

Yan, C. and Wang, T. 2025. A 3D discrete model for soil desiccation cracking in consideration of moisture diffusion. *Journal of Rock Mechanics and Geotechnical Engineering* 17(1), 614–635.

Yesiller, N., Miller, C.J., Inci, G. and Yaldo, K. 2000. Desiccation and cracking behavior of three compacted landfill liner soils. *Engineering Geology* 57(1-2), 105–121.

Yu, L. and Batlle, F. 2011. A hybrid method for quasi-three-dimensional slope stability analysis in a municipal solid waste landfill. *Waste Management* 31(12), 2484–2496.

Zajc, A. and Polanec, D. 2020. Ocena kakovosti strukture betona na osnovi rezultatov preskusa zmrzovanja/tajanja (Evaluation of the quality of concrete structure based on freeze/thaw test results). *Osnovni tehnološki parametri izvedbe sekundarne armiranobetonske obloge silosa odlagališča NSRAO = Basic technological parameters of the execution of the secondary reinforced concrete lining of the NSRAO disposal silo*, 127–141.

Zhang, M. and Reardon, E.J. 2003. Removal of B, Cr, Mo, and Se from wastewater by incorporation into hydrocalumite and ettringite. *Environmental Science & Technology* 37(13), 2947–2952.

Zhang, X., Sun, X. and Lin, Z. 2025. Improving soil moisture prediction using Gaussian process regression. *Smart Agricultural Technology* 11, 100905.

Zhang, Y., Yang, Z. and Ye, G. 2020. Dependence of unsaturated chloride diffusion on the pore structure in cementitious materials. *Cement and Concrete Research* 127, 105919.

Zhang, Y. and Zhang, M. 2014. Transport properties in unsaturated cement-based materials – A review. *Construction and Building Materials* 72, 367–379.

Zhou, J., Ni, J., Liu, S., Wang, Y. and Choi, C.E. 2025. Influence of plant root aging on water percolation in three earthen landfill cover systems: A numerical study. *Journal of Hydrology* 655, 132916.

Zibara, H. (2001) Binding of external chlorides by cement pastes, University of Toronto.

Zurmühl, T. and Durner, W. 1998. Determination of Parameters for Bimodal Hydraulic Functions by Inverse Modeling. *Soil Science Society America Journal* 62, 874–880.